Open Platform for Limit Protection with Carefree Maneuver Applications

A Thesis
Presented to
The Academic Faculty

By

Geoffrey J. Jeram

In Partial Fulfillment
of the Requirements for the Degree
Doctor of Philosophy in the
School of Aerospace Engineering

Georgia Institute of Technology
December 2004

Open Platform for Limit Protection with Carefree Maneuver Applications

Approved By:

Dr. J.V.R. Prasad, Advisor

Dr. Joseph Horn

Dr. Eric Johnson

Dr. William D. Lewis

Dr. Amy Pritchett

Dr. Daniel Schrage

11 October 2004

DEDICATION

To the last man,

still alive on earth,

You should have gotten off when you had the chance.

ACKNOWLEDGMENTS

This work is carried out under grant NAG 2-1418 originating at the Army/NASA Rotorcraft Division at NASA Ames. This project is funded by a research grant from the U.S. Army Aeroflightdynamics Directorate for in-flight demonstration of tactile cueing on the Rotorcraft Aircrew Systems Concepts Airborne Laboratory (RASCAL).

Regarding this work, the author is publicly thankful for:

- The Georgia Institute of Technology and its Guggenheim School of Aerospace Engineering for its intellectual challenges and its generosity with learning and research resources support, both tangible and intangible.
- Dr. JVR Prasad's luck at finding me as a potential graduate student, his wisdom in selecting me for this research project, and his invaluable advisement and instruction during my four year tour as a graduate student and doctoral candidate.
- The Army NASA Rotorcraft Division for its sponsorship of this research endeavor, particularly Matt Whalley and Dr. Mark Tischler for their special contributions of knowledge and advisement.
- The American Helicopter Society for the advancement and dissemination of aerospace knowledge and technology that extends beyond vertical takeoff and landing subjects.
- The considerable assistance of Weiliang Dai and Hossein Mansur for the use of RIPTIDE and their support and instruction for its use.
- My research collaborators and helpers, including: Suraj Unnikrishnan, Dr. Ilkay Yavrucuk, Nilesh Sahani, Dr. Joe Horn, Manuj Dhingra, Suresh Kannan.

TABLE OF CONTENTS

LIST OF TABLES

TABLE OF FIGURES

NOMENCLATURE

Symbols

ζ = 2nd order system damping coefficient

ω = 2nd order system natural frequency

μ = Force or position command switch

λ = Lagrange coefficient for Limit Margin. Positive values indicate "within limits".

τ_e = Effective time delay of a system

Δu_{crit} = Control margin

Δy = Limit margin

f , g , h= Vector functions

F = Force applied to Sidestick

j = imaginary number $\sqrt{-1}$

K = Scaling factor

M_H = Longitudinal Hub Moment

N = Limit Identifier

t = time, (Δt = time interval or sample interval)

u = Inceptor command to flight control system

$U(\omega_k)$ = discrete finite Fourier transform of inceptor signal at frequency ω_k.

V_H = Maximum horizontal airspeed within flight envelop limits.

w = number of intervals in a window

x = Aircraft State Vector of n elements, $x = [\, x_1 \;\; x_2 \;\; x_3 \ldots x_n \,]^T$

$X(\omega_k)$ = discrete finite Fourier transform for an aircraft state at frequency ω_k.

y = Aircraft Limit Vector of m elements, $y = [\, y_1 \;\; y_2 \;\; y_3 \ldots y_m \,]^T$

Y(s) = Transfer function of a subsystem

y_p = Predicted Limit Vector

 = A multimedia file is associated with this figure or text.

Superscripts and Subscripts

λ = Scaling or coefficient for Lagrange multiplier

δ = Inceptor physical displacement, (ex. $u_{\delta.long}$ is longitudinal position)

δu = Inceptor position to control command signal scaling

+ = Positive or Upper, as in upper critical control position, u^+_{crit}

- = Negative or Lower, as in upper critical control position, u^{-}_{crit}

ANN = Adaptive Neural Network

C = Aircraft characteristic, as in Y_C (s)

coll = Collective

crit = Critical

F = Force or Force-Feel characteristic, (ex. $u_{F.long}$ is applied longitudinal force)

f = Fast, as in fast states, x_f

Fu = Force applied to control command signal scaling

fut = Future

i = value for time index, as in $i\Delta t$

k = value for the k^{th} frequency

lat = Lateral (cyclic)

long = Longitudinal (cyclic)

M = main frequency

NN = Neural Network (implies static)

P = Pilot characteristic

p = Predicted

s = Slow, as in slow states, x_s

Acronyms

APC	Aircraft Pilot Coupling
CPU	Central Processing Unit
CWA	Cautions, Warnings, and Advisories
DARPA	Defense Advance Research Projects Agency
DFCS	Digital Flight Control System
HUD	Heads Up Display
HUMS	Health Usage Monitoring System
MTE	Mission Task Elements
NND	Normalized non-dimensional number (real values of –1 to +1).
OCP	Open Platform for Reconfigurable Control
OPLP	Open Platform for Limit Protection
RASCAL	Rotorcraft Aircrew Systems Concepts Airborne Laboratory
RIPTIDE	Real-Time Interactive Prototype Technology Integration Development Environment
SEC	Software Enabled Control
VMS	Vehicle Management System

SUMMARY

This Open Platform for Limit Protection guides the open design of maneuver limit protection systems in general, and manned, rotorcraft, aerospace applications in particular. The platform uses three stages of limit protection modules: limit cue creation, limit cue arbitration, and control system interface. A common set of limit cue modules provides commands that can include constraints, alerts, transfer functions, and friction. An arbitration module selects the "best" limit protection cues and distributes them to the most appropriate control path interface. This platform adopts a holistic approach to limit protection whereby it considers all potential interface points, including the pilot's visual, aural, and tactile displays; and automatic command restraint shaping for autonomous limit protection.

For each functional module, this thesis guides the control system designer through the design choices and information interfaces among the modules. Limit cue module design choices include type of prediction, prediction mechanism, method of critical control calculation, and type of limit cue. Special consideration is given to the nature of the limit, particularly the level of knowledge about it, and the ramifications for limit protection design, especially with respect to intelligent control methods such as fuzzy inference systems and neural networks.

The Open Platform for Limit Protection reduces the effort required for initial limit protection design by defining a practical structure that still allows considerable design freedom. The platform reduces lifecycle effort through its open engineering systems approach of decoupled, modular design and standardized information interfaces.

Using the Open Platform for Limit Protection, a carefree maneuver system is designed that addresses: main rotor blade stall as a steady-state limit; hub moment as a transient structural limit; and pilot induced oscillation as a controllability limit. The limit cue modules in this system make use of static neural networks, adaptive neural networks, and fuzzy inference systems to predict these limits. Visual (heads up display) and tactile (force-feedback) limit cues are employed. The carefree maneuver system is demonstrated in manned simulation using a General Helicopter (GENHEL) math model of the UH-60 Black Hawk, a projected, 53° field of view for the pilot, and a two-axis, active sidestick for cyclic control. Video Demonstration Link, 284 Mb 

CHAPTER I

INTRODUCTION

Every vehicle system has limits, whether we realize and understand them or not. In the past (and even today for newly discovered limits), overcoming or avoiding limits was an art, conquered by the individual aviator. As the field of aerospace engineering grew, so did the awareness and understanding of limits' origins, importance, and urgency. Limit protection (or elimination) grew into a science. When the operator drives the system beyond its limits, the results are unpredictable and include some sort of loss, such as wear, damage, destruction, injury, or death. Limit protection systems were designed to interact with elements of the overall vehicle control system. Those elements include the pilot's maneuver & trajectory planning, his bodily reactions, the display system, the inceptor system, the flight control system, the actuators, and the aerodynamic design of the vehicle itself. These limit protection elements have been successful, but typically attempt to interact with fixed elements along the control command path. For example, the protection system might be the conscious restraint of the pilot, but this compromises speed and adds the risk of human error, variability, and uncertainty.

During aircraft flight testing to determine an aircraft's practical limits, experimental test pilots may be allowed "carefree flight" which is defined by a National Aeronautics and Space Administration sponsored study[1] as "a type of flying in which the pilot is free to maneuver the aircraft in a 'carefree' manner with little or no concern for particular task constraints." With the advent of the digital avionics, limit protection systems have been designed into flight control system. Such advanced systems allow "carefree handling", a term used with varying meanings in technical and industry literature, that implies "the pilot can perform whatever action he wants with the stick, pedals and throttle and the aircraft's flight control system will protect the pilot and the aircraft by limiting parameters such as angle of attack, g-force and roll-rate, to a safe level."[2] Another term, "carefree abandon," used specifically with the F-22 Raptor aircraft has the same meaning, "'carefree abandon' translates into the ability of the fighter pilot to do whatever he wishes with the F-22, without fear of loss of control, loss of thrust or aircraft structural overstress."[3] But this automatic or autonomous limit protection purposefully overrides pilot authority and complicates control system design. The related term, "active control" or "active control system", also has a wide set of meanings, but in the context of limit protection, it refers to the technique of

using a control system in lieu of a physically stronger airframe to keep the aircraft within structural limits.

Active inceptors have now emerged that enable “carefree maneuver”. The term is synonymous with an extended meaning of “carefree handling”, and here implies that the aircraft’s display systems (visual, aural, tactile, etc) assist the pilot to find and follow the limit boundary without adding to his workload or requiring inordinate in-cockpit attention to systems gauges and readouts. “Carefree maneuver” is a form of limit protection that fits between the pilot’s conscious, active restraint (or lack thereof for “carefree flight”) and the flight control system’s automatic limit protection of “carefree handling”. This thesis will describe a platform designed as an open engineering system for limit protection that spans several elements of the vehicle control system and applies limit protection at the most appropriate level. The thesis places special emphasis on the active inceptor element, the newest and least developed element of the chain.

An inceptor, such as a steering wheel, a cyclic stick, or a sidestick, is an information interface between the human operator and the vehicle. It is one element in an aircraft-pilot system that includes the pilot, the inceptor, the vehicle digital control system, the actuators, the vehicle dynamics, and the display system feedback. Control system designers have included the inceptor as an element of the control system without feedback to the pilot, a reasonable approximation for passive inceptors. Whereas passive inceptors only allow the pilot to provide control intent information to the vehicle, an active inceptor can also provide information to the pilot. High fidelity active inceptors have recently become available for practical use. These inceptors can dynamically change their counter-force at relatively high bandwidths (changes on the order of a few hundredths of a second). This tactile cue capability introduces a proprioceptive feedback between the pilot and the active inceptor that invalidates the control system approach used for passive inceptors; introduces a host of design variables; and enables intuitive cue possibilities for carefree maneuver.

Significance of Limit Protection and Active Tactile Cueing

The purpose of a limit protection system is literally to prevent the aircraft from violating its limit boundaries. Conservative safety constraints can do the same. But safety constraints restrict the performance of the vehicle. Safety and performance are typically in opposition. The true value of a limit protection system is the reduction of the safety versus performance compromise.

We can consider the significance and value of limit protection systems featuring tactile cues with three example applications. The first application is aircraft systems limit protection. This is particularly important for aircraft that regularly fly at the maximum structural capabilities of the airframe and engine. Helicopters regularly operate in these conditions, near maximum gross weight and engine torque. Secondly, carefree maneuver systems can provide piloting force cues to assist pilots with basic aircraft control. General aviation pilots often fly many models of rental aircraft and do so less frequently than commercial or military pilots. Consequently, they can benefit much from proficiency cues. Thirdly, carefree maneuver applications can provide flight envelope limit cues for pilots of highly unconventional aircraft with very complex flight envelopes. Examples of these exotic configurations include tiltrotors such as the V-22 and Bell 609; and thrust vectored aircraft like the Joint Strike Fighter. Consider each of these potential applications in turn.

		
The V-22 Osprey	The Bell BA 609 Tiltrotor	The F-35 Joint Strike Fighter

Figure 1. Emerging Complex Aircraft with Limit Protection Systems.

Structural Limit Cues for Helicopters.

Helicopters regularly operate at their maximum gross weights and power levels. In extreme events, the pilot may fly the aircraft into a condition where catastrophic structural failure occurs and the aircraft crashes. This happens infrequently, but relatively minor limits are broken more frequently. Three commonly exceeded structural limits include engine overtorques, engine overspeeds, and rotor overspeeds. These rarely cause immediate failure, but rather require expensive maintenance inspections and parts replacements. An overtorque occurs when the pilot demands more power (torque) than the engine is rated to provide. An engine overspeed occurs when the turbine speeds beyond its rated limit and results when the engine speed governor lags after a pilot who

abruptly reduces main rotor thrust. Similarly, a rotor overspeed occurs when the rotor speeds beyond the fatigue limits of the main rotor hub and aircraft transmission system. All three of these limits are prototypical candidates for tactile limit protection cues.

According to the U.S. Army Safety Program[4], over the last three years, Army helicopters suffered an average of 26 of these relatively minor, non-fatal accidents for an average annual cost of $5.2 million (See Table 1). Approximately 80% of these accidents occurred in the Army's 3000 attack or scout helicopters. This equates to roughly $1,400 for every attack or scout aircraft every year. So a relatively simple limit force cue device retrofitted to cockpit collective levers could prove a cost effective, value added, carefree maneuver device for Army helicopters and their civilian analogues typically used for police work, news service observation, corporate travel, and medical evacuation.

Table 1. Costs for Non-Fatal Accidents due to Common Limit Violations

	Engine Overtorque		Rotor Overspeed		Engine Overspeed/temp	
	Number	Cost	Number	Cost	Number	Cost
FY 2003	9	$ 303 K	3	$ 161 K	13	$ 361 K
FY 2002	9	$ 734 K	1	$ 61 K	21	$ 1.22 M
FY 2001	10	$ 1.4 M	1	$ 197 K	13	$ 719 K

Source: U.S. Army Safety Center

Proficiency Cues for General Aviation.

A 2003 FAA sponsored study[5], explored four human factors for general aviation accidents, classifying the causal factors among three human error types (decision, skill-based, and perceptual errors) as defined by the Human Factors Analysis and Classification System (HFACS). It also considered willful disregard for FAA rules (violations). The study found that the skill based "stick-and-rudder" consistently accounted for nearly 70% of the seminal (precipitating) aircrew unsafe acts.

The same study also made a preliminary analysis of those skill-based errors. They included directional control (31% of skill based errors), airspeed (24%), compensation for winds (20%), aircraft control (18%), and visual lookout (8%). A related study[6] of commercial aviation, where the pilots have a higher average level of proficiency, found

similar results. Skill based errors were associated with 64% of FAR Part 121 carriers and 59% of FAR Part 135 carriers. A limit protection system with tactile cues either embedded in the aircraft autopilot system or added as a stand alone active inceptor system has the potential to considerably reduce the first four of these errors.

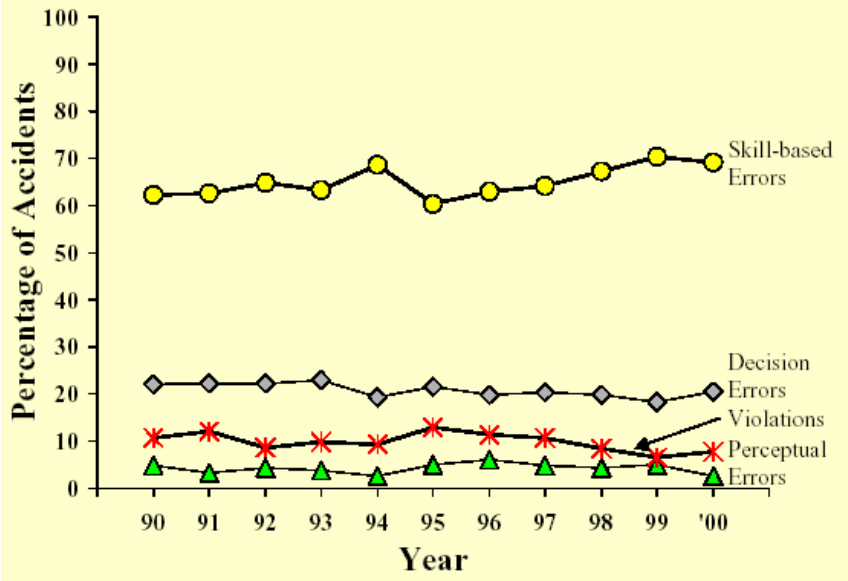

Figure 2. HFACS analysis of GA accidents.

Flight Envelope Cues for Complex Aircraft.

There are several active developmental aerospace programs that are attempting to create highly unconventional aircraft with complex flight envelopes. The Bell BA609[7] is a nearly 17,000 pound tiltrotor with a 5,500 lb payload and applications in the Coast Guard, corporate transport, emergency medical service, offshore utility, and search and rescue. This aircraft has a variable force-feel system build into its cockpit controls. The manufacturer decided not to incorporate a pure fly-by-wire active inceptor system in its initial version. This aircraft has a hybrid control system that is not easily convertible to a pure active inceptor retrofit. However, a basic carefree maneuver algorithm could be embedded in its variable force feel system.

The V-22 Osprey[8] is a nearly 60,000 pound tiltrotor designed for the U.S. Navy, Marines, and Air Force. It has diverse mission applications that include amphibious assault, V/STOL heavy transport, and search and rescue. The first $1.45 billion contract was awarded to in 1997 to begin production of the first 425 aircraft for the Marine Corps.

This aircraft has a fly-by-wire control system with customized passive cockpit inceptors. It is a potential after-market customer for an active inceptor upgrade with a carefree maneuver system.

The Joint Strike Fighter (JSF) program is arguably most technically challenging production aircraft program in the world today. The aircraft is a supersonic jet fighter with vectored thrust and an in-fuselage vertical lifting fan that enables vertical take-off and landing. Like the aforementioned tiltrotors, its flight regime ranges from hovering flight to high-speed forward flight, but also extends to transonic speeds. This is the only aircraft in development today designed from the outset to include a digital fly-by-wire control system, an active inceptor cockpit, and some sort of carefree maneuver system. Lockheed Martin manufactures the aircraft in partnership with BAE Systems. The aircraft is planned as a platform with several variants for the U.S. Air Force, the U.S. Navy, the U.S. Marine Corps, and the U.K. Royal Navy. In all, some 2783 aircraft are planned for these initial customers with additional orders likely from other countries around the world. The total contract, which will exceed $200 billion dollars, is potentially the largest contract ever to be secured by a military aircraft manufacturer.

Figure 3. Stirling Dynamics Active Sidestick.

BAE Systems, a leading manufacturer of flight quality active inceptors, will manufacture the active inceptor system for the JSF[9]. An example of sidestick with two active axes is shown in Figure 3. BAE Systems has announced its intention to develop a carefree maneuver system for the JSF.

The utility and value of active force-feedback inceptor systems is exemplified in these three applications. Notice also the various environments in these examples. The types of aircraft are very different, and employ either fly-by-wire or fly-by-cable flight control systems. The proficiency and experience of the pilots varies across the examples from civilian private pilots, to military helicopter pilots, to custom trained aviators for complex aircraft. Consider that tactile cue systems also have analogous applications for automobiles and industrial equipment. A closed design approach could produce the control systems required for all these varieties of tactile cue systems, but an open design approach would greatly simplify the lifecycle tasks, reduce the total cost of development, and shorten the time to completion for each new application.

Motivation and Goals

Essential limit protection systems have been designed into flight control systems and added to the aircraft separately, in a fixed, ad hoc manner. The latest limit protection research, described in chapter 2, has focused on algorithm development, using closed, design approaches that facilitated the research. The goal of this thesis is the creation of a holistic, systematic open design approach that guides the design of limit prediction mechanisms and intelligently applies limit protection to the most effective points along the control signal path, allowing voluntary limit protection where possible. Objectives include:

- A detailed taxonomy of limit protection functions and design choices.
- A modular architecture where major functions are decoupled.
- A level of definition that provides a balanced compromise between design freedom and practical structure.
- An extensible structure with replaceable, upgradeable functional modules and robustness to change in its application.

The hypothesis is that satisfying these objectives will lead to a limit protection system with that can be applied to current research and existing aircraft, and may be indefinitely renewed and extended to accommodate new technologies and applications.

CHAPTER II

PRIOR ART AND ONGOING DEVELOPMENT

The preceding terms and definitions have emerged in the past decade of limit prediction and carefree maneuver literature. Aircraft limit prediction systems linked to tactile cues in flight controls enable carefree handling and help the pilot make the most of an aircraft's flight envelope[10]. Recent studies such as the Helicopter Maneuver Envelope Enhancement (HELMEE) program have shown as much in the NASA Ames' Vertical Motion Simulator[11]. Other ongoing projects such as the Helicopter Active Control Technology program sponsored by the U.S. Army and carried out by Boeing continue to explore the potential of active cueing[12]. The Army/NASA Rotorcraft Division continues to develop its Rotorcraft Aircrew Systems Concepts Airborne Laboratory (RASCAL) in a JUH-60 Blackhawk airframe[13]. With a two-axis active sidestick controller and a full-authority fly-by-wire flight control system, the RASCAL facilitates active control and limit cueing research. The Army/NASA Rotorcraft Division Flight Mechanics and Cockpit Integration Branch and the School of Aerospace Engineering at the Georgia Institute of Technology are developing the control system for the RASCAL active sidestick. One product of the endeavor is this holistic approach and open design architecture. It is intended for the RASCAL active control system and is applicable to other haptic applications.

Open Engineering Systems

An Open Engineering System (OES) is one that changes and evolves over time with changes in technology, application, market, and so on. This differs from a closed engineering system, which targets a specific (static) environment, has limited ability to evolve, and may or may not have any utility beyond its targeted design application and environment.

> *Open engineering systems are systems of industrial products, services and processes that are capable of indefinite growth and development by both incremental technological advance and major technological change stemming from an existing base.*[14]

The tactile cueing and active limit protection system designs to date, such as the HACT, HELMEE, and Georgia Institute of Technology studies described below, focused on algorithm development for specific aircraft. They have targeted specific aircraft and, with the exception of the HACT project[15], have also limited the design to a bijective mapping of limits to inceptor axes. These limit protection systems design might follow control systems design methods that include non-real time simulation with a mathematical pilot model (i.e. the classical "crossover model," the modern "optimal control model," the "pursuit model," and so on). These projects have also enjoyed controlled evaluation and testing environments using piloted simulation at their later stages.

The open engineering systems approach or philosophy is now well developed theoretically and practically for physical products. It is also becoming widely used for software applications. The theory and explanation for the open platform design used in this design is expounded in engineering, design, and management literature.

Nam Suh's design axioms[16] play an important role in the open design philosophy. He proposes two primary axioms for designs that relate design parameters to functional requirements: the Independence Axiom and the Information Axiom. The Independence Axiom states that sections of the design should be separable so that changes in any one section would have no (or as little as possible) effect on any others. The Information Axiom states that the information inherent in a product design and its sections should be minimized. From these two axioms, several corollaries follow:

- Decouple the design sections to minimize interactions,
- Minimize functional requirements to simplify the design,
- Integrate sections where possible without compromising other principles to reduce the number of parts and complexity,
- Standardize sections and interfaces to reduce information content,
- Symmetrize sections to reduce the information content,
- Allow large tolerances for functional requirements to reduce the information content,
- Uncouple and minimize components to reduce complexity & interdependence.

Each of these axioms and corollaries can be applied to control systems design and more specifically to limit protection systems that include active inceptors.

When Karl Ulrich detailed the role of product architecture for design[17], he described the open engineering philosophy and its relevance to five areas of managerial importance: product change, product variety, component standardization, product performance, and

product development management. He defined design architecture as: (1) the arrangement of functional elements; (2) the mapping from functional elements to physical components; and (3) the specification of the interfaces among interacting physical components.

Ulrich defines many of the terms of design topology to be incorporated into the active control system platform of this thesis. He makes the distinction between modular architecture, which uses a one-to-one mapping from functional elements to physical components, and integral architecture, which includes complex (non one-to-one) mapping from functional elements to physical components and / or coupled interfaces between components. Erens and Verhulst deepened Ulrich's work[18]. They considered architecture for product families, platform longevity, and platform renewal.

Object Oriented Software

Object oriented programming[19,20] (OOP) is a computer programming paradigm that emphasizes an open engineering systems approach. The fundamental aspect of OOP is the use of objects as a basis for modularity and structure. The other main aspects of OOP include Abstraction, Encapsulation, Polymorphism, and Inheritance. The first two of these aspects (Abstraction and Encapsulation), taken together, satisfy Suh's corollaries by capturing the basic functions of a program and hiding the inner workings of the programming objects so that only the essential information is exchanged among the objects. The remaining two aspects (Polymorphism and Inheritance), strive toward the realization of the programming as an open engineering system capable of indefinite growth and development that stems from the existing base. Polymorphism is the object's ability to apply its function to different types of variables and data. Inheritance is nature of a programming object to pass on its function or class to new combinations and extensions for new applications and larger modular structures. The object-oriented approach has applied to many aerospace software endeavors including flight simulation[21,22], aerodynamics[23,24,25,26], aircraft design[27,28,29], and flight control[30].

Open Control Platform

The Open Control Platform (OCP) developed at the Georgia Institute of Technology and the Boeing Phantom Works under a DARPA Software Enabled Control (SEC) Program adopts an open engineering systems approach to control systems design[31]. It overcomes the limitations of current control systems design practices that follow from the traditional closed engineering approach. Those limitations include:

- Complex, brittle, data interchange where the interaction of control system components is based on communication protocols or hardware, sometimes proprietary, that is not amenable to replacement or change.
- Computational limitations related to the stringent technological constraints of low weight, low power systems require an integral design, optimized for performance within the constraints of the environment.
- Tight coupling of information requirements among the functional modules, subsystems, and components, fostered by the need for an optimized design, makes the pieces very difficult to singly update or upgrade without a complete review and recreation of the larger control system.
- Closed and proprietary systems may protect commercial investment and represent competitive advantage, but they limit interchangeability, reconfigurability, and distributed and concurrent processing.

The OCP is a hardware and software platform that echelons low-level, mid-level, and high-level control systems functions. These echelons roughly correspond to the time scale of control action. The OCP provides for real-time distributed computing, prioritized event-based communication for dynamic reconfiguration, dynamic scheduling, adaptive resource management, and a reconfigurable controls set. The platform exemplifies an open engineering systems approach that can accommodate new technologies and control systems applications, whether for aerospace applications, manufacturing such as the limit protection platform presented in this thesis.

Vehicle Limit Protection

Limit prediction and protection mechanisms can be loosely classified by the time scale of limit protection, that is, the immediacy of the need for limit protection action and the proximity of the protection mechanism to that protected element. For the sake of this analysis, the time scale classification has been simplified to three (Table 2). The time scale is approximate and in many cases of prior art for limit protection, elements of the vehicle control system, particularly the flight control system, are used to protect limits in other time scales. While not relevant for this introduction, these categories could be extended forward of the flight control system to very fast limit protection within the actuators or to the longer time scale of risk management prior to flight (described later in Figure 4).

Table 2. Time Scales for Limit Protection Systems

Purpose	Stability & Control	Maneuver Control	Trajectory planning
Action or Reaction time	Less than 0.1 sec	0.1 sec to 1.0 sec	Greater than 1.0 sec
Lowest Elements of Control	Flight Control System, Actuators	Body & Inceptor	Mind
Human involvement	None or involuntary	Non-cognitive or Reflexive	Cognitive, Thoughtful

The first category of limits, such as those that are highly sensitive to control surface movements, are appropriately addressed at the aircraft flight control system level without cueing to or input from the pilot. Control system adjustments for this category must be made quickly, on the order of hundredths of a second or faster. This is too fast for human reaction. A joint U.S./France study[32] of helicopter limits identified 39 limits that fall into the remaining two categories. These limits are most effectively cued through combinations of visual warning lights and instruments, aural warning and caution tones, verbal (voice) warnings, and tactile cueing through the cockpit controls. The second category includes the limits that are sensitive to inceptor position and speed over displacement within a few tenths of a second. This thesis primarily addresses the maneuver control category, but the approach presented here may be extended to include stability & control and trajectory planning. Examples for such maneuver limits include: vertical load factor, main rotor blade stall, main rotor flapping, main rotor speed, and transmission torque. The third category, which includes limits that vary slowly, over seconds and longer, are appropriately cued by non-tactile means.

Aircraft Programs

Aircraft have always had various forms of limit protection and cue devices, but they have mainly taken the form of systems gauges and readouts in the cockpit. The pilot remained the agent responsible for the limit protection and he included those gauges in his instrument cross check. Other common cues have been aural, such as the stall buzzer or simple stick shaker. More sophisticated limit protection systems were pursued in several aircraft development programs (See Figure 3).

Table 3. Survey of Limit Protection Systems in Operational Aircraft.

Aircraft Program	Limits	Method of Protection or Cue
Eurofighter[33]	Angle of Attack Load Factor	Integral to FCS
Airbus A319/320[34]	Load Factor Airspeed Stall	Integral to FCS
Boeing 777[35]	Stall Overspeed (airspeed) Bank Angle	Visual, Audio, Tactile (Tactile cues include softstops and shakers)
RAH-66 Comanche[36]	Main Rotor Torque Speed Sideslip angle	Visual, Audio
V-22 Osprey[37]	Rotor flapping (incl. transient) Rotor yoke bending Driveshaft torque Nacelle conversion actuator Vertical downstop load Angle of Attack	Integral to FCS
C-17A Galaxy[38]	Deep stall	Audio

A notable debate continues with regard to pilot-in-the-loop limit protection versus autonomous, involuntary limit protection. The Airbus A319/320 and the Boeing 777 both have systems that protect stall and airspeed limits, but the manufacturers adopt different approaches. Airbus integrates limit protection into the aircraft flight computers to make limit protection automatic and involuntary*. Boeing chose to provide protection through sensory cues, including basic tactile cues, to communicate imminent limits and encourage voluntary protection. The Airbus approach emphasizes the safety of the aircraft, as defined by its built-in limit protection, and de-emphasizes pilot judgment. In the extreme case, this approach would ultimately place the safety decision with the aircraft manufacturer and its limit protection systems designers. The Boeing approach allows the pilot greater discretion during a limit boundary encounter and it would be the pilot

* Autonomous limit protection, including this Airbus example, is not strictly involuntary. The pilot may still disable the protection system by means of a switch or circuit breaker. But this pro-action may be overlooked or may be too difficult during limit boundary encounters and high-workload events, such as emergency situations.

ultimately decides whether or not to violate the flight envelope. It also, arguably, leads to greater workload for pilots who choose to override the limit cues.

University Research

Limit prediction and avoidance is a research topic of interest at the Georgia Institute of Technology. Limit prediction, flight envelope protection, and tactile cueing research has been sponsored variously by the Defense Advanced Research Projects Agency (DARPA), the Center for Excellence for Rotorcraft Technology (CERT), and the Army NASA Rotorcraft Division (See Table 4). The products of that research have been mainly the concept of dynamic trim limit prediction[39,40] and the use of adaptive neural network algorithms for that prediction[41,42,43]. The research focused on the limit algorithms themselves for simulated manned application and autonomous applications. The system architecture was not the focus of the research, which used a straightforward application of limit protection algorithms with modeled tactile cues for manned simulation or direct interdiction of control signals for autonomous applications.

Table 4. Survey of Tactile Limit Avoidance Research Programs

Research Program	Limits	Type of Cues
HELMEE (UH-60A)	Engine Torque Main Rotor Blade Stall	Longitudinal Softstop Collective Softstop
CERT (XV-15)	Vertical Load Airspeed Torque Longitudinal Flapping	Tactile Longitudinal Softstop
HACT (AH-64)	Load Factor Main Rotor Stall Transmission Torque Rotor Speed Tail Rotor Torque Main Rotor Flapping	Longitudinal Softstops, detents, and tactile gates Yaw Softstop Collective Softstop

A portion of the Software Enabled Control[44] project includes a limit protection goal that incorporated an adaptive limit prediction algorithm and protected the vehicle from limit violation at the command level for an autonomous rotorcraft, the GTMax[45]. The project is notable in that the overall vehicle control system is based in an open software architecture.

The Traffic Alert and Collision Avoidance System[46] (TCAS) has been employed for two decades. Recent research, particularly at the Massachusetts Institute of Technology, continues to advance the use of visual and aural pilot advisories and alerts. One study[47] proposed the use of performance metrics based on probabilistic models for false alarms and correct detections to improve system efficacy. A related study[48,49] considered multiple alerting systems and the potential conflicts among them. Traffic alerting systems (for collision avoidance) have been integrated with air traffic procedure displays[50] and tested in flight simulation[51]. The work adopts visual and aural displays as decision aids for the pilot.

HACT

The Helicopter Active Control Technology (HACT) program, sponsored by the U.S. Army and executed in its later development phase by Boeing Helicopters advanced several technologies pertaining to advanced flight control, including various tactile cues.[52] The HACT program took an integrated approach to active limit protection and tactile cueing and incorporated its carefree maneuver system into the Vehicle Management System (VMS). The carefree maneuver system used static neural network based limit prediction algorithms with complementary filters to eliminate steady state errors. It is the most comprehensive tactile avoidance cueing program to date.[15, 53, 54, 55]

Federal Aviation Administration

In the 1970's, the Federal Aviation Administration (FAA), in an effort to standardized cockpit alerting systems, reviewed military and commercial warning and alerting systems in three studies[56,57,58]. The studies found that pilots were overwhelmed with warnings. The Boeing 747, as an example, had over 400 separate cockpit warnings; nearly all were visual and auditory in nature.

In 1998, the FAA certified an integrated cockpit alerting system[59] that combines and prioritizes the visual and aural alerts and warnings for an aircraft's Traffic Alert and Collision Avoidance System (TCAS), Reactive and Predictive Wind shear Detection Systems (RWS and PWS), and Ground Proximity Warning System (GPWS). The Allied Signal product was created after coordination with both Airbus and Boeing and agreement over the priorities of these systems.

Defence Research Agency

The United Kingdom's DRA researched methods for providing carefree maneuver capabilities to pilots. The studies[60, 61] considered different cueing methods, including heads up display symbols, auditory tones, and tactile cues in the collective lever. The

tactile collective cue showed great promise – it reduced instances of over-torque while improving performance and reducing workload for a number for maneuvers. Other European helicopter research also explored the general considerations for active control technology[62, 63]. These research efforts identified potential benefits of active tactile cues, but did not delve deeply into the design of limit protection systems.

HELMEE

The Helicopter Maneuver Envelope Enhancement (HELMEE) study was conducted as a series of studies by the Army Aeroflightdynamics Directorate. The first[64] was qualitative in nature. It was conducted by Sikorsky and provided general insights into helicopter limit cueing. The second[11] was conducted by the Aeroflightdynamics Directorate at Ames Research Center. It explored helicopter limit cueing for transmission torque, main rotor underspeed, and main rotor overspeed. Cues included stick force feedback, aural tones, voice warnings, and heads up display symbols. The tactile cue was found to be the most immediate and strongest cue. Pilots preferred to have multiple cues for corroboration, especially combinations of tactile and HUD cues. The HUD, tone, and voice cues had little or no effect on task performance. There were concerns that the aural cues might interfere with cockpit and radio communications. The HUD cues were discrete and, as such, had little information content and no corrective suggestion. The pilots found them useful as corroboration of the tactile limit cues and preferred trials that included multiple forms of cues.

CHAPTER III

OPEN PLATFORM FOR LIMIT PROTECTION

The Open Platform for Limit Protection (OPLP) presented here is the definition and description of functional structures and their outputs (deliverables). It is presented as a template that will structure and facilitate the design and prototyping of limit protection systems. It can be implemented in a variety of commercial tools for control systems design, including MATLAB/Simulink[65] and Advanced Real-Time Control Systems[66]. The intent of the OPLP is to balance the design freedom needed by the control systems designers with the practical functionality required for a system with potentially multiple cues and multiple control path interfaces. The structure of this platform was chosen to accommodate prior and ongoing research and foreseeable future control systems theory and applications. This chapter defines this OPLP template and explains where and how the prior art fits into this platform. The succeeding chapter documents several limit protection systems designed, prototyped, and tested in the context of this platform.

A vehicle control system typically contains many elements. Starting with the vehicle dynamics and moving toward the source of the control command, the control signal path includes subsystems for the control surface actuators, a digital flight control system, and for a manned system, a cockpit control inceptor and a pilot. The overall control system includes inner-loop signal feedback at each element and may include branches from other sources of control, such as multiple inceptors, cockpit switches for aircraft configuration changes (ex. landing gear), changes in the local flight environment (ex. tethered or released from a towing aircraft, mothership, or formation flight interaction). The control system may use an outer loop autonomous control system in lieu of the human pilot. Within the pilot's physical-biological system, there are numerous control feedback signals and elements. Most notably in the context of this thesis, these include the "body knowledge" and reflexive restrain that the experienced pilot uses to maintain control of the aircraft within its limits. Even preceding flight maneuvers or take-off, there are mission decisions that influence whether an aircraft and pilot system will be prone to limit violations and their corresponding risks.

This Open Platform for Limit Protection (OPLP) adopts a holistic approach for limit protection and imposes protection constraints at appropriate points across the control path as shown in (Figure 4).

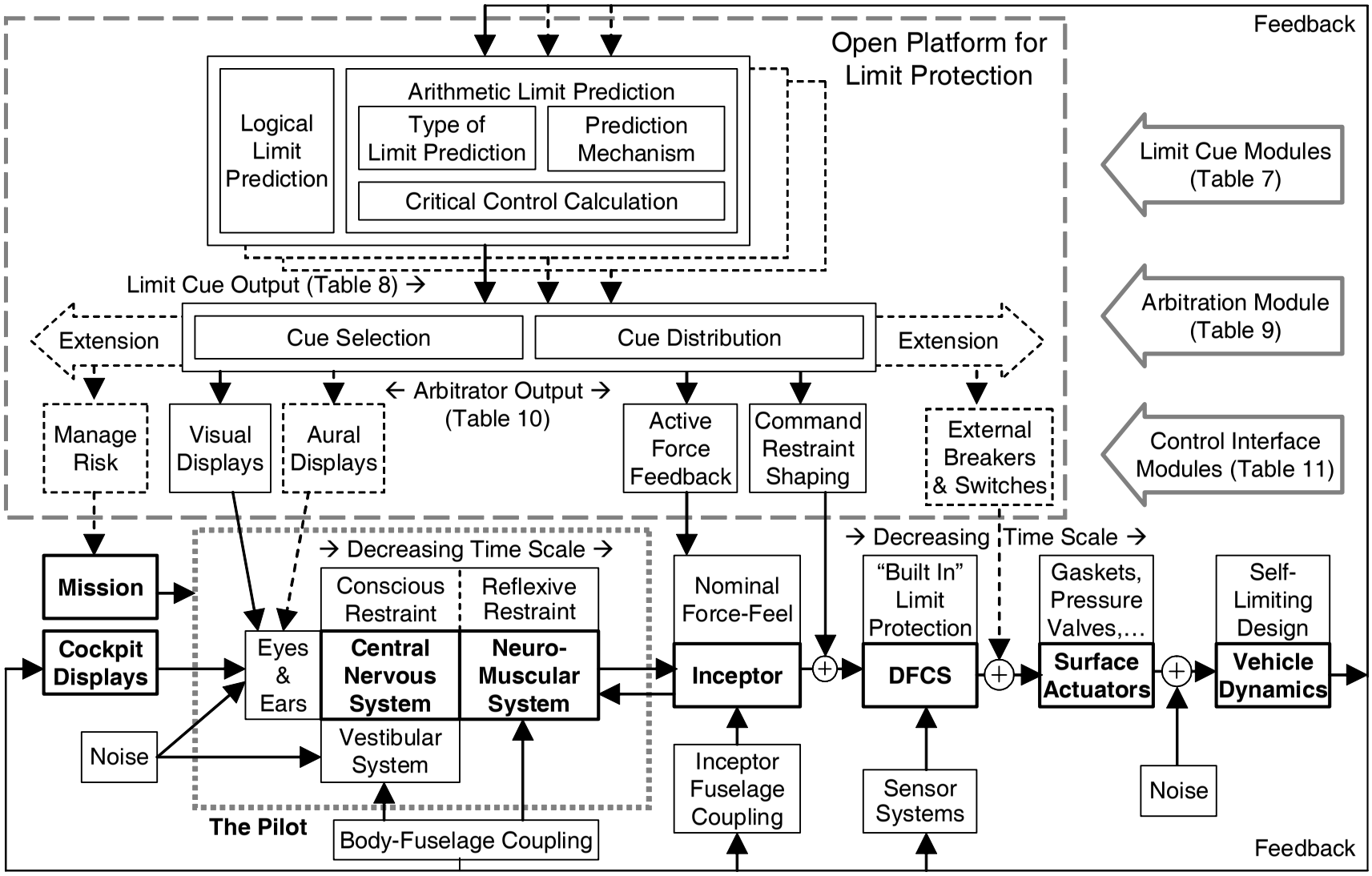

Figure 4: Open Platform for Limit Protection and Vehicle Control System

In a manned vehicle system, such as that depicted in the figure, the pilot uses a control strategy based on his or her understanding of the aircraft and the goals for the flight and the maneuver. The control strategy is communicated to the aircraft through the cockpit control levers, the inceptors. The inceptor creates the digital control signals for the digital flight control system (DFCS). The DFCS then commands the actuators and their control surfaces to affect the progress of the flight maneuver. The states of the aircraft feed back to affect the control commands all along the control path. The DFCS used the sensor information to rapidly update its commands in accordance with its aeronautical design standards. The dynamics of the moving aircraft affects the physical control subsystems, including the human pilot and the limb-inceptor system. The pilot senses the movement of the vehicle and adjusts his control commands to move the system toward his goals. Figure 4 depicts dominant elements of the closed vehicle control system, but the true system involves many more control signals and nested feedback signals.

Limit protection is often present in every sub-system along the control path, traditionally and still primarily in the deliberate control and conscious restraint that the pilot exercises during flight. The force-feel system of the inceptor has physical limitations of stiffness, damping, inertia, and nonlinear artifacts such as dead band, hysteresis and so on. Commonly in modern complex aircraft such as the V-22, the JSF, and the V-22 mentioned earlier, the Flight Control System (FCS) is designed with integral or "built-in" protection for significant foreseeable limits. Forward of the FCS, control surfaces and actuators; whether hydraulic or electrical; have limit protection mechanisms such as overpressure valves, blow-out gaskets, droop stops, and circuit breakers. The vehicle itself may also have limit protection integral to its aerodynamic design, such as a canard designed to stall before the main wing. These are the common methods of limit protection today: limit protection integral to each control subsystem or element of the control system.

The model for pilot sub-system, shown as the dotted grey line in the figure, is adapted from models proposed by Jex[67] and Hess[68] and chosen because it depicts the different manner in which visual, aural, tactile, and vestibular senses process information. Cockpit visual and aural displays are sensed by eyes and ears with neural direct neural interface to the brain. The vestibular sense of spatial orientation also uses a direct interface with the central nervous system. Depending on the complexity of the visual and aural signals, the brain requires time to process and interpret this information. The pilot can then exert intentional conscious control and restraint to keep the vehicle within its limits. Tactile cues through the cockpit controls and the pilot's hands and feet are interpreted by the

neuromuscular system as the information is passed to the central nervous system. With regard to tactile cues, the neuromuscular system can react reflexively and with pre-trained muscular control with little or no cognitive processing delay.

In Figure 4, the Open Platform for Limit Protection is boxed with the dashed line. Its development grew from a design for limit avoidance solely through voluntary (overrideable) tactile cues. But, as was found in the HELMEE research[11] and again during prototyping of the blade stall cue described in the next chapter, such cues worked best when combined with corroborating visual cues. Moreover, there were instances when the limit protection tactile cue was too rapid for the pilot to follow, felt jittery, and suggested the need for automatic or autonomous protection for faster, high frequency limit avoidance. Consequently, an open design for tactile cueing[69] was extended to encompass limit protection across the control command path. The solid signal lines in the figure represent the elements of the platform that have been prototyped and tested with this thesis. The blocks and signals indicated with dashed lines represent envisioned logical extensions to the approach that are yet unrealized.

Among the modules, information flows in one direction only, allowing a decoupled set of replaceable subsystems and an open platform that can be easily renewed and extended. There are three stages of functional modules: 1) the Limit Cue modules, 2) the Arbitration module, and 3) Control Interface modules. The first stage is the set of limit cue modules which combine the limit prediction and control cue calculation functions. These functions are distinct, and the designer may choose to decouple them, but in practice, their algorithms are tightly coupled and they form an integral module that provides both functions. An example of an essentially decoupled limit cue module is the HELMEE main rotor blade stall cue module described later in this paper (page 65). The limit cue may be separated into its static neural network based limit predictor and its inverse partial derivative critical control calculator. An example of a necessarily coupled limit cue module is the second blade stall cue (page 69). In that limit cue module, the adaptive dynamic trim algorithm is called iteratively by the critical control calculation algorithm to arrive at a solution for the dynamic trim control constraint.

Likewise, the second major module treats cue selection and distribution together as integral functions in one module. Depending on the algorithms involved, the two functions may be executed sequentially, in a decoupled fashion (this is the approach used for the applications in this work). However, an arbitrator realized through heuristic logic or fuzzy inference would combine the two functions in the same algorithm. The third module is

actually a class of modules that have the common function of influencing control commands, but do so in different ways using different signal interfaces.

The use of decoupled modules facilitates change and renewal. This platform adopts three stages of functional modules to realize this advantage, but does not mandate further decomposition of the limit cue, arbitration, and control interface modules. The design for these modules may be integrated or modular depending on the requirements and resources of the limit protection system designer. This subordinate module design choice is made after weighing the advantages of the flexibility and growth of a modular design against the high performance possible with a more integral design.

Table 5. Nature of the Protected Limit

Considerations	Possibilities	Limit Examples
Knowledge	Control the mean	Vortex Ring State
	Process Capability	Pilot Induced Oscillation
	Characterized Process	Engine Torque
Origin	Aerodynamic	Main Rotor Blade Stall
	Structural	Engine or Transmission torque
	Controllability	Pilot Induced Oscillation
	Regulatory	Assigned altitude block
	Physical	Terrain, Antennae
Time Scale (in human terms)	"Immediate" ($< 10^{-1}$ sec)	Engine Overspeed (Surges)
	"Reflexive" (10^{-1} to 10^{0} sec)	Vertical Load
	"Cognitive" ($> 10^{0}$ sec)	Acrobatic attitudes
Risk	Soft limit (fatigue wear, increased risk)	Maximum Engine Temperature Minimum Safe Altitude
	Hard limit (Catastrophic)	Max Flapping (Fuselage contact),

Nature of the Limit

When designing a limit protection algorithm, the maximum or minimum limit values may already be defined by the vehicle's design criteria and can then be considered as given rather than chosen. As the nature of the limit is understood, the appropriateness of the remaining design choices becomes clear for the design of the limit cue module and for the later arbitration and control system interface modules. Considerations of the limit are

shown in (Table 5) with examples from a continuum of possibilities. Elements of this table are described in more detail below.

Knowledge

When a new phenomenon (such as a vehicle limitation) is discovered, the operators, designers, and society at large progress through stages of technological knowledge about the phenomenon. It is a progression through ignorance, awareness, measurement, and ultimately, fine control. These stages of technological knowledge[70], shown in Table 6, guide the design choices for a limit cue module and its output, the limit cue itself.

For example, when technological knowledge reaches the pre-technological stage (stage 3) where at least some basic "rules of thumb" are known about when the limit margin improves and which control inceptors affect it positively or negatively, then these rules could be built into a basic logical limit cue. When the limit itself can be defined (i.e. the maximum or minimum value) and measured (stage 4), then at least an alert cue can be used. As more complete knowledge is gained, the dynamical nature of the limit is characterized. Then (after stage 5), the limit can be predicted and the critical control positions determined so that a constraint cue may be used.

Table 6. Stages of Knowledge applied to vehicle limits

Stage	Name	Character	Typical Forms and → Locations of Knowledge
1	Complete Ignorance		None → Nowhere
2	Awareness	Pure Art	Tacit → In each user's head
3	Measure	Pre-technological	Discussed and Written → In user community
4	Control the Mean	Scientific method is feasible	Written & embodied in hardware → Gross measure & control mechanisms
5	Process Capability	A solution found. Local "recipes"	Hardware and operating manuals → Institutional & proprietary designs
6	Process Characterization	Tradeoffs & Optimization	Empirical equations → Databases, Lookup-Tables, Journal papers
7	Know Why	Science	Formulae, analytical solutions, algorithms → Technical literature, textbooks, libraries.
8	Complete Knowledge	Nirvana	Absolute and comprehensive → Omnipresent

Source: Adapted from Bohn[70].

When new limits and phenomena are first recognized, their gross qualities are learned and aviators adapted their mission planning and maneuvering to accommodate them. After more rigorous research, engineers are able to design control systems for the new phenomenon. In the first case, limit protection requires human knowledge and involvement, perhaps through a cockpit visual or aural display. In the later case, the knowledge is captured in a limit protection system that can drive tactile cues or automatic protection. An advanced stage of knowledge is a prerequisite to greater understanding of the nature of the limit's origin, time scale, and risk.

Origin

But whether given or chosen, vehicle limits ultimately trace to one of a few characteristic origins. The laws of fluid mechanics impose aerodynamic limits. The natural laws of materials and physical environment impose structural limits. Controllability limits are imposed by human capabilities. Regulatory limits are imposed by society over the system. Obstacles such as trees or regions of dangerous icing impose physical limits. Structural limits commonly have numerical handles – they can be monitored through sensor measurements of stresses, strains, forces, and accelerations. In contrast, while some controllability measurements (limits) are defined numerically (ex. ADS-33[71] limits on pitch (roll) oscillations), others are qualitative or pseudo-quantitative, (ex. Cooper-Harper handling qualities levels). So while arithmetic limit cues have been commonly and effectively used for structural limits, a logical, heuristic based limit cue was developed within this OPLP for Pilot Induced Oscillation, a controllability limit. Interpreting physical obstacles as limits is a way of addressing obstacle avoidance as another form of limit avoidance.

Time Scale

The time scale (as described with regard to Table 2) of limit protection action also guides design choices with regard to where and how the limit should be protected. The limit protection designer should consider whether the limit is so volatile and fast that it would require practically instantaneous, autonomous limit protection, or whether it is slow enough for voluntary protection within normal pilot workload and useable cue environment, and so could be presented as a visual or tactile cue. Whenever possible, whether the limit can be influenced quickly or not, the volatility of the limit dynamics suggests how far limit parameter control may be addressed by the pilot (after due consideration of an informative visual or aural cue), or handled reflexively (guided by a tactile cue), or protected automatically (through command restraint shaping).

Taken together, the time scale and the origin of the limit reflect the controllability of the limit parameter at a given point along the control path, even within the control planning of a human pilot. A qualitative model[72] of human interactions with complex dynamical systems considers the human as a triune that includes a behavior generator, a sensory information processor, and a set of internal models. The human pilot maintains a set of internal models that narrow in scope from a world model that is too general to be actionable to a domain, a locale, a surround, and ultimately to an element that can be acted upon. In the context of limit protection, the pilot maintains a mental concept of the aircraft and its systems, including its limits and its inceptors. When the limit can be affected (controlled) directly though the inceptors, the pilot can maintain his internal element model and merely adjust his maneuver to follow tactile limit avoidance cues. If, however, the limit cannot be adequately protected within the context of the maneuver, more information about the limit and the situation must be presented to the pilot, visually and aurally, so that the pilot can use a higher level model (the surround or locale model) to plan a new maneuver and adopt a new actionable element model. Put another way, when the limits cannot be satisfied within the context of the present flight profile, the pilot needs more information and more time to develop an alternative course of action. The new course of action may an entirely new maneuver, a decision to override the limit, a decision to abort the flight, or any number of other options that are possible within the pilot's greater world model.

Risk

Finally, when considering the nature of the limit, the risk of limit violation guides some design choices. Depending upon how a structural limit is defined, it may be the ultimate load limit of a vehicle component or, more likely, a conservative value accounting for fatigue wear and the uncertainties of design and use. When the consequences of limit violation are severe or catastrophic (a so called "hard" limit), then the designer may choose to protect the limit autonomously, without allowing the pilot to override the protection. If the consequences are not catastrophic, but instead are fatigue wear and reduced component life, then more liberty may be afforded to voluntary and participatory limit cues for the pilot.

Limit Cue Module Design

Limit prediction and critical control calculation are two functions that, in practice, are so interdependent and tightly coupled that they need to be designed as an integral module. There may be many limit cue calculation modules in the OPLP using disparate

sources as inputs. For example, there may be a hub moment limit module that uses instrumentation signals from sensors attached directly to parts of the transmission, or there may be a vertical load limit module that monitors a common avionics data bus for the information it needs. The character of the input information is left open to allow flexibility for the limit prediction algorithm designers. As new aircraft are designed, its creators may foresee the need to protect particular limits and build the requisite sensor telemetry into the aircraft's Vehicle Management System (VMS) or Health and Usage Monitoring system (HUMS). In these cases, the limit prediction modules may share identical or common information interfaces with the VMS or HUMS. When the need for limit protection is identified for pre-existing aircraft, the limit prediction module may use pre-existing VMS/HUMS information if available, or may use instrumentation added to the aircraft in an ad hoc fashion and dedicated to the limit protection.

Table 7. Limit Cue Definition and Design Choices

Module	Aspect	Choices	Definitive Applications
(Arithmetic) Limit Cue Prediction	Type of Limit Prediction	Fixed Time Horizon	UH-60 Rotor Blade Stall[11]
		Dynamic Trim	XV-15 Angle of Attack[39]
		Worst Case	UH-60 Hub Moment[73,74]
		Probabilistic	Air Traffic Collision[47]
	Prediction Mechanism	Math Model	AH-64 Energy Mgt,[54]
		Static Neural Network	UH-60 Blade Stall[11]
		Adaptive Neural Network	UH-60 Blade Stall[75]
		Iterative Simulation	Air Traffic Collision[47]
	Critical Control Calculation	Inverse Gradient	UH-60 Blade Stall[11]
		Pseudo-Inverse	XV-15 Angle of Attack[39]
		Weighted Pseudo-Inverse	None
		Algorithmic Search	UH-60 Hub Moment[73,74]
	Type of Cue	Constraint	UH-60 Rotor Blade Stall[11]
		Alert	UH-60 Rotor Blade Stall[11]
		Transfer Function	Pilot Induced Oscillation [76]
		Friction	Pilot Induced Oscillation [76]
(Logical) Limit Cue Calculation	All the above listed options of arithmetic cues are available.		
	Prediction and Control	Crisp IF-THEN	None
		Fuzzy Inference	Pilot Induced Oscillation[76]

Note: Underlined references refer to limit cues first developed within this OPLP

The internal design of the limit cue module's limit prediction and critical control calculation algorithms presents design choices for limit prediction and avoidance algorithms (listed in Table 7). The design choices can be characterized by the ultimate limit they address, the type of prediction uses, the mechanism used in the limit modeling algorithm, and the method of calculating the corresponding critical control position. Limit prediction has relied on analytical methods, labeled here as "Arithmetic", whereby the vehicle limit is given a numerical handle. This handle may be a direct sensor measurement, such as airspeed or vertical load, or it may be found indirectly from related measured parameters. Some limits may have no implicit numerical handle but are given a number with a correlation function. Main rotor blade stall is an example where an empirical value, Equivalent Retreating Indicated Tip Speed (ERITS), provides a convenient correlated numerical value[11]. But besides arithmetically based cues, this thesis acknowledges "Logical" limit cues that are understood through known or suspected cause and effect relationships and rule-based heuristics. The limit protection control cues may also be heuristically determined. This approach brings emergency conditions and emergency procedures within the realm of limit protection.

Arithmetic Limit Cue Design

Arithmetic cues rely on a state space dynamical *aircraft model* to represent the system of aircraft states, inputs, and outputs.

$$\dot{x} = g(x,u) \qquad\qquad y = h(x,u) \qquad\qquad (1)\quad (2)$$

The *state*, x, is a defining set of aircraft motion characteristics and the *input*, u, is the set of physical displacements of the cockpit controls. With information about the states and the controls, and an accurate model of the dynamic interaction between them, the mathematical solution provides the future state of the aircraft. The limited parameter y, (or *limit vector* of several limit parameters), is an algebraic function of the present states and inputs. Often, a limit parameter is identical to the value of a state.

Depending on the context, the word *limit* may refer either to the name of the limited parameter (such as Vertical Load or Airspeed) or to a critical value of that parameter (such as 4 G's or 150 Knots). The *future limit margin* is defined as the difference between the limited parameter critical value and the value of that parameter at some future time.

$$\Delta y^{+}_{fut} = y_{lim} - y_{fut} \qquad \Delta y^{-}_{fut} = y_{fut} - y_{lim} \qquad (3)\ (4)$$

An *inceptor* is the physical lever that is the interface between the pilot and the vehicle's flight control system. It translates the control command from applied forces and displacements into an information medium that the Flight Control System can use. The *control margin* is defined as the difference between the present control command input and that critical value that would lead to a limit violation. The value and units of the control margin are based on the form of the control command. For example, with a cockpit inceptor, the *critical control position* is the location (in inches or degrees) where, if the pilot displaced the inceptor to that position, the aircraft would reach the critical limit value, *the limit*. A limit (i.e. the maximum or minimum allowable value) may be a function of the control configuration and flight condition, $y_{lim}(x,u)$, but could be a constant maximum or minimum allowable value. A *limit* has a corresponding *upper control margin* when there exists a *critical position* greater than the present control position. Likewise, a limit has a *lower control margin*, when there exists a corresponding *critical control position* less than the present control position. By convention, whether referring to maximum limits or minimum limits, limit margin and the control margin are both considered positive while the system is within the limit boundary.

$$\Delta u^{+} = u_{crit} - u_o \qquad \Delta u^{-} = u_o - u_{crit} \qquad (5)\ (6)$$

In the general case, the relationship between the *future limit margin* and the present *control margin* is non-causal, non-linear, and non-bijective. To establish a causal relationship and enable practical limit avoidance cueing, every limit prediction model makes a *future transition assumption* for each limit. With this assumption, the present aircraft state, x_o, and the control position, u_o, a limit prediction model provides a *predicted limit vector*, $y_p(x_o,u_o)$, or *predicted limit*, y_{ip} . The *predicted limit margin* is defined as the difference between the *predicted limit* and the critical limit value or *limit*.

$$\Delta y_p = y_{lim} - y_p \qquad (7)$$

In a limit avoidance cue, the system approximates a mapping between the *predicted limit margin* and the *present control margin*. This mapping of a predicted limit to the critical control position is the essence of effective limit avoidance tactile cueing (Figure 5).

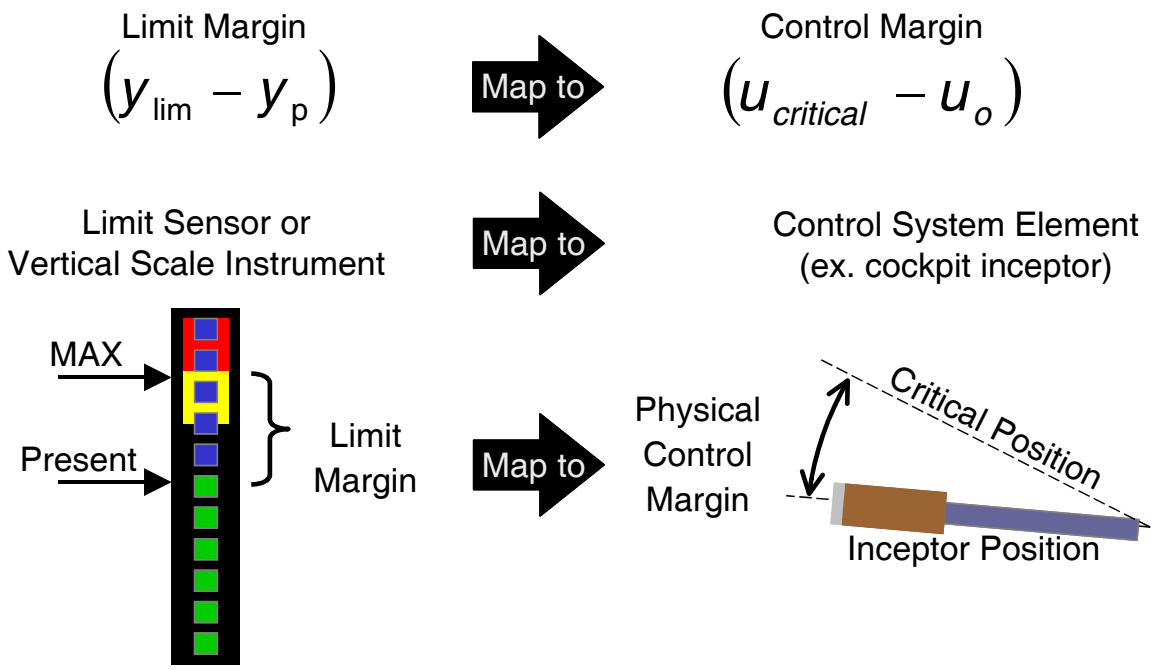

Figure 5. The Key to Effective Tactile Constraint Cueing

Limit Prediction Type

The defining differences among the types of limit predictions are the assumptions about the transition from the present to the future. The fixed time horizon prediction calculates the value of the limit parameter at a fixed distance in the future. In this case, the future transition assumption is an assumed future time history for the controls. The dynamic trim prediction, calculates the limit parameter value for the aircraft dynamical system in a quasi-steady equilibrium. The future transition assumption in this case, is an assumed transition for the states.

Fixed Time Horizon (FTH)

This type of prediction assumes that the controls will follow some defined path to a chosen point in the future. The fixed time horizon prediction may assume the controls follow the worst-case path. More commonly, the controls are assumed to follow a path similar to the path followed by the pilot during actual or simulated test flights that provide time history data. The fixed time horizon method maps the relationship between the vector of states and controls at each time, t_o, to the limit value at time, $t_o + \Delta t$. This mapping can be captured in any number of ways, most effectively in neural networks as described below. The advantage of this method is that the time scale for the prediction is known and, depending on the nature of the limit, can be reasonably accurate to a few

tenths of a second or more into the future. For example, the limit predictions of the HELMEE study used time horizons (Δt) of 0.25 to 0.46 seconds[77].

$$\begin{array}{ccccccc} \begin{bmatrix}\mathbf{x}(t_o)\\ \mathbf{u}(t_o)\end{bmatrix} & \cdots & \begin{bmatrix}\mathbf{x}(t_o+\Delta t)\\ \mathbf{u}(t_o+\Delta t)\end{bmatrix} & \cdots & & & \\ \mathbf{h}\downarrow \quad \searrow \mathbf{f} & & \mathbf{h}\downarrow \quad \searrow \mathbf{f} & & \cdots & & \\ \mathbf{y}(t_o) & \cdots & \mathbf{y}(t_o+\Delta t) & \cdots & \mathbf{y}(t_o+2\Delta t) & \cdots & \mathbf{y}_{pFTH}=\mathbf{f}(\mathbf{x},\mathbf{u}) \end{array} \tag{8}$$

These prediction times are far enough to give the pilot time to react, but not so far that the prediction loses accuracy. More distant time horizons loose accuracy due to pilot self-determination. That is, the pilot is likely to choose a future control path unlike control path of the aggregate training data for the prediction model.

Dynamic Trim (DT)

The dynamic trim prediction[78,79] separates the n aircraft states into k "slow" states that vary slowly with time, and (n-k) "fast" states that vary quickly and reach a steady value during a maneuver.

$$\mathbf{x}=\begin{bmatrix}\mathbf{x}_{slow}\\ \mathbf{x}_{fast}\end{bmatrix}\in R^n \qquad \mathbf{x}_{slow}\in R^k \qquad \mathbf{x}_{fast}\in R^{n-k} \tag{9}$$

The future transition assumption is that the controls and the predicted slow states do not change while the fast states have changed and settled to a constant. The predicted limit follows from the solution to the dynamical system (1) and (2) in the form:

$$\begin{bmatrix}\dot{\mathbf{x}}_{slow}\\ 0\end{bmatrix}=\mathbf{g}(\mathbf{x},\mathbf{u}) \ , \quad \mathbf{y}_{pDT}=\mathbf{h}(\mathbf{x},\mathbf{u}) \tag{10) (11}$$

The manner in which the fast states transition to steady and the time this takes is neglected. Consequently, the prediction time is not defined. In practice, the dynamic trim solution can be difficult to find for complex dynamical models, but an adaptive technique[80] can approximate the dynamic trim prediction model from time history *a posteriori*.

The dynamic trim prediction is well suited for limit variables that reach their maximum or minimum values in quasi-steady state. It gives good predictions for the worse case limit values possible during a maneuver, especially a quasi-steady maneuver such as a banked

turn or pull-up. While the minimum prediction time horizon is undefined, this characteristic is generally evident from inspection of the time history of the prediction and the actual limit value. This prediction time would vary with the flight condition and type of maneuver.

Worst Case

A peak response prediction, which may also be considered a worst case prediction, is a systematic search of all potential limit parameter responses across a proximate subset of states and controls. The extent of the proximate subset used for the worst case search is a key design choice for this type of prediction. This type of prediction is deliberatively conservative, yet may be appropriate for critical limits whose violations lead to catastrophic results.

Probabilistic

Whereas the fixed time horizon and dynamic trim predictions can be considered "single path" predictions and the peak response estimation can be called an "all path" prediction, the probabilistic type of limit model explicitly addresses uncertainties in guidance, structure, pilot, and other variables in the limit prediction model. Probabilistic approaches have been proposed for visual and aural collision avoidance cues[81,82,47].

Prediction Mechanism

Math Model

This prediction method uses a model for predicted limit, y_p, derived from *a priori* understanding of the aircraft dynamics.

$$\mathbf{y}_p = f(\mathbf{x},\mathbf{u}) \tag{12}$$

This method solves the state equation (1) based on the future transition assumption. For the dynamic trim prediction, the assumption defines values for the fast states and assumes the controls are held at the current position during the maneuver. For the fixed time horizon prediction, the assumption defines the control future time history. The one special form of the math model that requires no future transition assumption is the zero time horizon prediction, which is not a prediction at all. In that case, the present limit is used as the prediction, y_p=y. The math model produces a virtual table of limit predictions for given states and control values. This can take the form of an actual look-up table for use with multiple argument interpolation as a preliminary step to create neural network training data.

Static Neural Networks

An artificial neural network is a mathematical construct, such as a polynomial or a combination of vector functions called basis functions (such as the sigmoid, tan-sigmoid, and radial basis functions). Based on error back-propagation, this construct has parameters that self-adjust to provide a target output. Neural networks capture the *a posteriori* relationship between the controls and the predicted limits based on representative pattern and target data. Math model solution sets can provide this data directly or the time history data from flights and simulations can provide it. Static network training is completed with all the data available.

$$y_p(t) = f_{NN}(\mathbf{x}(t), \mathbf{u}(t)) \tag{13}$$

Type	Training Patterns		Training Targets
Dynamic Trim	$x_{slow}(t)$, $u(t)$	→ $f_{NN}(x,u)$ ←	$y_{DT}(t)$
Fixed Time Horizon	$x(t)$, $u(t)$	→ $f_{NN}(x,u)$ ←	$y(t+\Delta t)$

Prediction error is a common practical difficulty with math model and static neural network predictions because aircraft parameters and flight conditions change, as when the center of gravity shifts or pilot control characteristics change. The HELMEE and HACT projects correct prediction errors using complementary filters that effectively eliminate steady state prediction errors. But while this technique performs an essential function, the filters cloud the output from the prediction model.

Adaptive Neural Networks

Adaptive neural networks offer an alternative method to correct real time prediction errors and, unlike filters, they improve the prediction function to capture local or transient variations in the dynamical relationship of states, limits, and controls[43]. Unlike a static network, an adaptive network adjusts the neural network weights incrementally, as additional pattern and target pairs are presented. In other words, the adaptive neural network uses time history data in real time to reduce the prediction error and improve the prediction model. In order to use an adaptive network to approximate the predicted limit, it must have a measured or inferred value for the limit parameter to use as its real time target.

Iterative Simulation

When the limit protection system has a dynamical model of the limit parameter and adequately fast processing capability, it can use iterative simulations. The method is

needed for worst-case limit predictions and Monte Carlo simulations for probabilistic predictions. This iterative method has been demonstrated for aircraft conflicts (collisions) to generate alert cues[82]. The iterative probabilistic approach also has the potential to define constraint cues (for tactile softstops) to guide the pilot along a "best" or "safest" path.

Critical Control Calculation

When the limit parameter is adequately understood, the limit cue module can establish a relationship between a limit and the controls and a constraint can be calculated in the control domain. Local sensitivity methods depend on the limit gradient or the limit vector Jacobian, also called the limit sensitivity matrix. This method approximates a linear limit-to-control relationship using the tangent to the limit surface defined by the math model, $y_p=f(x,u)$, or neural network $y_p=f_{NN}(x,u)$. If the limit prediction mechanism (math model or neural network) is sufficiently well understood, the predicted limit Jacobian may be derived analytically. If not, the local limit sensitivity may be found through perturbation methods, iterating on its limit prediction system as a subsystem or subroutine. For the non-predictive limit models, $y_p=y$, the critical control position equals the current control position, $u_{crit}=u_o$

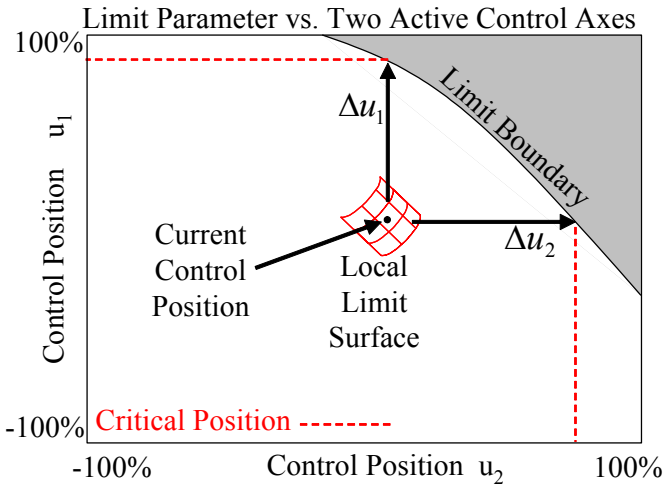

Figure 6. Critical Position from Limit Partial Derivative

These methods have the advantage of computational speed. The disadvantages are those inherent in the linearization. The limit surface may be highly nonlinear and local

sensitivity values may vary considerably with small changes in the state or control. Also, it is not uncommon for the current control position on the limit surface to lie at a local minimum or maximum where the same limit is reached whether a control is moved one direction or the opposite. Linearization will fail to predict accurate critical control positions for these conditions.

Inverse Partial Derivative

This simple method finds the control margin by dividing the limit margin by the limit sensitivity for each control axis (Figure 6).

$$\Delta u_j = \left(\frac{\partial f_i}{\partial u_j} \right)^{-1} \left(y_{\lim_i} - y_{p_i} \right) \tag{14}$$

This limit sensitivity method estimates the critical position for each active axis independently. The HELMEE study used this method effectively to cue each limit along a distinct active control axis. But in that study, the sensitivity was set at a constant value that was appropriate and approximately correct for the flight profile of the evaluation.

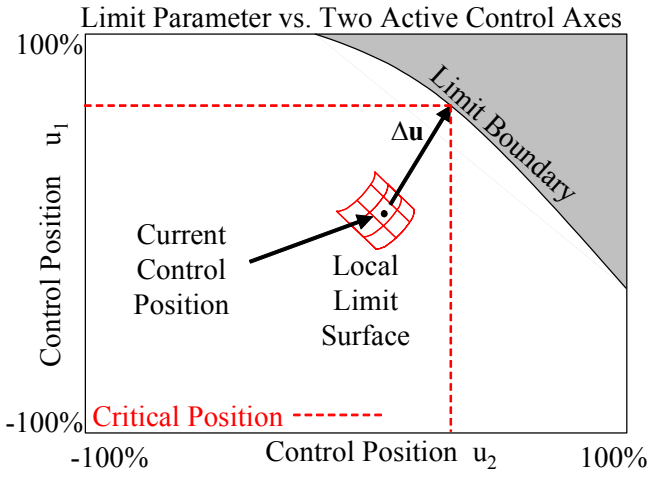

Figure 7. Pseudo-Inverse of Limit Gradient .

Pseudo-Inverse of Limit Gradient

An alternative method[39] treats the controls together as a vector and uses the Jacobian's pseudo-inverse to find the control margin vector to the "nearest" control

combination that zeros the limit margin. This nearest distance is the least-squared distance of each axis control margin. This method weights each of the controls equally.

$$\Delta \mathbf{u} = \left(\frac{\partial f_i}{\partial \mathbf{u}} \right)^{+} \left(y_{\lim_i} - y_{p_i} \right) \tag{15}$$

The critical control position for each axis follows directly from the control margin vector decomposition. This method works fairly well when one limit is moderately influenced by two or more active control axes.

Weighted-Inverse of Limit Gradient

A variation of the previous method multiplies the pseudo-inverse by a weight matrix. This weight vector may be a function of the states to emphasize or de-emphasize control axes at different flight conditions

$$\Delta \mathbf{u} = \mathbf{W}(\mathbf{x}) \left(\frac{\partial f_i}{\partial \mathbf{u}} \right)^{+} \left(y_{\lim_i} - y_{p_i} \right) \qquad \mathbf{x} \in R^n,\ \mathbf{u} \in R^k,\ \ \mathbf{W} : R^n \rightarrow R^{k \times k} \tag{16}$$

Algorithmic Limit Search

This approach emerged in two variations: as a first order vertical load limit cue and as a transient peak limit for hub moment. This approach uses an algorithmic surface search algorithm to find the critical control position. This method begins a search at the current state, x_o, and samples the prediction models, $y_p(\mathbf{x_o},u)$, at increasing and decreasing positions for each of the active control axes in turn. Throughout the search, the present (instantaneous) state vector is used. When the resulting prediction for a limit parameter first moves into a set of prohibited values, the control position at that point becomes the critical control position. A prohibited value for the limit parameter is one beyond the maximum or minimum allowable or an internal subset of values. The algorithm finds any critical control positions above or below the current positions of each of the axes.

This method does not necessarily assume a positive or negative relationship between the control and the limit. It does allow the possibility that the non-linear inverse may not be one-to-one. It has these advantages over the local sensitivity methods described earlier. Its chief drawback is its computational demand. Without a capable active control system computer, the designers may need to simplify the complexity of the neural network used for the limit prediction or reduce the resolution of the limit surface search. The latter option

is usually best since the prediction is itself only an approximation and there is no need to search to high precision a limit surface of lower precision.

The Mesh Surface (Figure 8) represents a predicted limit (vertical loading, N_z) with respect to collective and longitudinal control axes. The algorithm treats it as one with a first order response, or at least one where other time values (transient peaks) of the limit parameter are not considered. At the depicted instant in time, during a pull up maneuver, when the control and limit coordinate is positioned at (u_{coll}, u_{long} ,y), the search algorithm begins at the predicted limit for the current control position (u_{coll}, u_{long} ,y_p). The algorithm varies each control position in the prediction function away from the start position, along the admissible control positions shown as black lines. When the prediction exceeds the limit (in this example y_{lim+}= $N_{z(max)}$=1.5), that control position is defined as the critical control positions for each axes for that instant. Those upper critical control positions are indicated in red and blue lines. Note in this example that the predicted limit decreases at very high collective positions. Had the limit been set a little higher (i.e. $N_{z(max)}$=1.6), the algorithm would not find a critical position for collective because no position along the collective search path exceeds the limit.

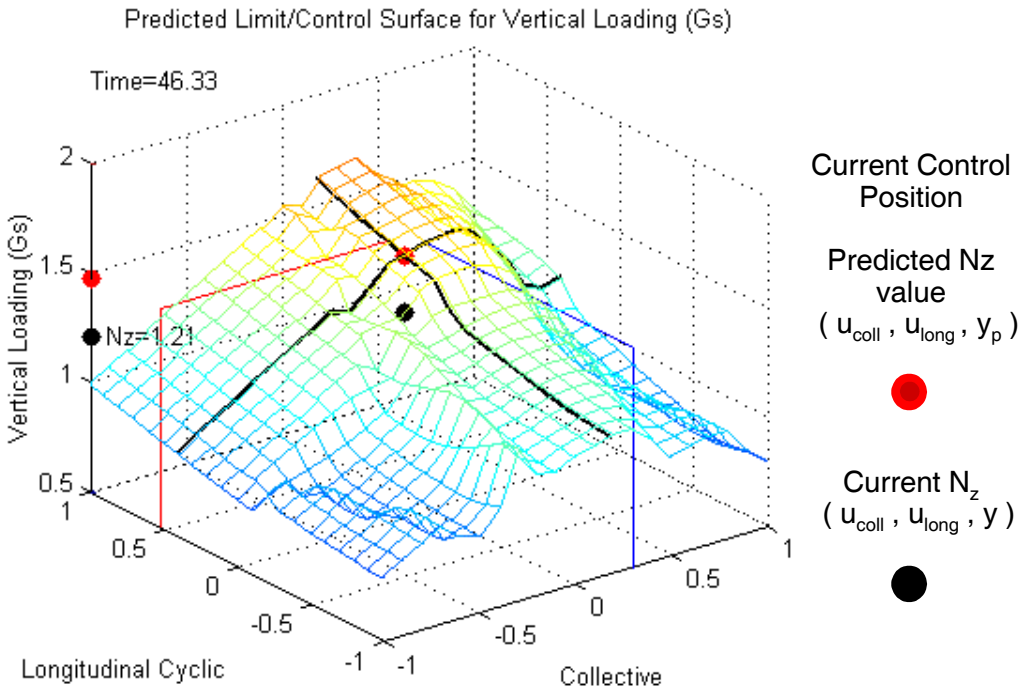

Figure 8. Algorithmic Limit Search (1st Order, 2D).

Figure 9 depicts another sort of algorithmic search where the transient peak is a chief concern. In this case, the limit model provides a prediction of the time response of the limit parameter as a function of a control input, such as a step change in longitudinal cyclic. The search algorithm then finds the maximum peak of the parameter response for a set of control inputs and then defines the critical control position as the input that first results in a transient limit. A method such as this was used to predict hub moment transient limits.

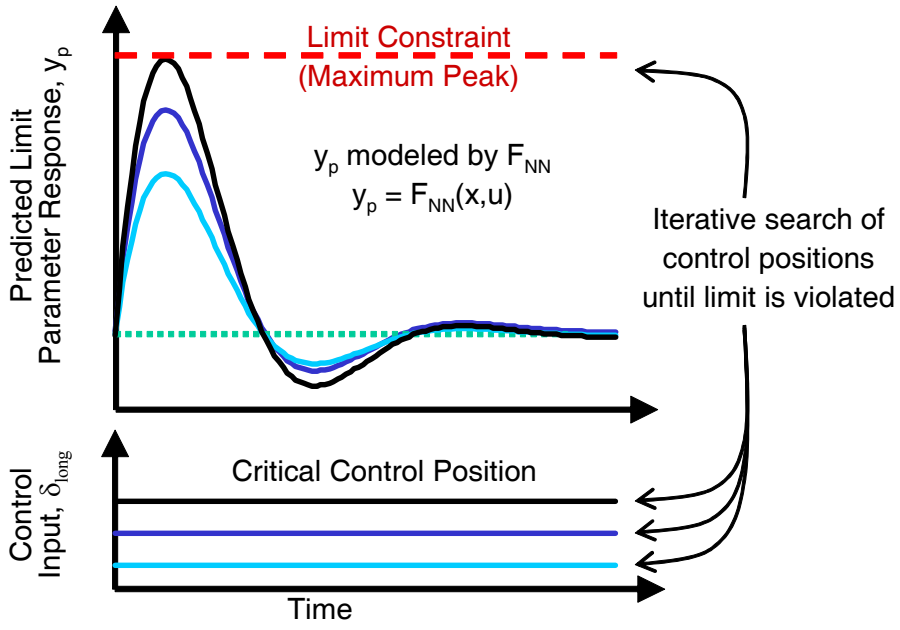

Figure 9. Algorithmic Limit Search (2nd Order, 1D).

Logical Limit Cue Design

Logical limit cues rely on rule based decisions. Generally these take the form of logical syllogisms, either the "crisp" logic or "fuzzy" logic. They are effective in detecting both limits and emergency conditions. Logical limit detection can also provide limit cues when the nature of the limit is not yet well understood and the stage of technological knowledge is inadequate to calculate a control constraint.

Crisp IF-THEN logic

The basic Aristotelian syllogism draws a conclusion from two premises. In the context of logical limit prediction or detection, the first premise defines the limit in terms of some function of aircraft states. The second condition reports a related condition during flight. The conclusion determines whether the vehicle is within limits or not, and can trigger limit

cue for the pilot or an autonomous limit protection mode. This is the very common approach for visual cockpit indicators of aircraft system status. Such limit syllogisms are hard wired sensor switches that open or close the illumination circuits for cockpit warning indicator panels. Caution, warning, and advisory panel lights for helicopters are commonly provided for engine chip detection, main rotor overspeed, main rotor underspeed, low fuel, main transmission oil pressure, fuel pressure, and so on. An example for an oil pressure indicator lamp takes the form:

If sensed oil pressure is greater than 120 psi

Then close "High Oil Pressure" warning lamp circuit.

Sensed oil pressure is greater than 120 psi.

Therefore close "High Oil Pressure" warning lamp circuit.

Such limit protection cues rely on the pilot to make the appropriate limit protection action or to execute a pre-trained emergency procedure. Alternatively, this type of limit detection logic can trigger task tailored flight control laws to accommodate limit proximity or emergency conditions.

Fuzzy Inference

In contrast to crisp logic, fuzzy logic allows possibilities and degrees of limit violation or emergency condition fulfillment. The aircraft states, controls, and limits become fuzzy variables for a fuzzy inference system. For example, airspeed as a fuzzy variable is not operated on as a numerical value of 60 knots. Instead it is described by membership function such as "cruise speed", "hover", or "below ETL". Likewise, an output, such as collective position, can have fuzzy membership functions such as "forward", "centered", or "aft". Each membership function is a unimodal possibility distribution across a universe of discourse, analogous to a function domain.

A fuzzy inference system follows five steps. First, it fuzzifies the input, converting it from a numerical value into a membership function. Second, it applies the fuzzy operators analogous to the logical AND, OR, and NOT. Third, it applies an implication method. This is a rule described as an IF – THEN relationship. Fourth, the results for all the rules are considered simultaneously and aggregated. Finally, aggregate result is defuzzified to number. The rules are defined from *expert* knowledge such as pilot experience, aircraft technical manuals and handbooks, and aviation textbooks. For example, the rules for an emergency procedure cue are a pilot's answers to: "What are the indications that make

you realize and identify an emergency condition?" and "What do you do to remedy the emergency?" These become fuzzy IF-THEN relationships that infer the logical cue.

As an example, consider settling with power as flight region beyond controllability limits. If the vortex ring state could be well defined as a numerical limit, an arithmetically based limit avoidance cueing system would apply. The HACT Program takes this approach to provide a power settling avoidance cue on the collective control axis[55]. However, when the condition is not explicitly defined but is generally understood, an expert model assesses the possibility of the condition and sets tactile avoidance cues and non-tactile cues. This vortex ring avoidance cue treats the condition not as an arithmetic cue as does the HACT program, but as a logic based cue. While not usually addressed in helicopter operator's manuals, flight schools include settling with power as an important topic of instruction. School manuals[83] describe the conditions conducive to settling with power as: a vertical or nearly vertical descent of at least 300 feet per minute, low forward airspeed, and normal-high engine power (from 20 to 100 percent). From this knowledge, an abridged fuzzy inference system takes a form depicted in Figure 10.

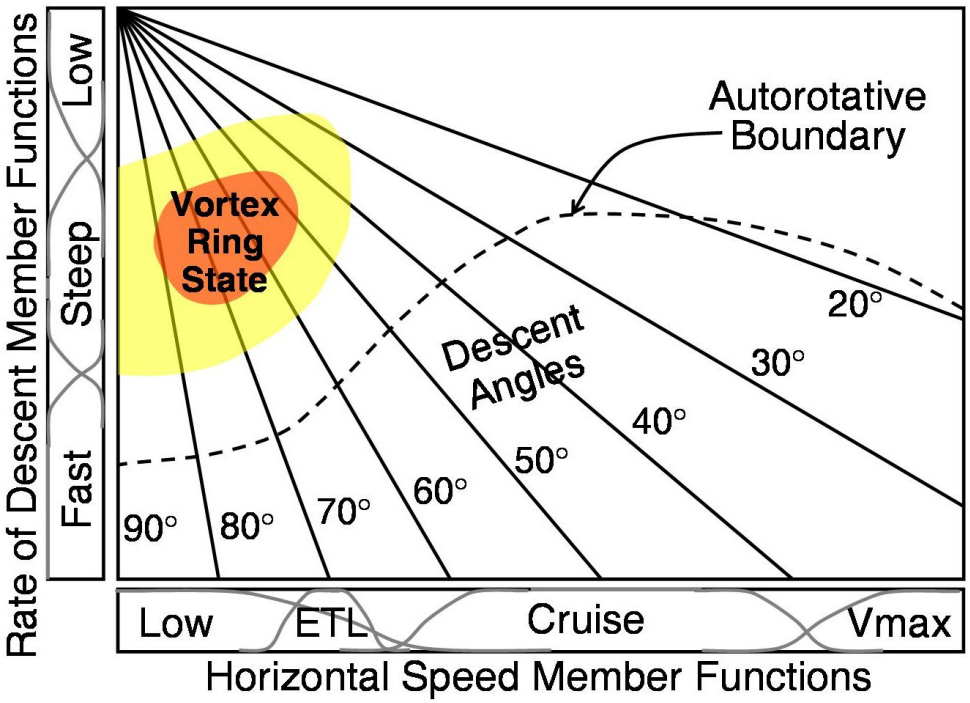

Figure 10. Depiction of Fuzzy Inference Vortex Ring State Estimator

Limit Cue Module Outputs

While the inputs to this entry echelon of limit modules for the OPLP may vary, the character of their output should be standardized to facilitate the practical application of a limit protection system. So, while the interface protocol will change, the carefree maneuver applications described later in this paper adopted the interface standardized to shown in Table 8. The limit cue modules communicate constraint, urgency, dynamics, and non-linear qualities and take the form of column vectors. The values within these vectors are non-dimensional and normalized to span -1.0 to 1.0. For example, a cyclic inceptor with a 0 to 10 inch range of positions has a 5-inch radius centered at 5 inches. Forces are similarly normalized by a base force equal to that required for full inceptor deflection. These normalized values become dimensional displacements or forces at the tactile interface module if the limit protection ultimately takes the form of a tactile cue.

Table 8. Limit Cue Module Output

Theory		As Implemented and Tested		
Intent	**Structure**	**Data Types**	**Units**	**Example**
Constraint	$\begin{bmatrix} N_{lim} \\ u_{cue} \\ \Delta h_{cue} \\ \Delta \ell_{cue} \\ y \\ y_{lim} \\ \lambda_{\Delta y} \end{bmatrix}$	$\begin{bmatrix} \text{Integer} \\ \text{Float} \\ \text{Float} \\ \text{Float} \\ \text{Float} \\ \text{Float} \\ \text{Float} \end{bmatrix}$	$\begin{bmatrix} \text{ND} \\ \text{NND} \\ \text{NND} \\ \text{NND} \\ \text{Varies} \\ \text{Varies} \\ \text{Varies} \end{bmatrix}$	$\begin{bmatrix} 3 \\ .24 \\ 1.0 \\ 0.04 \\ 400 \\ 300 \\ 100 \end{bmatrix}$
Alert	$\begin{bmatrix} N_{lim} \\ A_{cue} \\ \omega_{cue} \end{bmatrix}$	$\begin{bmatrix} \text{Integer} \\ \text{Float} \\ \text{Float} \end{bmatrix}$	$\begin{bmatrix} \text{Integer} \\ \text{NND} \\ \text{rad/sec} \end{bmatrix}$	$\begin{bmatrix} 1 \\ 2.0 \\ 108.0 \end{bmatrix}$
Transfer Function	$\begin{bmatrix} N_{lim} \\ \omega \\ \zeta \\ K_0 \\ K_2 \\ \mu \end{bmatrix}$	$\begin{bmatrix} \text{Integer} \\ \text{float} \\ \text{float} \\ \text{float} \\ \text{float} \\ \text{float} \end{bmatrix}$	$\begin{bmatrix} \text{ND} \\ \text{rad/sec} \\ \text{ND} \\ \text{ND} \\ \text{ND} \\ \text{NND} \end{bmatrix}$	$\begin{bmatrix} 0 \\ 18.85 \\ 0.7 \\ 1.0 \\ 1.0 \\ 0 \end{bmatrix}$
Friction	$\begin{bmatrix} N_{lim} \\ \mu_d \\ \mu_s \end{bmatrix}$	$\begin{bmatrix} \text{Integer} \\ \text{Float} \\ \text{Float} \end{bmatrix}$	$\begin{bmatrix} \text{ND} \\ \text{NND} \\ \text{NND} \end{bmatrix}$	$\begin{bmatrix} 4 \\ 0.2 \\ 0.2 \end{bmatrix}$

The output of the limit cue modules provides essential information for limit protection and additional non-essential but useful information regarding the limit and the preferred limit protection mechanisms. The identifier is an example. It provides a handle for the limited parameter that the OPLP can communicate to the vehicle operator. The Arbitrator module accepts these limit cue vectors as inputs may adopt the preference information or may supersede preferences depending on its design. The order of the elements starts with an identifier, continues with information about the cue, then information about the limit, and ends with an indicator for the module designer's preferred control system interface (i.e. visual, tactile, and so on).

Constraints

Equality and Inequality constraints are communicated as a seven-element column vector. The first element (n_{lim}) identifies the system limit being protected. The second, third, and fourth elements, (u_{cue}, Δh_{cue}, $\Delta \ell_{cue}$), provide the control constraint position as the limit protection cue, its height, and its length. The sign of the cue height defines whether it is an upper constraint (positive height) or a lower constraint (negative height). When the constraint manifests as a tactile softstop, the height value corresponds to the start of the softstop force increase at the constraint position. The length allows the cue designer to adjust the abruptness of the constraint. A length of zero creates a step force soft stop while longer length creates a more gradual cue. The fifth, sixth, and seventh elements, (y, y_{lim}, λ_{lim}), provide the value of the limited parameter, its limit, and a Lagrange multiplier. The Lagrange multiplier will be positive while the parameter is within limits, zero while $y_p = y_{lim}$, and negative while the limit is violated.

$$y_{lim} \text{ is a minimum} \Leftrightarrow (y_p > y_{lim} \text{ AND } \lambda > 0) \text{ OR } (y_p < y_{lim} \text{ AND } \lambda < 0) \quad (17)$$

$$y_{lim} \text{ is a maximum} \Leftrightarrow (y_p > y_{lim} \text{ AND } \lambda < 0) \text{ OR } (y_p < y_{lim} \text{ AND } \lambda > 0) \quad (18)$$

The purpose of the Lagrange multiplier element is two-fold. Its basic purpose is to indicate whether the limit is a maximum or minimum and this is done through its sign. But the second purpose of this seventh element is to facilitate future forms of limit protection algorithms that incorporate optimal control theory to determine the "best" path to a limit constraint. As an example, consider an altitude limit, which may a regulatory (airspace) limit or by physical obstacles at ground level. Altitude is typically not affected directly by

the cockpit controls. Rather, the cockpit controls affect rate of climb or descent or acceleration upwards or downwards. An optimally set constraint for an altitude limit could guide the aircraft to arrive at the limit boundary at a tangent with minimized overshoot and time-to-limit without violating other related limits such as maximum vertical load or angle of attack. For this type of limit cue algorithm, the Lagrange multiplier provides performance cost information to the arbitration cue. The units of the Lagrange multiplier and the optimal cost function should be common among the modules in the limit protection system and would be defined by the aircraft's mission. The units may be in probability of catastrophic failure, in hours of fatigue lifespan, or in dollars (in which case would describe a literal cost function).

The Cue Position is the only essential element of the constraint vector, but the additional elements provide for richer limit protection. This constraint information allows the limit cue designer to request specific qualities for a potential softstop cue. The limited parameter value and its limit may be presented as a cockpit display. Although a true Lagrange multiplier facilitates optimal control algorithms in the arbitration module, the sign of the multiplier, along with the parameter and limit values, serves as a flag to communicate whether this constraint refers to a maximum or minimum.

Alerts

When the intent of the module designer is to attract attention to a limit or situation, an alert vector of four elements is used. The first element identifies the limit. The second and third elements provide frequency and amplitude of the alert signal. The fourth element communicates a preferred control interface. If the alert ultimately manifests as a tactile cue, the frequency and amplitude define a shaker cue. If the cue is visual, the frequency and amplitude define color and brightness. If the cue is aural, the frequency and amplitude define the sound pitch and loudness.

Transfer Function

The transfer function allows the limit protection designer to introduce a transfer function in the control path. In general, a transfer function can take many forms, including cubic and higher order terms. A relatively simple transfer function with zero order and second order terms in the control path has the form:

$$T(s) = \mu K_0 + \frac{(1-\mu) K_2 \omega^2}{\left(s^2 + 2\zeta\omega s + \omega^2\right)} \qquad (19)$$

This form can model the spring and damper dynamics of a cockpit inceptor and may be applied elsewhere along the control path. When applied to the post inceptor command signal, the transfer function would add a second order delay. When applied to the inceptor, it defines the force-feel dynamics and whether it uses a position command or force command. The zero order coefficient, K_0, becomes the force-to-command scaling coefficient, K_{Fu}, and the second order coefficient, K_2, becomes the position-to-command scaling factor, $K_{\delta u}$.

$$T(s) = \mu K_{Fu} + \frac{(1-\mu) K_{\delta u} \omega_F^{\,2}}{\left(s^2 + 2\zeta_F \omega_F s + \omega_F^{\,2}\right)} \qquad (20)$$

As a force-feel dynamical response, the natural frequency, ω_F , and damping, ζ_F , define the time response. The force or position command switching value, $\mu \in [\,0\ 1\,]$, allows a mix of zero order and second order response. Parameters, $K_{\delta u}$ and K_{Fu} , amplify or diminish the normalized signal. In the case of a force feel transfer function, the output is normalized by the force gradient, k_f.

A limit protection designer might choose to manifest a transfer function cue as a visual or aural display for synthetic vision or virtual cockpit systems. As a visual cue, the transfer function might define a recursive frame algorithm that leads or trails the current display frame. To the pilot or viewer, such a manifestation would make motion appear shadowy or blurry. The blur could be used to visually communicate the transmission time lag for a remotely piloted vehicle and encourage the remote pilot to expect a sluggish response and encourage a slow, steady maneuver strategy that reduces the visual blur. As an aural cue, the transfer function may define an echo or reverberation.

Friction

A motion discontinuity cue is included in Table 8. Like the transfer function, this may have little relevance for relation to visual or aural cues, but it can define frictional cues in an inceptor and hysteresis in the post-inceptor signal.

While the transfer function and discontinuity cues are available, the limit protection designer must use caution with these elements, whose functions are more properly addressed within the flight control system. These two elements may introduce intentional nonlinearities and effective time delays to the overall control system, to the detriment of the vehicle's overall controllability and handling qualities.

Arbitration Module Design

The Arbitration module performs two major functions (Figure 11): it selects among simultaneous limit cues for each control axis and it distributes limit protection to appropriate points across the control signal path. These functions are distinct and may be executed sequentially in either order or simultaneously.

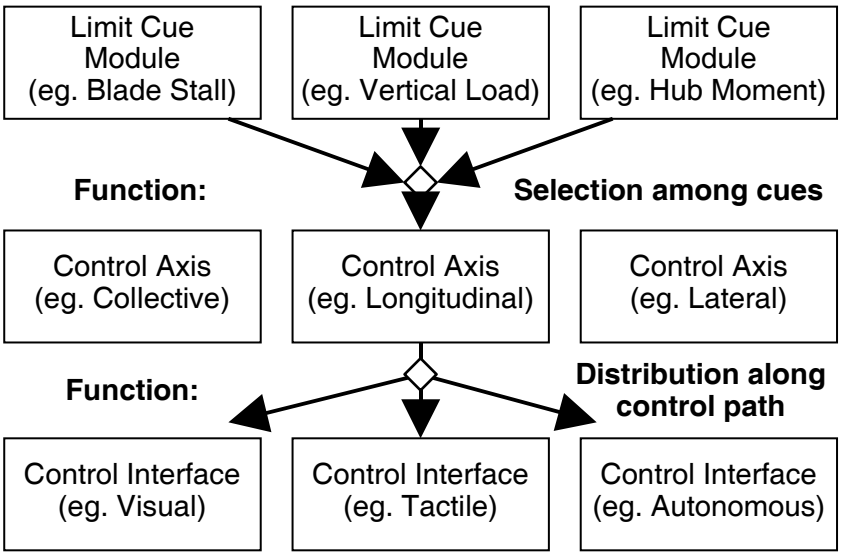

Figure 11. Major Functions of the Arbitration Module

Table 9. Arbitration Definition and Design Choices

Module	**Function**	**Choices** or **Considerations**	**Applications**
Arbitration	Limit Cue Selection	One-to-One	HELMEE[11]
		Most Conservative	HACT[53]
		Intelligent Selection	Not yet demonstrated
	Control System Distribution	Fixed	Common
		Frequency Distribution	Not yet demonstrated
		Deadband Shaping	

Limit Cue Selection

One-to-One

With multiple limit constraints for each control axis, a limit cue selector is needed to select which will serve as the constraint and which will serve as the alert cue for each of the active control axes. The module defines the cue position, u_{cue}, which the tactile interface module will use and any control shaping based on the control margin, Δu. For simple limit protection systems with only a few limits, the limit to control axis may be a bijective mapping. This was the approach used for the HELMEE[11] project, which mapped engine torque directly to collective and main rotor blade stall directly to longitudinal cyclic. In this case there was no possibility of conflict between the cues.

Most Conservative of Several Limit Cues

For systems with multiple control axes - each with multiple limit cues - the most conservative cue for each control axis may be used. For example, consider a moment of forward flight when the longitudinal cyclic position is forward at -5%. The Critical Control Positions for two limits are 30% aft for vertical load limit and 45% aft for the main rotor blade stall limit. The most conservative method chooses 30% aft as the combined critical control position.

Intelligent Selection

But it is not always appropriate to cue every control for the most conservative limit. At times the cues may conflict with one another as when one limit is exceeded because a control axis is too far left while another limit is exceeded because the same control is too far right. In such cases, the arbitrator may need a rule-based method of prioritization and de-confliction and appropriate cue selection. In cases when the aircraft flies beyond two or more limits simultaneously, the limit cue constraints may be in conflict. For more complex systems, intelligent control algorithms with decision heuristics may be needed in the Arbitration module to deal with multiple conflicting cues and assign precedence among cues based on the flight environment and control mode. The rules that resolve this conflict rely on the knowledge of interrelated limits and the consequences of control movements. Examples of interrelated limits are vertical loading and main rotor blade stall. When the aircraft approaches those limits together, as in a pull up maneuver, both avoidance cues would push the longitudinal collective forward. In extreme cases, the cue would push the collective forward and put the aircraft into a dive that would exacerbate the problem. The arbitration module must select the most urgent limit for autonomous protection or a tactile cue, or it must elevate that conflict decision to the pilot through a visual or aural cue.

Distribution across the Control System

The design for limit protection distribution relies heavily on an understanding of the nature of the limit, particularly the risk of limit violation and the time required for protection actions. Autonomous limit protection can be made as rapidly as its flight control hardware can operate, often at a 50 Hertz update rate and greater. Tactile force feedback cues are limited by the reflex reaction time and physical dynamics of the limb-manipulator system, on the order of 0.1 to 1.0 seconds. Visual and aural cues that require cognitive processing and textual and verbal cues require still more time. In maneuvering flight, limit parameters are dynamic and, at times, their corresponding control constraints may move rapidly. When driving visual cues (i.e. Heads Up Display readouts), the limit display may be changing too rapidly for the pilot to discern and accommodate. Extreme constraint volatility may also exceed the physical bandwidth of the limb-manipulator system or lead to a force feedback cue that degrades handling qualities or that the pilot finds objectionable.

Fixed Distribution

Nearly all current limit protection systems were designed to interface at fixed points along the control signal path. For example, the stall warning buzzer common in general aviation aircraft is fixed as an aural display and does not manifest as a visual or tactile cue. In modern cockpits, the cockpit display subsystem may present a visual “pop-up” limit cue accompanied by an aural warning tone. But these would not autonomously protect the limit. They remain visual or aural. The carefree handling systems in complex aircraft autonomously protect critical, fast limits such as rotor yoke bending and drive shaft torque.

Frequency Distribution

The frequency distribution approach (Figure 12) splits limit protection between tactile cues and autonomous protection based on the frequency content of the constraint. A low pass filter can slow a volatile tactile constraint cue to a speed where it is acceptable to the pilot, but such a filter adds an effective delay that offsets the advantage of limit prediction. By using the high frequency remainder for autonomous limit protection, the system still provides voluntary tactile avoidance cues for the pilot while automatically protecting the system against high frequency limit constraints. In addition to or instead of a low pass filter shown in the figure, a rate limiting element may be used to slow the speed of a tactile cue. The figure depicts the concept as it would apply to an upper constraint limit that the pilot is flying along or beyond. There would be some additional logic (not shown) that would set whether this frequency distribution feature is active or disabled based on whether the physical pilot command is within or beyond the limit boundary.

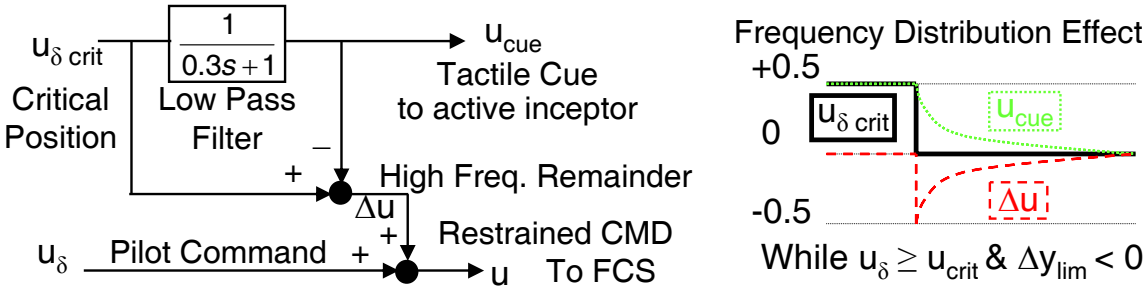

Figure 12. Frequency Based Distribution

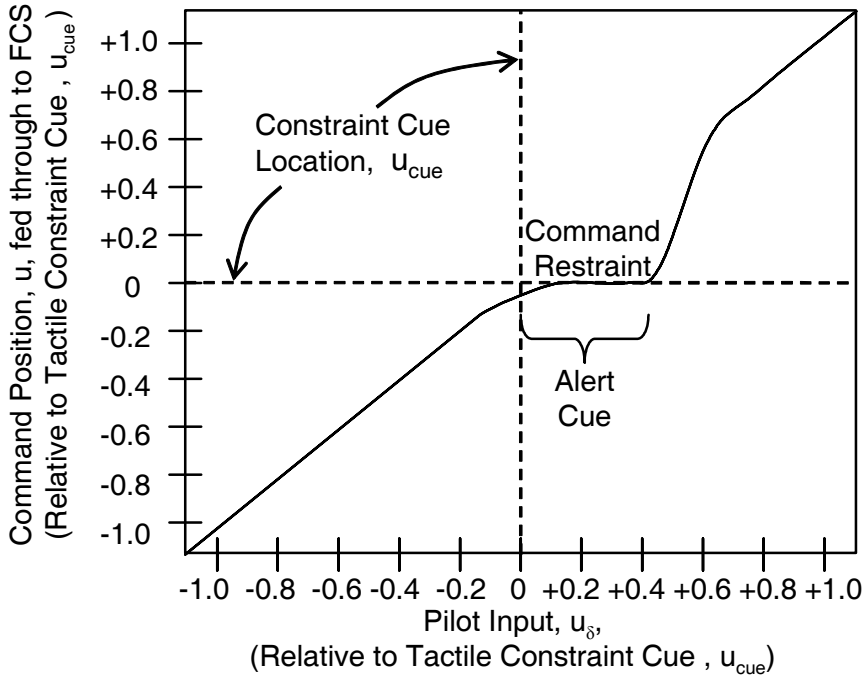

Figure 13. Deadband Split

Deadband Split

Another approach* to cue distribution applies a deadband split (Figure 13) to the nominal position command signal (that is, the physical position of the inceptor, u_δ) at the location of a limit protection constraint. The fed-through, post-inceptor, FCS input, u, is initially restrained as the pilot pulls through the location of the tactile constraint cue. While the fed through command is restrained, an alert cue is active in the form of a stick shaker.

* Concept proposed by Nilesh Sahani and Dr. Joseph Horn of Pennsylvania State University.

Arbitration Module Output

The Arbitration module provides limit protection cues to modules that interface with the control system. The structure of output varies among these destinations. While Figure 4 shows many potential interface points, only autonomous command restraint shaping; and visual, aural, and tactile limit cues will be practical in the foreseeable future and appropriate for a real time limit protection system during flight. Consequently, only these four modules and their corresponding outputs are considered here. In general, this module provides the essential information required for limit protection, plus the most helpful and useable supplemental limit cue information as shown in Table 10.

More limit and cue information is provided where the control channel is richer and can communicate more information to the pilot or aircraft. The visual display is the richest of those available for conscious limit protection and nearly all the constraint and alert information is included. The length and height of the cue, which may only have meaning for a tactile cue, are omitted from the visual and aural channels. The aural display similarly offers a large bandwidth and the same information is provided. The transfer function and friction cues have no meaning for the visual and aural. The tactile channel, which is also a form of cockpit display, has a smaller information capacity. But it does have the capacity to alter the control command with or without pilot input, and the transfer function and friction cues are provided for that purpose. Finally, autonomous (involuntary) limit protection is possible through command restraint shaping that uses the control margin and transfer function limit cues. These concepts (Table 10) are described in detail below.

Control Interface Module Design

The overall control system offers more points for limit protection cues than are indicated in Figure 4. The pilot has senses for vision, hearing, and touch as already described. Additionally, human pilots have proprioceptive and vestibular senses of accelerations. Forward of the human element, a limit protection can alter the post-inceptor command. Still other limit protection controls are available prior to flight in mission planning and forward of the pilot in the flight control system and the control surface actuators. These possibilities are discussed briefly here, with special emphasis on the tactile force feedback interface. The Control Interface is the last module of the Open Platform for Limit Protection with the design choices listed in Table 11. As such, the module outputs are specific to aircraft subsystems and are not standardized like the two information interfaces internal to the OPLP.

Table 10. Arbitration Module Outputs

Theory			As Implemented and Tested		
Destination	**Intent**	**Structure**	**Data Types**	**Units**	**Example**
Visual	Constraint	$\begin{bmatrix} N_{lim} \\ u_{cue} \\ y \\ y_{lim} \\ \lambda_{\Delta y} \end{bmatrix}$	$\begin{bmatrix} \text{Integer} \\ \text{Float} \\ \text{Float} \\ \text{Float} \\ \text{Float} \end{bmatrix}$	$\begin{bmatrix} \text{ND} \\ \text{NND} \\ \text{Varies} \\ \text{Varies} \\ \text{Varies} \end{bmatrix}$	$\begin{bmatrix} 1 \\ .24 \\ 325 \\ 300 \\ 25 \end{bmatrix}$
	Alert	$\begin{bmatrix} N_{lim} \\ \omega_{cue} \\ A_{cue} \end{bmatrix}$	$\begin{bmatrix} \text{Integer} \\ \text{Float} \\ \text{Float} \end{bmatrix}$	$\begin{bmatrix} \text{ND} \\ \text{rad/sec} \\ \text{NND} \end{bmatrix}$	$\begin{bmatrix} 1 \\ 120 \\ 1.0 \end{bmatrix}$
Aural	Constraint	$\begin{bmatrix} N_{lim} \\ u_{cue} \\ y \\ y_{lim} \\ \lambda_{\Delta y} \end{bmatrix}$	Not Implemented		
	Alert	$\begin{bmatrix} N_{lim} \\ \omega_{cue} \\ A_{cue} \end{bmatrix}$	Not Implemented		
Tactile (per axis)	Constraint	$\begin{bmatrix} u_{cue} \\ \Delta h_{cue} \\ \Delta \ell_{cue} \end{bmatrix}$	$\begin{bmatrix} \text{Float} \\ \text{Float} \\ \text{Float} \end{bmatrix}$	$\begin{bmatrix} \text{NND} \\ \text{NND} \\ \text{NND} \end{bmatrix}$	$\begin{bmatrix} 2 \\ 1.0 \\ 0.04 \end{bmatrix}$
	Alert	$\begin{bmatrix} A_{cue} \\ \omega_{cue} \end{bmatrix}$	$\begin{bmatrix} \text{Float} \\ \text{Float} \end{bmatrix}$	$\begin{bmatrix} NND \\ rad/\text{sec} \end{bmatrix}$	$\begin{bmatrix} 2.0 \\ 18.8 \end{bmatrix}$
	Transfer Function	$\begin{bmatrix} \omega_n \\ \zeta \\ K_0 \\ K_2 \\ \mu \end{bmatrix}$	$\begin{bmatrix} \text{Float} \\ \text{Float} \\ \text{Float} \\ \text{Float} \\ \text{Float} \end{bmatrix}$	$\begin{bmatrix} \text{rad/sec} \\ \text{ND} \\ \text{ND} \\ \text{ND} \\ \text{NND} \end{bmatrix}$	$\begin{bmatrix} 7 \\ 0.1 \\ 1.0 \\ 1.0 \\ 1.0 \end{bmatrix}$
	Friction	$\begin{bmatrix} \mu_d \\ \mu_s \end{bmatrix}$	$\begin{bmatrix} \text{Float} \\ \text{Float} \end{bmatrix}$	$\begin{bmatrix} \text{NND} \\ \text{NND} \end{bmatrix}$	$\begin{bmatrix} 0.2 \\ 0.2 \end{bmatrix}$
Autonomous (per axis)	Constraint	$[\Delta u]$	[Float]	[NND]	$[-0.08]$
	Transfer Function	$\begin{bmatrix} \omega_n \\ \zeta \\ K_0 \\ K_2 \\ \mu \end{bmatrix}$	$\begin{bmatrix} \text{Float} \\ \text{Float} \\ \text{Float} \\ \text{Float} \\ \text{Float} \end{bmatrix}$	$\begin{bmatrix} \text{rad/sec} \\ \text{ND} \\ \text{ND} \\ \text{ND} \\ \text{NND} \end{bmatrix}$	$\begin{bmatrix} 100 \\ 1.0 \\ 1.0 \\ 0.0 \\ 1.0 \end{bmatrix}$

Table 11. Control Interface Design Choices

Module	Aspect	Choices
Mission	Risk Management	Aircraft model, loading, altitude, etc.
Visual Aural	Limit Identity	Textual/Verbal, Lamp/Tone
	Urgency	Caution, Warning, Advisory
	(Priority)	1 – 23…
Tactile	Force Feedback (for each control axis)	Softstops
		Detents & Gates
		Shakers
		(Bobweight) Dynamics
		Friction (Dynamic & Static)
	Other	Surface Texture
		Inceptor / Lever Shape
		Temperature
		Electrical potential (charge)
Neural Stimulation		
Proprioceptive		
Vestibular	Somatogyral	
	Somatogravic	
Command Restraint Shaping	command shaping	Subtract/Add control margin

Mission Planning

The subject of limit protection can be extrapolated beyond control during the flight itself. Mission planning is a critical phase of flight where performance is estimated based on equipment on board, weight and balance, environmental conditions, and so on. The aircraft is evaluated in the context of its estimated performance and its mission. Shortcomings are discovered and risks are assessed. Risks of limit violations can be managed and mitigated through the choices of aircraft, loading, altitude, speeds, and so on.

Visual and Aural

The visual and aural cue interfaces may use industry standard or pre-existing cockpit warning and alert systems, such as the Allied Signal Integrated Alerting Cockpit Alerting Safety System[59]. In doing so, this interface need only provide high level information such as the identity (name) of the limit and its relative priority or at least its level of alert urgency

(caution, warning, or advisory). The cockpit interface would then internally combine, prioritize, and arbitrate the maneuver limit cues (and other alerts) and divide them between visual and aural displays.

At a lower level the visual/aural cockpit alerting system serves as the greatest conduit of information that pilots possess and it is the primary source of information regarding aircraft systems and limits. As a channel for limit protection cues, vision displays offer multiple cues for both simple and complex information. The size of a limit cue is its portion of the visual field of view. The cue can assume various shapes, such as the sector arcs of analog gauges. Particular shapes, such as letters and numbers, are symbols that carry very detailed information about limits and controls, however, the additional cognitive processing step of interpreting symbols and strings of symbols (i.e. words) adds a small delay to the control process. Color is commonly used to indicate an alert status or urgency. The notable examples are: green to indicate nominal range, yellow to indicate a transient limit, and red to indicate a maximum or minimum peak limit. Visual displays may also provide cue information through both stereoscopic and ocular focal distance.

The sense of hearing also has a high capacity for information that can be presented from different sides (left or right), at different frequencies (high pitched to low pitched), and at different intensities (quiet or loud). This information may be simple, non-verbal tones or tonal compositions with a remarkable capacity for eliciting emotional reactions such as peace or alarm. The aural analogues to visual text messages are the verbal messages that can likewise carry detailed systems and limit information at the cost of additional cognitive processing time. Verbal cues may be masculine or feminine and can carry emotional content.

Tactile Cues

The sense of touch encompasses many distinct sensations potentially useful as limit cues. The inceptor surface *texture* may be smooth, fuzzy, prickly, wet, sticky, and so on. Active texture cues may be used to communicate such things as the aerodynamic performance of aerodynamic surfaces (laminar versus turbulent boundary layers). The *shape* of the cockpit control levers is commonly used as an identification tool in cockpits. Active shape changing inceptors have been used to provide flight control and limit cues (ex. Angle of Attack cue using a handgrip protrusion[84]). With active heating and cooling element, an inceptor could use temperature to intuitively communicate temperature related limits and system performance such as engine turbine temperature or rotor blade icing. Mild shock may be a useful as a limit alert cue.

The primary forms of tactile cue considered for this limit protection platform are the force-displacement cues of an active cockpit inceptor. Force-feel characteristics, physical control dimensions, and cockpit placement have been the subject of many studies[100,101,102,103,104,105]. Depending upon its design capabilities, an active inceptor can generate a counter-force function based on the inceptor position, on time, and on higher dynamical states of the inceptor and the vehicle. The cue force is a combination of the nominal force displacement curve, softstops, the detents, oscillations, damping and natural frequency response. Because human pilots have different degrees of strength and control for the different control axis, it is appropriate to decompose this function into its active control axis components and tailor them to pilot physiology.

$$F = F(u,\dot{u},t) = F_{nom} + \sum_i F_{ss_i} + \sum_j F_{\det_j} + F_{\omega} + F_{\omega_n\zeta} + F_{fric} \tag{21}$$

Range of Motion

Traditional cyclic sticks move several inches in two axes. An active sidestick may move approximately 25 degrees or more longitudinally and laterally and may provide a third axis (twist) about a vertical axis. Smaller ranges of movement, such as 5 or 10 degrees from neutral, are useful when force is the only interaction between the pilot and the active system. Larger ranges of movement, such as 15 to 30 degrees from neutral, allow both force and displacement as information channels between the pilot and the active control system. However, very large ranges of movement in a sidestick can be awkward for the pilot. Also, a larger range magnifies the movement of limit avoidance cues to the point where they may be objectionable to the pilot. The range of movement may best be left adjustable for pilot preference.

Nominal Force-Displacement Relationship (F_{nom})

An inceptor uses a nominal force-displacement relationship where the pilot feels a centering force that increases gradually and nearly linearly as it is pushed away from its neutral position.

$$F_{nom} = F(u) = k_f(u - u_0) \tag{22}$$

The zero-force intercept is the neutral position where the inceptor will settle when left untouched. An active sidestick can offer cues and guidance by changing the zero-force position and how the counter-force increases as pilot applies force. The force-displacement relationship can be nearly flat, $k_f = 0$. This is the typical feel of a traditional

helicopter cyclic stick without friction. Another relationship uses a preload force. With a preload, the control will not move from the neutral position until the breakout force is reached. The force gradient is the key parameter used to dimensionalize the limit protection cues generated by the preceding limit protection modules. a normalized non-dimensional cue (such as constraint height of $\Delta h_{cue} = 1.33$) is multiplied by the stick force required for maximum static deflection (30 Newtons) to arrive at the softstop height (40 Newtons).

Force Inversely Proportional to Control Margin (F_{ss})

One tactile softstop cue is the use of a force Inversely Proportional to Control Margin (Figure 14). This form of a softstop, used successfully with V-22 simulations[39], creates a counter force that opposes the pilot as he pushes the control towards a limit. The magnitude of the counterforce is approximately inversely proportional to the control margin and increases to a maximum counter-force at the critical control position. This method can be implemented with minor variations, but its defining characteristic is the gradual increase in counter-force as the critical control position is approached. This method does not provide a precise cue regarding the limit and this reflects the true indistinct nature of many (perhaps most) limits, which are based on subjectively defined safety margins added to structural failure loads or control system domain boundaries.

Step Force at Critical Control Position (F_{ss})

Another successful form of softstop uses a step increase in counter-force at the critical control position (Figure 15). The cue provides a precise indication to the pilot about the location of the edge of the flight envelope defined by the limit prediction algorithms. However, when the critical control position varies rapidly while the pilot is following the cue, it can seem jittery and may be objectionable.

Detents and Inverse-Detents (F_{det})

A force detent superimposed on the nominal force-displacement relationship serves well as a trim cue or an autopilot cue. The sidestick will remain in a detent “force-well” until the pilot provides a sufficient break away force (Figure 14). Then the stick would follow the nominal force-displacement relationship. The inverse detent, also called a tactile gate, has the opposite effect (Figure 15). It pushes the stick away from the inverse-detent position to one side or the other. Such a cue can steers the pilot away from high-risk flight conditions, such as very steep, high power approaches where vortex-ring state is predicted as imminent.

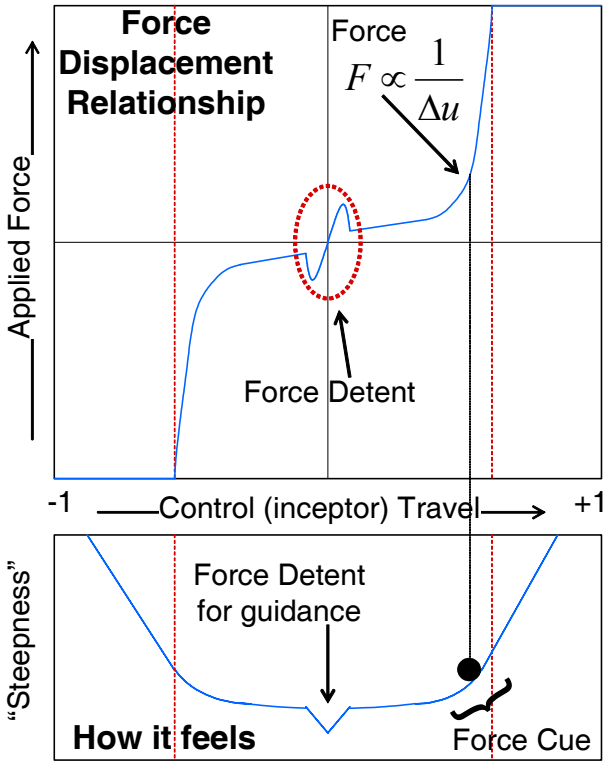

Figure 14. Inverse Force Softstop with Detent

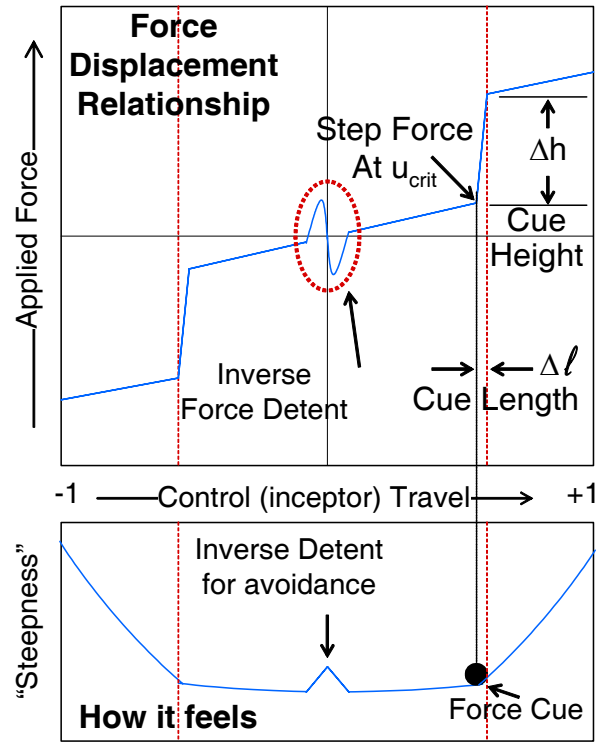

Figure 15. Step Force Softstop with Gate

Shaking and Vibration ($F\omega$)

Shaking and vibration is a very useful supplemental cue. It is used to indicate that the aircraft is already beyond a limit. It can also cue impending limits whose indications involve vibration. For example, a high frequency vibration can cue loss of tail rotor effectiveness and tail rotor malfunctions. A low frequency, 1/rev, can cue main rotor stall and other main rotor limits.

$$F = F(t) = A\sin(\omega t) \tag{23}$$

Damping and Natural Frequency Response ($F\omega_n\zeta$)

The frequency response of an active inceptor can imply agility or sluggishness to convey the maneuvering capability of an aircraft in varying flight regimes. Damping as a force cue, may be effective for transient limits such as maximum flapping with respect to cyclic. It is the only force cue listed here that depends directly on control speed. Maximum transient limits depend primarily on fast control movements rather than control positions.

$$F_{\omega_n \varsigma} = M(\ddot{u} + 2\omega_n \varsigma \dot{u} + \omega_n{}^2 u) \tag{24}$$

Friction (F_{fric})

Friction is a constant force that opposes the direction of movement. It may have use as a cue, but mainly it helps the pilot hold the control at a constant position despite airframe vibrations or those occasions when the pilot removes his or her hand.

Proprioceptive and Vestibular

Proprioceptive perception combines the force and motions sense of touch among the body's joints and muscles with other intra-organism cues of weight or weightlessness. Vestibular perception senses inertial and angular acceleration. The otolith organ and semicircular canals located in the inner ear provide for the somatogravic and somatogyral cues. Besides the active force feedback cues of active inceptors, there is not yet a feasible interface with these forms of perception.

Neural Stimulation

Direct neural interface has recently emerged as a potential control channel.[85,86] But the research has focused on translating neural or cortical signals into useable digital control signals and not on translating digital information (such as limit cues) into neural signals.

Control Restraint Shaping

The inceptor serves as an interface between the physical world where the pilot resides and the digital domain where the flight control system operates. Command restraint shaping is a form of autonomous limit protection where a portion or all of the control margin is added or subtracted to the post-inceptor command signal when a limit violation is predicted. The “restrained” command signal becomes the input for the flight control system.

CHAPTER IV

DESIGN, PROTOTYPING, AND SIMULATION ENVIRONMENT

The structure of the Open Platform for Limit Protection was refined over three years of tactile cueing and limit prediction work at the Georgia Institute of Technology and the Army NASA Rotorcraft Division. The lessons learned guided the platform compromises between generality that allows design freedom and specificity that closes design freedom, but facilitates practical testing of real limit protection algorithms. Using the structure of the Open Platform for Limit Protection, four distinct limit protection projects were developed, tested individually, and combined in an OPLP based carefree maneuver system. The first project validated the RIPTIDE prototyping environment and the hardware integration of the active sidestick. The work helped define the precursor to the OPLP, an open design for tactile cueing systems[69]. With that project, the taxonomy of limit protection systems was laid out and reviewed with regard to ongoing limit protection and active control research, especially the HACT[15] program. That review led to the development of a tactile avoidance cue for Pilot Induced Oscillation[87,76]. This second project addressed three untried aspects of the limit protection: 1) It addressed a controllability limit, 2) It used a logic based limit predictor, and 3) it used inceptor dynamics as a transfer function cue. Because of the qualitatively dissimilar nature of the PIO cue, it is explained in a separate chapter. The third and fourth projects returned to arithmetic limit cue methods and to the softstop as the primary tactile cue. But they advanced other novel aspects of limit protection including cues for transient peaks[74] and adaptive prediction mechanisms[75].

The following sections describe the development of this carefree maneuver system starting with a description of the design, prototyping, and testing environment. Then the limit protection performance metrics and the test maneuvers are explained. The design and performance of each functional module is explained in turn. The combined carefree maneuver system is summarized in Table 12.

Table 12. Carefree Maneuver System Design Choices

Module	Aspect	Choices
Main Rotor Blade Stall Arithmetic **Limit Cue**	Nature of Limit	Aerodynamic
	Type of Prediction	Fixed Time Horizon
	Prediction Mechanism	Static Neural Network
	Critical Control Calculation	Inverse Partial Derivative
	Type of Cue	Constraint and Alert
Pilot Induced Oscillation Logical **Limit Cue**	Nature of Limit	Controllability
	Prediction and Control	Fuzzy Inference System
	Type of Cue	Transfer Function and Friction
Main Rotor Blade Stall Arithmetic Cue **Limit Cue**	Nature of Limit	Aerodynamic
	Type of Prediction	Dynamic Trim
	Prediction Mechanism	Adaptive Neural Network
	Critical Control Calculation	Inverse Partial Derivative
	Type of Cue	Constraint
Hub Moment Arithmetic **Limit Cue**	Nature of Limit	Structural
	Type of Prediction	Transient Peak Search
	Prediction Mechanism	Static Neural Network
	Critical Control Calculation	Inverse Partial Derivative
	Type of Cue	Constraint
Arbitrator	Limit Cue Selection	Constraints and Alerts: Most Conservative
		Transfer Function and Friction: One-to-One
	Control System Distribution	Fixed
Visual **Control Interface**	Symbols	Text showing Constraint Cue, Name and value of limit
	Colors	Green – Nominal Red – At or Beyond Limit
Tactile **Control Interface**	Force Feedback: Softstop	Driven by Constraint Cue
	Force Feedback: Shaker	Driven by Alert Cue
	Bobweight Dynamics	Driven by Transfer Function Cue
	Friction	Driven by Friction Cue

Development and Prototyping Environment

This Open Platform for Limit Protection was realized as a control system block diagram within Simulink®[65]. It was auto-coded and compiled using MATLAB's Real-Time Workshop. The Real-Time Interactive Prototype Technology Integration Development Environment (RIPTIDE)[88] served as a prototyping environment that facilitated iterative improvement of the control system. RIPTIDE applies the SIMULINK® based control system to the vehicle math model, which, for the applications presented here, was a General Helicopter Model (GENHEL)[89] of the UH-60A Black Hawk helicopter, whose states are rendered as a pilot's view with OpenGL Performer™. While the development of the control system began at Ames Research Center, California, under a grant from the Army NASA Rotorcraft Division to develop and demonstrate in-flight tactile cueing on the Division's Rotorcraft Aircrew Systems RASCAL[13]; the majority of the development and testing was conducted in an active sidestick workshop assembled at the Georgia Institute of Technology as shown in (Figure 16) using the equipment listed in (Table 13).

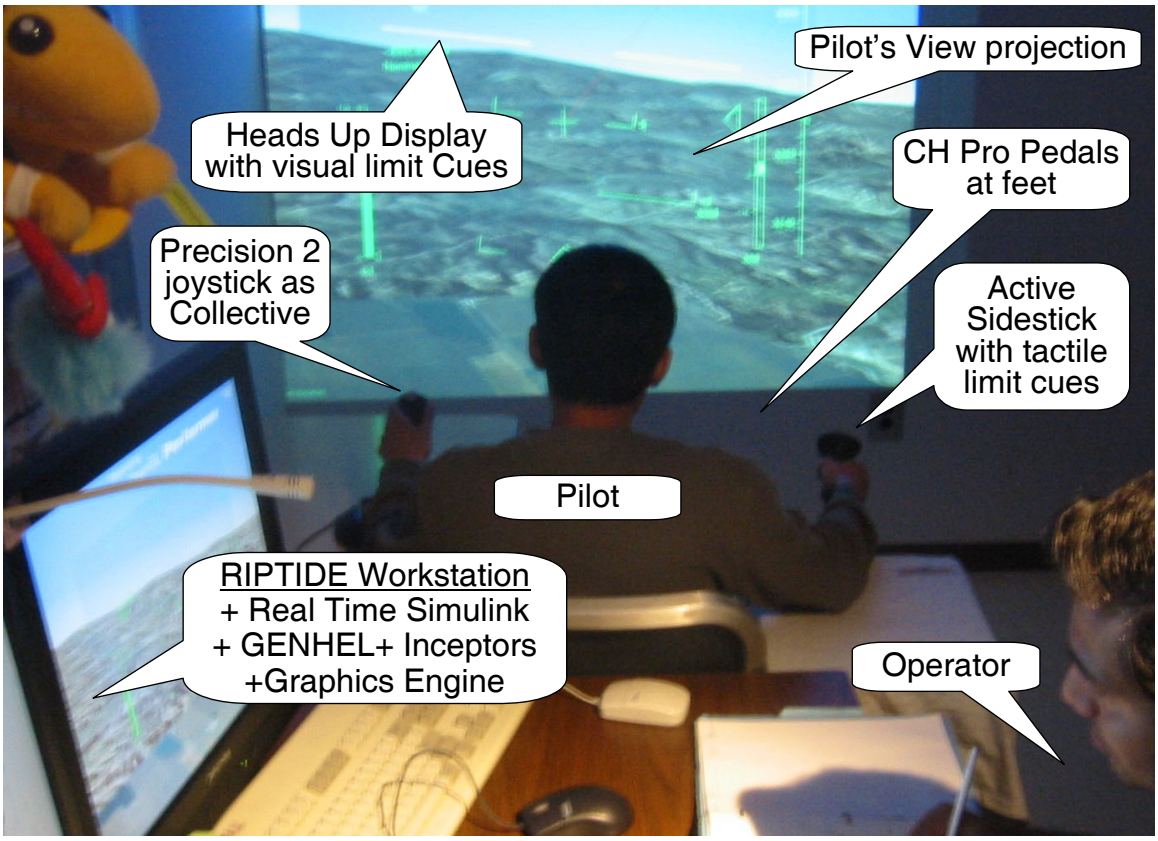

Figure 16. Active Sidestick Workshop.

Table 13. Active Sidestick Workshop Equipment

Hardware	
Workstation	Dell Precision 530 Workstation
Processors	Symmetric (twin) 1.7 GHz Xeon® microprocessors
Memory	1 Gb static random access memory
Storage	18 Gb SCSI, 7200 RPM, SCSI hard disk for Windows XP 34 Gb SCSI, 7200 RPM, SCSI hard disk with two partitions for: Data & Documents (20 Gb) and Linux with RIPTIDE (10 Gb)
Graphics	NVIDIA® Quadro 700, with 64 Mb
Displays	Twin Planar 120PL 20 in flat panel displays (dual display setup)
Projection	Dell 3200MP projector (1024x768 resolution) split from right display.
Imaging	Two Logitech USB cameras (640x480 still, 320x240 at 30 fps)
Active Sidestick	Stirling Dynamics active sidestick model SA-S-2D-1
Network	Two 10bT Ethernet cards (one for LAN, a second for active sidestick)
Joystick	Microsoft Precision 2 joystick
Pedals	CH Pro USB Pedals
Miscellaneous support equipment	VGA signal splitter, USB Hub, USB extensions, Surge protector, keyboard, mouse, monaural microphone, second PC with microphone and web cam used for teleconferencing and video recording.
Software	
System	Linux Red Hat 7.3 upgraded to kernel 2.4.23 smp with CH Pro patch.
Graphics	NVIDIA Linux driver, release 2880
Prototyping	Real Time Interactive Prototype Technology Integration Environment (RIPTIDE) release 7.3 mod 4
Rendering	SGI OpenGL Performer version 6.1 demo
Capture tools	Xvidcap; Ksnapshot, ImageMagick,

Limit Protection Performance Metrics

The purpose of a limit protection system is literally to prevent the aircraft from violating its limit boundaries. Conservative safety constraints do the same. But this approach restricts the performance of the vehicle. Safety and performance are typically in opposition. The true value of a limit protection system is the reduction of the safety versus performance compromise, so quantitative assessment of the limit protection systems used a two dimensional evaluation for: 1) vehicle performance or "agility" and 2) limit protection. Additionally, especially for the early designs evaluated in this platform, a qualitative assessment of the performance was made through examination of time history data of Mission, Task, Element (MTE) maneuvers.

The time required to perform a MTE maneuver to its standard is the primary measure of aircraft performance or agility served at the primary vehicle performance metric. The elapsed time begins with the initiation of the first maneuver element and it ends with the completion of the final element of the maneuver.

$$T = t_F - t_0 \tag{25}$$

This agility time may be left in a dimensional form (i.e. seconds) or may be normalized by a standard time span such as the "theoretical" time, T_0. This theoretical time is that time required to perform the maneuver to standard with full use of the flight envelope, but without limit violation. This nondimensional term is called an agility factor (AF):

$$AF = \frac{T_0}{t_F - t_0} \tag{26}$$

Two types of limit protection metric are used to measure peak and integrated limit violations. The Peak Violation (PV) is simply the most extreme value of the limit parameter, whether maximum or minimum. The value may be normalized in various ways, typically by dividing by the difference between maximum and minimum limits (the "limit span").

$$PV^{+} = \max(y) \tag{27}$$

$$PV^{-} = \min(y) \tag{28}$$

The Integrated Limit Margin (ILM) is the time integral across the maneuver of the limit margin. This may be the first power integral (ILM_1) or the integral of the square or higher power (ILM_2). By definition, the limit margin is positive while the system satisfies the limit constraint and negative when the limit is violated, so this metric only integrates the amount of violation, not the underutilization of the flight envelope.

$$ILM_n = \int_{t_0}^{t_F} \left|\min(0, \Delta y_{\lim})\right|^n dt \tag{29}$$

A Normalized Integrated Limit Margin (NILM) may be calculated by dividing the ILM by both the standard time span and the limit span:

$$NILM_n = \frac{\int_{t_0}^{t_f} \left|\min(0, \Delta y_{\lim})\right|^n dt}{(t_f - t_0)(y_{\max} - y_{\min})} \tag{30}$$

Another metric, called the Effectiveness Factor or Safety Factor creates a normalized limit protection metric analogous to the Agility Factor for vehicle performance.

Manned Simulation and Testing

Three pilots were used for the iterative development and prototyping of the carefree maneuver system using the mission task maneuvers described below. The first and second pilots were U.S. Army aviators with approximately 1000 flight hours each. Both had rotary wing and fixed wing ratings, but only one had flown the UH-60 Blackhawk as his primary aircraft. A third pilot was a fixed wing aviator competent with simulated rotary wing flight control but without actual helicopter flight experience. Most of the results shown below for the limit cues were generated by the two helicopter aviators intermittently over two years as each limit cue was developed and tested. The primary purpose of the manned simulation test flights was to demonstrate the carefree maneuver systems and their designs within the context of this platform. A secondary purpose of the testing was to examine the performance of the specific limit protection algorithms.

Mission Task Elements for Limit Protection Evaluation

Existing aeronautical design standards (ex. ADS-33[71]) establish Mission Task Elements (MTE) for the purpose of evaluating aircraft handling qualities. The ADS-33 MTE performance metrics standardize maneuvers for fair and consistent evaluation of handling qualities levels. In some cases, these maneuvers do intentionally put the aircraft near limit boundaries and are suited to test limit protection systems. One maneuver that does is the ADS-33 Pullup/Pushover maneuver. It was used to qualitatively evaluate a limit avoidance tactile cue that validated the RIPTIDE based active sidestick experimental setup.

But in order to more effectively explore the effectiveness of limit protection systems, two additional maneuvers, the "Attitude Capture" and "Swoop" maneuvers, were created with standards that put the vehicle at its limit boundary for hub moment and blade stall. The maneuvers were patterned after ADS-33 maneuvers, particularly the Pullup/Pushover maneuver. They are described on the following two pages using the imperative grammatical style found in the ADS-33 MTE maneuver descriptions. The two maneuvers are depicted in Figure 17 and Figure 18.

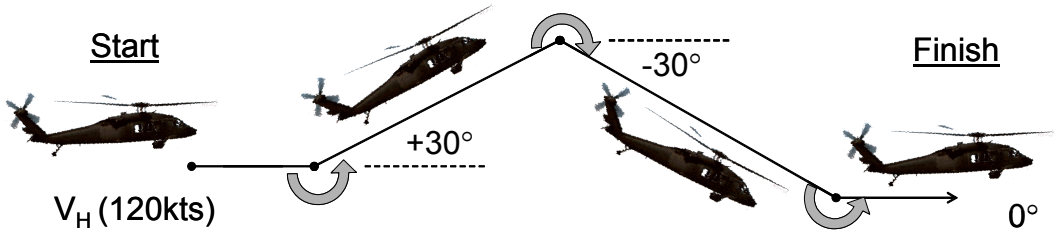

Figure 17. Attitude Capture Maneuver.

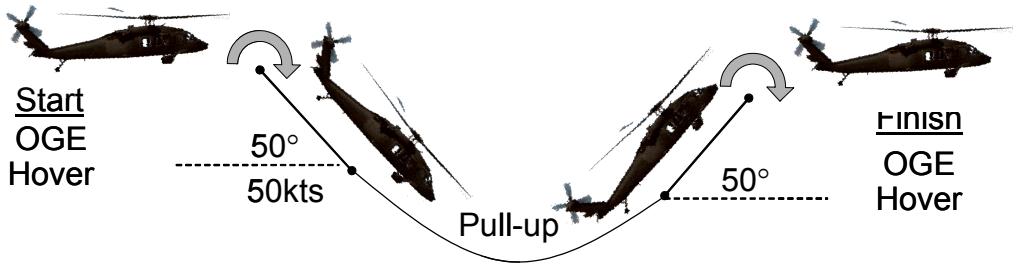

Figure 18. Swoop Maneuver.

The Attitude Capture Maneuver

Objectives.

- Check handling qualities, pilot workload, and limit protection for pitch acceleration and pitch rate related limits, whether steady or transient, in high speed flight. These limits may include hub moment, flapping, vertical load, and main rotor blade stall.
- Check handling qualities at vehicle limit boundaries.
- Check for ability to maneuver aggressively, at maximum vehicle performance, without violating operational limits.
- Check for ability to rapidly target fixed weapons in high speed flight.

Description of maneuver

From level unaccelerated flight at the lesser of V_H or **120 knots**, using an abrupt aft cyclic command, attain a maximum pitch rate in a symmetrical pullup to a 30 degree nose high attitude. Pause briefly at this attitude. Transition, with an abrupt forward cyclic via a symmetrical pushover, to a maximum (downward) pitch rate to a -30 degree, nose down, attitude. Pause briefly at this attitude. Complete the maneuver with an abrupt pull-up and maximum pitch rate to recover to level flight as rapidly as possible. The entire maneuver should resemble a doublet control input maneuver. The maximum or minimum pitch rate is defined by the relevant limits of the vehicle. The pause at the target nose high or nose low attitudes need only be long enough to verify overall pitch controllability. Collective pitch remains constant throughout the maneuver.

Description of test course.

This maneuver may be accomplished up-and-away, and no test course is required.

Performance standards for pilot.

Table 14. Performance – Attitude Capture

	Desired	Adequate
• Attain target pitch attitudes, +30°.	± 5°	± 15°
• Maximum pause at nose high attitude.	0.5 sec	1.0 sec
• Attain target pitch attitudes, -30°.	± 5°	± 10°
• Maximum pause at nose down attitude.	0.5 sec	1.0 sec
• Return to level flight attitude, 0°	± 10°	± 15°
• Maintain angular deviations in roll and yaw within ±X degrees from the initial unaccelerated level flight condition to completion of the maneuver.	10 deg	15 deg
• Collective pitch remains constant throughout the maneuver.	✓	✓

The Swoop Maneuver

Objectives.

- Check handling qualities, pilot workload, and limit protection for pitch acceleration and pitch rate related limits, whether steady or transient, in dynamic maneuvering from hover to high speed flight. These limits may include hub moment, flapping, vertical load, and main rotor blade stall.
- Check handling qualities at vehicle limit boundaries.
- Check for ability to maneuver aggressively, at maximum vehicle performance, without violating operational limits.

Description of maneuver

From OGE hover, using an abrupt cyclic command, rapidly pitch down -50 degrees nose down attitude. Hold this attitude, allowing the diving aircraft to accelerate, until the airspeed reaches 50 knots. Via a steady but rapid cyclic command, execute a symmetrical pull-up, to a nose high +50 degree attitude. Hold this cyclic climb as the aircraft decelerates. At an appropriate airspeed, execute a rapid pitch down to return to an OGE hover. The collective pitch setting (for OGE power) remains fixed throughout the maneuver.

Description of test course.

This maneuver may be accomplished up-and-away, and no test course is required.

Performance standards for pilot.

Table 15. Performance – Attitude Capture

	Desired	Adequate
• Begin at OGE Hover	± 5 kts	± 15 kts
• Attain target pitch attitude, -50°.	± 5°	± 10°
• Begin pull-up at target airspeed, 50 kts.	± 2 kts	± 5 kts
• Attain target pitch attitude, +50°	±10 deg	±15 deg
• Complete maneuver at OGE Hover	± 10 kts	± 15 kt
• Maintain angular deviations in roll and yaw within ±X degrees from the initial unaccelerated level flight condition to completion of the maneuver.	± 10 deg	± 15 deg
• Collective pitch remains constant throughout the maneuver.	✓	✓

CHAPTER V

CAREFREE MANEUVER DESIGN FOR STRUCTURAL LIMITS

Limit Cue Module: HELMEE Main Rotor Blade Stall

Prototype development for in-flight tactile cueing on the RASCAL aircraft began in the summer of 2001 at the Army/NASA Rotorcraft Division. The active inceptor was the Sterling Dynamics Active Sidestick System model SA-S-2D-1 and the development environment was an SGI IRIX version of the Real-Time Interactive Prototype Technology Integration/Development Environment (RIPTIDE). This blade stall limit cue was the first one tested in the RIPTIDE environment. As a validation project, this limit cue module recreated a previously researched and fairly well known tactile cue algorithm.

The Nature of the Limit

Retreating blade stall is a well known and serious helicopter limitation. When violated, the helicopter pitches up violently and rolls to the retreating blade side. It is an aerodynamic limit that quickly leads to controllability and structural limits. Violation can be catastrophic if it occurs near the ground. But "blade stall" is not a numerical parameter that can be handled as a limit by itself. Knowledge of the limit is at Stage 6 (of Table 6): it is fairly well understood, measured, and controlled using an empirical approximation. When treated empirically as a first order limit, where transient peaks are not important causes, the limit violation can be precipitated or prevented in a time scale roughly equal to a quarter rotation of the main rotor (a gyroscopic delay) plus any time delays in the flight control system. This puts the time scale on the order of a few tenths of a second, and so makes it appropriate for tactile cues and autonomous protection, but too quick for cognitive cues.

Limit Cue Design

The Main Rotor Stall limit was defined numerically as Equivalent Retreating Indicated Tip Speed (ERITS). The empirical version of ERITS used here is:

$$\text{ERITS} = \frac{\left(\Omega R \frac{\rho}{\rho_o} - V_{eq}\right)}{N_z} \frac{W_o}{W} \qquad (31)$$

The prediction model was the same polynomial static neural network developed for the HELMEE study*. It provided a prediction for a fixed time horizon of 0.253 seconds. A complementary filter between the neural network and the instantaneous ERITS value eliminated steady state prediction error. ERITS values below 250 were considered beyond the limit, and were signaled with a stick shaker defined by an alert cue. An ERITS prediction of 300 is the trigger for a softstop constraint cue.

$$y_{\lim}^{-} = 300\,fps \;\; (ERITS) \tag{32}$$

The critical control position was calculated with a simple partial derivative inverse:

$$u_{crit}^{+} = u_{\delta} + \left(\frac{\partial y}{\partial u_{\delta}} \right)^{-1} \left(y_p - y_{\lim}^{-} \right) \tag{33}$$

This longitudinal cyclic axis cue had a negative limit sensitivity, meaning that the negative (minimum) limit lead to a positive (upper) critical control position. The limit sensitivity was set at the same constant value that was used in the HELMEE study.

Limit Cue Output

Both an alert (the stick shaker) and a constraint (the softstop) were used. Blade stall was made limit number 1. The critical control position was used as the constraint position. The softstop height was set at 1.33, which would create a softstop cue force a third greater than the force required for maximum static deflection. Ultimately, as described later, this would become 40 Newtons. A short length of 0.04 was chosen to create nearly a step force softstop. The last three elements of the constraint cue, while not needed for a tactile cue, could be displayed as a corroborating visual display.

$$\left[\mathrm{N}_{\lim} \quad u_{cue} \quad \Delta h_{cue} \quad \Delta \ell_{cue} \quad \mathrm{y} \quad \mathrm{y}_{\lim} \quad \lambda_{\Delta \mathrm{y}} \right]^T = \left[1 \quad u_{crit}^{+} \quad 1.0 \quad 0.04 \quad \mathrm{y}_{\mathrm{p}} \quad 300 \quad \Delta y_{\lim} \right]^T \tag{34}$$

$$\left[\mathrm{N}_{\lim} \quad A_{cue} \quad \omega_{cue} \right]^T = \left[1 \quad 2.0 \quad 108.0 \right]^T \tag{35}$$

---

* Mr. Matt Whalley, the principle investigator of the HELMEE study provided paper printouts of the C code programming used at the NASA Ames Vertical Motion Simulator for the Piloted Evaluation if the HELMEE longitudinal cues. The neural network was reconstructed from that code into a Simulink block diagram

The alert was a simple binary switch that set the shake force amplitude to zero when the aircraft was within limits. When the actual limit parameter, y, (not the prediction, y_p) dropped below 250, the alert amplitude was set to 2.0, or twice the force required for maximum static stick deflection. The alert frequency was set to 108 rad/sec or 17.2 Hz. This frequency was chosen to resemble the UH-60 main rotor speed (27 rad/sec) times its four blades.

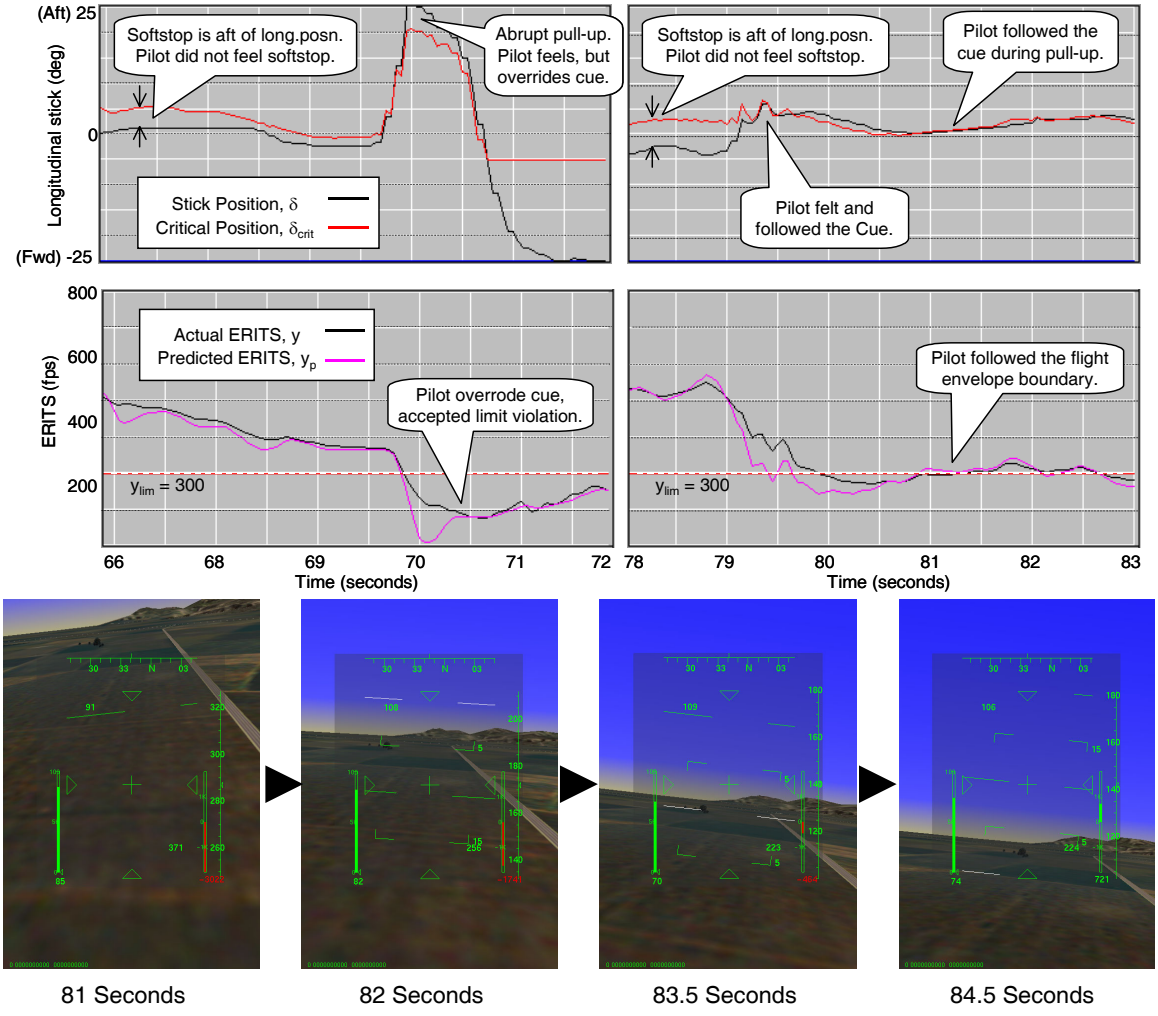

Figure 19. Main rotor blade stall limit cueing during pull-up maneuver.

Limit Protection Performance

The performance of the active control system in piloted simulation of two consecutive pull-up maneuvers is shown in Figure 19. The position of the softstop and stick are shown

in the top graphs. The predicted control margin is the area below the softstop (in red) and above the stick position (in black). In both maneuvers, the aircraft begins in an accelerating dive where the limit parameter, ERITS, is approaching its limit. Consequently, the control margin is narrowing. When the predicted ERITS reaches its limit as the stick moves aft, the pilot encounters the softstop cue. In the first maneuver (at left), the pilot overrides the softstop to make an abrupt pitch up. He exceeds the limit as ERITS drops to 175 fps. At critical times, the pilot may need to do this to avoid sudden obstacles (i.e. wires) and a tactile softstop does not prevent him. In the second maneuver (at right), the pilot encounters and follows the softstop, and in so doing, safely gets the most out of the maneuver envelope.

The performance of the same limit cue was also tested in a banked (50°) turn at high speed (100 kts) as shown in Figure 20. During the maneuver, the pilot had been steepening the bank angle of his turn while maintaining altitude. At 14.5 seconds, the combination of high speed and steep bank put the aircraft at its blade stall limit. At that point, the blade stall limit tracking is added to his workload. But instead of adding to his busy visual or aural information channels, the limit is monitored solely though the tactile cue. Between 14.5 and 16.0 seconds, the pilot encounters the softstop and begins to follow it. Then, until 20 seconds, he smoothly maneuvers along the edge of the flight envelope, commanding the lateral cyclic from visual cues to maintain altitude, while allowing the tactile cue to drive the longitudinal cyclic position. Between 20 and 21 seconds, he adjusts the collective first up then down. This affects the neural network limit prediction and the softstop position. The softstop nudges the longitudinal forward at 20 seconds and then recedes by 21 seconds. The pilot is able to feel and follow the longitudinal softstop as it reacts to his commands on other axes.

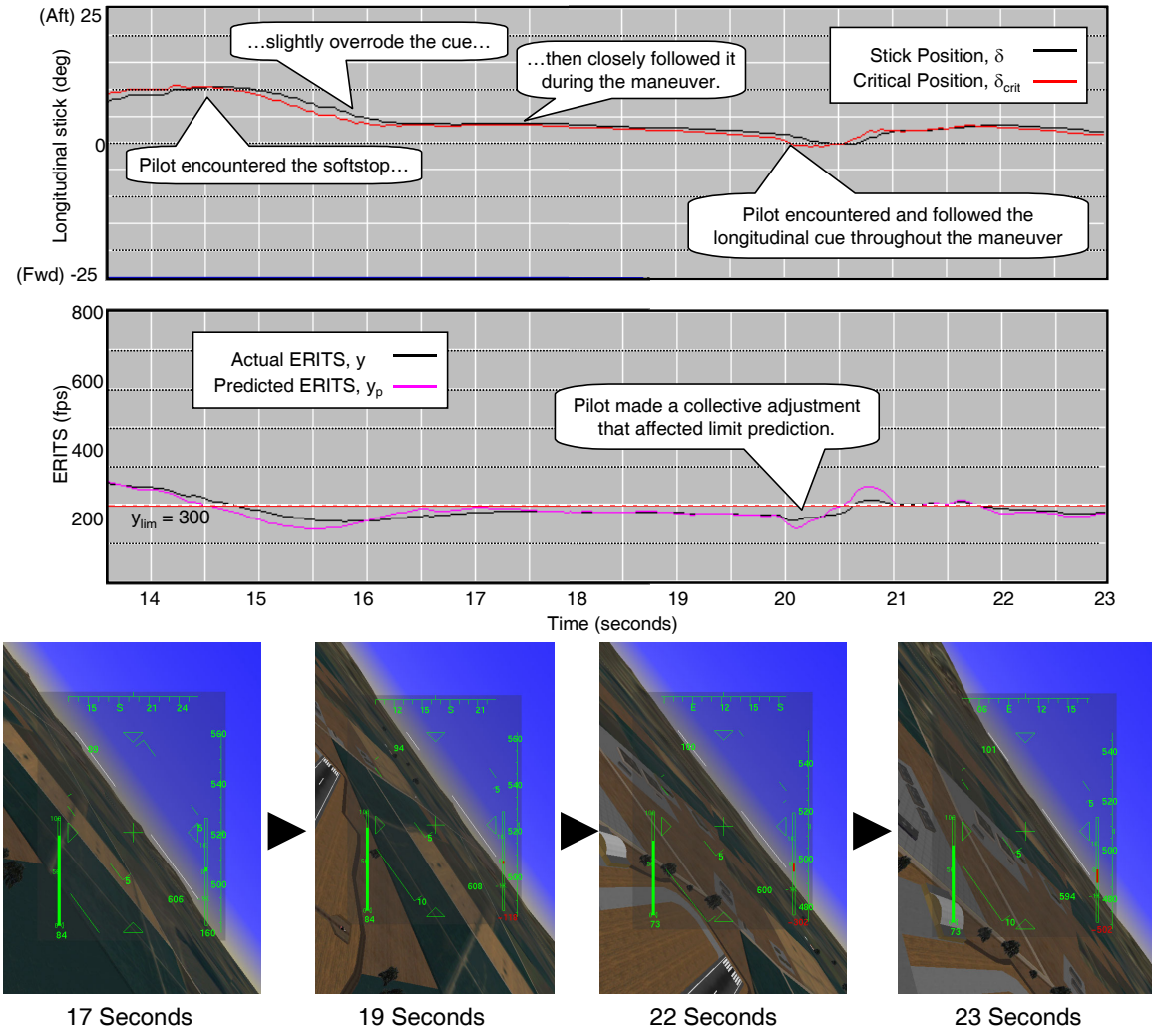

Figure 20. Main rotor blade stall cueing during banked, high-speed turn.

Limit Cue: Adaptive Neural Network Limit Protection for Blade Stall*

An adaptive dynamic trim limit prediction mechanism[90, 91] requires no *a priori* training. The adaptive network augments an approximate dynamical limit model to improve the real-time estimation of the limit parameter dynamics. Neural network weights are updated on-line based on weight update laws derived using Lyapunov analysis[92]. A Single Hidden Layer (SHL) neural network can approximate a continuous function to an arbitrary degree of accuracy. The weight update laws are designed such that the neural network output cancels the modeling error of the chosen approximate model. Main Rotor Blade Stall,

* This limit cue module was prototyped and tested in collaboration with Suraj Unnikrishnan and Dr. J.V.R. Prasad. Its construction is explained in detail in Ref. 75.

which was used in the HELMEE validation described above, provided a familiar, yet highly nonlinear parameter that would challenge the limit prediction algorithm.

Limit Cue Design

This approach (Figure 21) uses a linear approximate model and a Single Hidden Layer (SHL) Adaptive Neural Network (ANN), updated online, to estimate the limit parameter dynamics. The critical control position is computed from this estimated model using the method of dynamic trim. The method of dynamic trim, for limit detection and avoidance, is applicable only to limit parameters that achieve their maximum value in steady state.

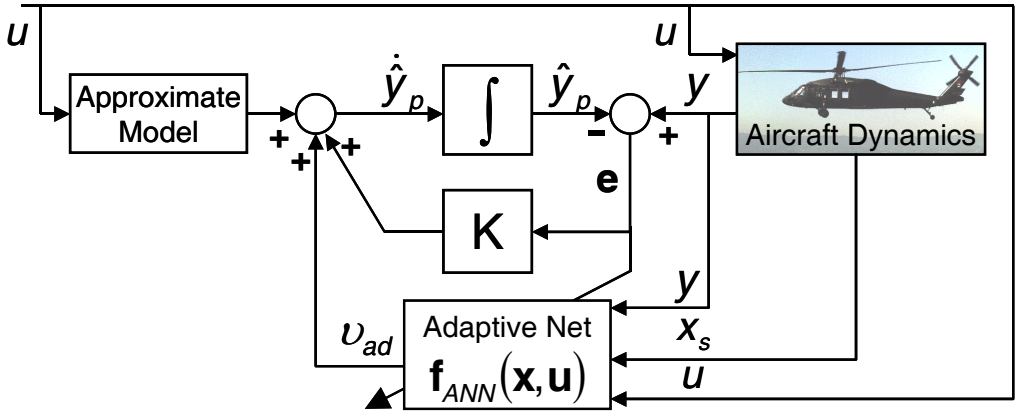

Figure 21. Limit Prediction using Adaptive Neural Network

The approximate model takes a linear state space form. With an error feedback term and the ANN dynamic correction, the dynamical limit model takes the form:

$$\dot{\hat{y}}_p = A\hat{y}_p + Bu + \upsilon_{ad}(y_p, x_s, u) + K(y_p - \hat{y}_p) \tag{36}$$

The critical control position is calculated from an analytical solution to the dynamic trim equation:

$$0 = A\hat{y}_{\lim} + Bu_{crit} + \upsilon_{ad}(y_{\lim}, x_s, u_{crit}) \tag{37}$$

To reduce the computational demands, the calculation is made recursively. If the matrix is not square, the pseudo-inverse is used:

$$u_{crit}(t) = B^{-1}\{\upsilon_{ad}(y_{\lim}, x_{slow}, u_{crit}(t-\Delta t) + Ay_{\lim})\} \quad (38)$$

This critical control position is used as a constraint location manifested as tactile softstop and as a color coded textual visual display.

Limit Cue Output

This adaptive dynamic trim module was limit number 3 and used a softstop constraint cue. The softstop height was set at 1.0 and its length was 0.04 (1° of stick travel for the ±25° Radius of Motion). The cue position was placed 0.04 before the critical control position so that the constraint would begin before the critical position was reached. The softstop force would reach its maximum at the critical control position.

$$u_{cue} = u_{crit}^{+} - 0.04 \quad (39)$$

$$\left[N_{\lim} \quad u_{cue} \quad \Delta h_{cue} \quad \Delta \ell_{cue} \quad y \quad y_{\lim} \quad \lambda_{\Delta y}\right] = \left[3 \quad u_{cue} \quad 1.0 \quad 0.04 \quad y \quad 300 \quad \Delta y_{\lim}\right] \quad (40)$$

Limit Protection Performance

The UH-60 GENHEL model was flown in manned, RIPTIDE based simulation. The pilots flew numerous swoop maneuvers with and without the limit cue and the performance of the limit protection for blade stall was examined.

Figure 22 depicts the results of one of the maneuvers without any limit protection. The pilot simply flew the maneuver in a “carefree” manner. At 161 seconds, the pilot initiates the maneuver with full cyclic (u_δ = -1 or 25 ° forward) from out of ground effect (OGE) hover. By 166 seconds, the blade stall limit (ERITS = 300) is reached and violated. During much of the pull-up, the pilot chooses to use full cyclic (where u_δ=1). The limit violation lasts over three seconds while the aircraft pulls out of the high speed dive and reaches a (minimum) peak of 220 fps. The average maneuver time was 10.21 seconds.

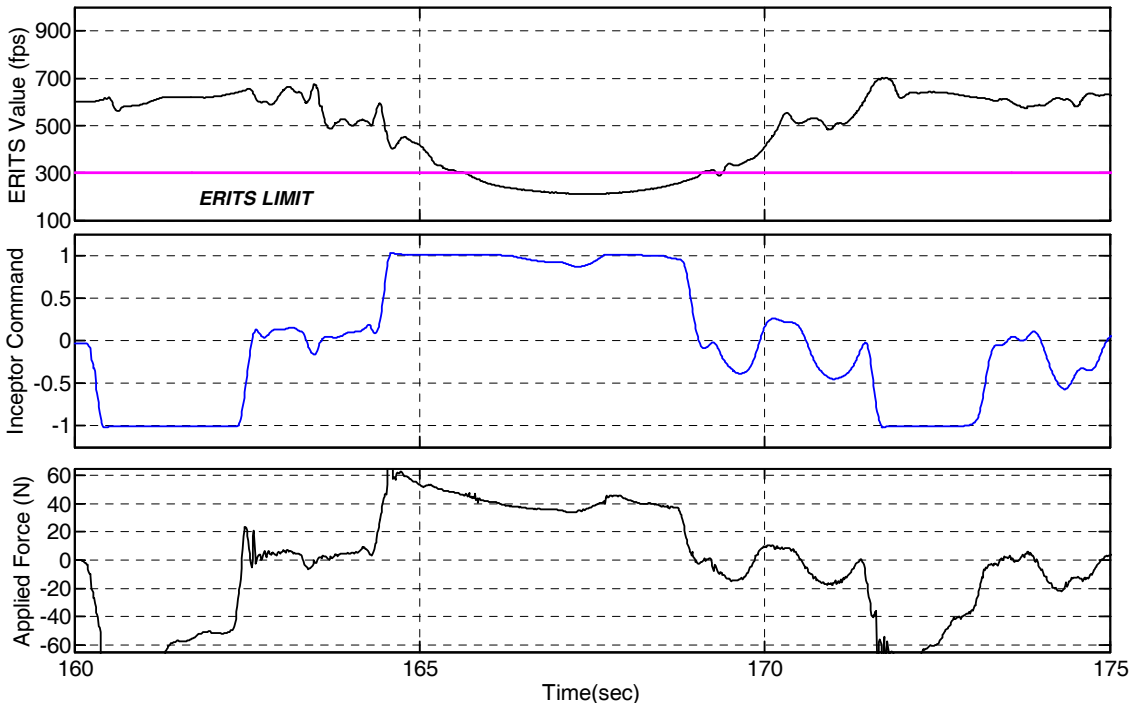

Figure 22. Blade stall ERITS parameter in swoop Maneuver without cue.

The swoop maneuvers executed with a tactile softstop constraint resulted in fewer and less severe limit violations. A characteristic example such a maneuver is shown in Figure 23. As before, the pilot initiates the maneuver from an OGE hover with full forward cyclic. But during the pull-up, instead of using full cyclic, the pilot allows the constraint to guide him. He encounters and follows the softstop (where $u_\delta = u_{SS} = u_{cue}$) from 171.5 to 174.0 seconds. The maneuver shows the pilot following along the edge of the limit boundary. Notably, the limit prediction and softstop cue oscillate from 169 to 171 seconds as the algorithm adapts to changing limit parameter dynamics and converges to a solution. This oscillation is exacerbated by biodynamic interaction of the softstop cue and the limb-manipulator system.

Conclusions

The adaptive neural network, a more sophisticated mechanism than the static network, required careful design of its update laws to ensure dynamic stability. But relative to a static neural network, it succeeds with fewer neurons and no significant *a priori* training. The static networks created for the HELMEE and HACT programs required extensive training databases from simulation time histories or math models. The Static Neural Network required a complementary low pass filter to eliminate its steady state

prediction errors. This mechanism, coupled with the limited update speed of the active sidestick, sometimes led to objectionable contact with receding softstops.

The adaptive neural network approach also suffered a soft-stop bumping problem that was caused by a volatile dynamic trim prediction while the aircraft was far from the limit boundary. While the adaptive prediction algorithm itself is stable, the oscillations during its convergence to a prediction may couple with biodynamic effects of the cue to create an objectionable cue which degrades the basic handling qualities of the aircraft. Such objectionable oscillations occurred many times during the evaluation of this limit cue. Although more detailed consideration is needed to find the best solution for these oscillations, it is clear that the proper choice of the network learning rate and error correction gain is important.

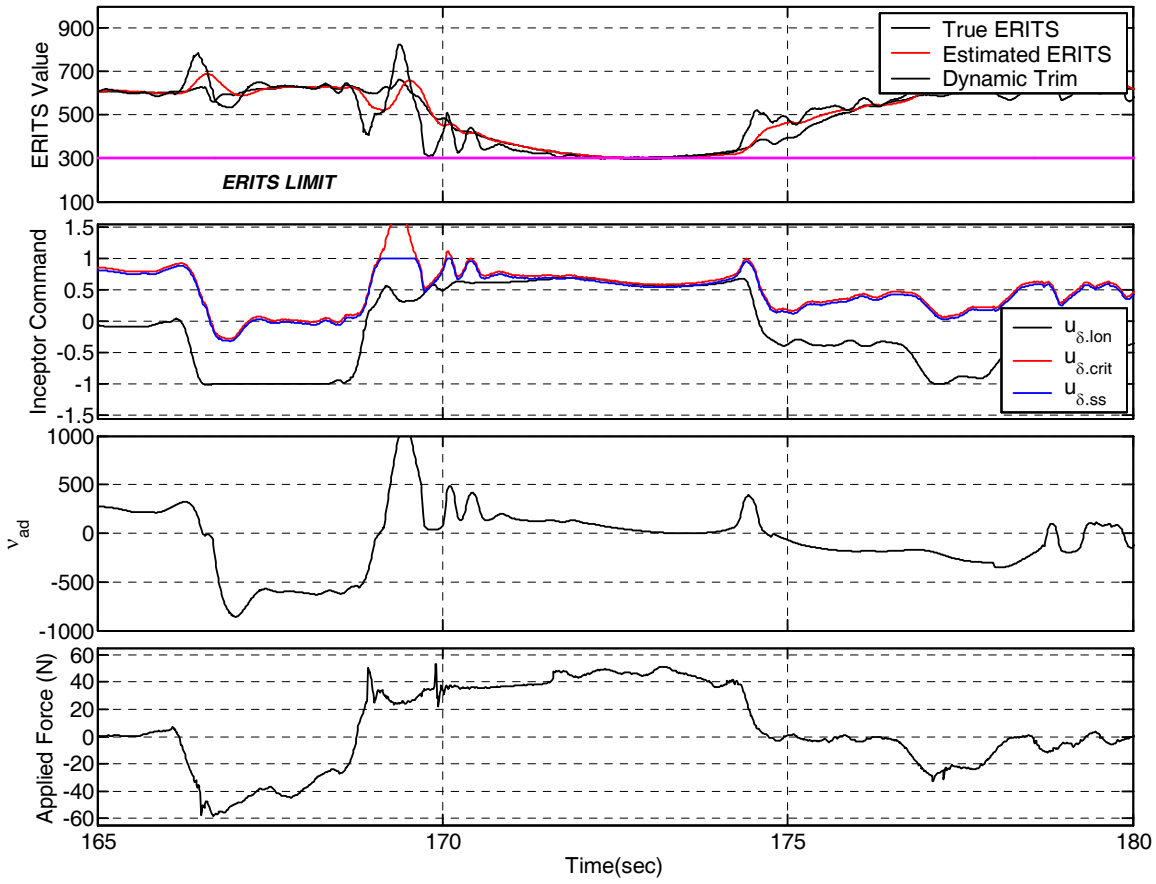

Figure 23. Blade stall ERITS parameter in swoop maneuver with constraint cue.

Limit Cue: Transient Peak Limit Protection for Hub Moment*

Static load limits on the main rotor hub, also known as mast bending limits, present a difficult challenge for the development of a carefree maneuver system. Limits on the maximum main rotor hub moment can be approached during highly aggressive maneuvers, when the CG is near operational limits or during ground operations when the attitude of the aircraft is constrained. In flight, hub moment is a highly dynamic parameter, and limits tend to be reached during the peak response immediately after a large control input or control reversal. After the initial control input, the magnitude of the hub moment tends to subside as the airframe responds to the applied moment. Hub moment limits are most likely to be exceeded in the longitudinal axis because of the higher moment of inertia and larger cyclic control range in the longitudinal axis.

Limit Cue Design

In order to predict the future response of the longitudinal hub moment, the dynamic system is modeled as a single input single output system (SISO) with longitudinal stick position ($u_{\delta.long}$) as the control input. The off-axis control coupling effects are negligible and ignored. The limit prediction static neural network was trained using a non-real-time simulation model. Though it was possible to generate them by perturbing the variables in non-real-time simulation, the approach was not used. Instead, the functions were extracted using non-real-time simulations in order to demonstrate how these functions can be obtained from flight test data. The training data was generated by performing standardized step and doublet type control inputs. The process was repeated for different trim conditions to obtain training data to adequately cover most flight speeds. The forward velocity in level trim flight was varied from 60 knots of backward flight to 120 knots of forward flight through variations of 20 knots.

Using the Dynamic Trim approach, the aircraft states are partitioned into slow states (x_s) and fast states (x_f). In the quasi-steady-state response (or dynamic trim) the fast states are assumed to reach equilibrium, and the slow states are varying in time. In the transient response, the fast states are represented by dynamical equations and the slow states assumed to be unchanged.

In this study, the peak response estimation algorithm[39] has been modified so that the transient response of the fast dynamics need not be modeled strictly using linear time

---

* This limit cue module was prototyped and tested in collaboration with Nilesh Sahani and Dr. Joseph Horn. The algorithm is explained in full detail in Ref 74 .

invariant equations. Instead the response of the limit parameter to a step input is represented by a series of functions as shown in the equation below.

$$y(x_s,t) = y_0(x_s) + \sum_{i=1}^{n} f^i(x_s,t)\, g^i(\Delta x_{f0}) + H(x_s,t)\Delta u \qquad (41)$$

This approach has two advantages: the dynamics need not necessarily be linear and the unknown function. The functions g^i , f^i and H can be readily identified using time domain methods. In the above equation, Δu is a step input from trim position. f^i and H are functions of only slow states and time. The control margin is calculated with an iterative search algorithm (see Figure 24) for the maximum stick input (the change from the current position) that would cause the predicted hub moment to reach its peak value.

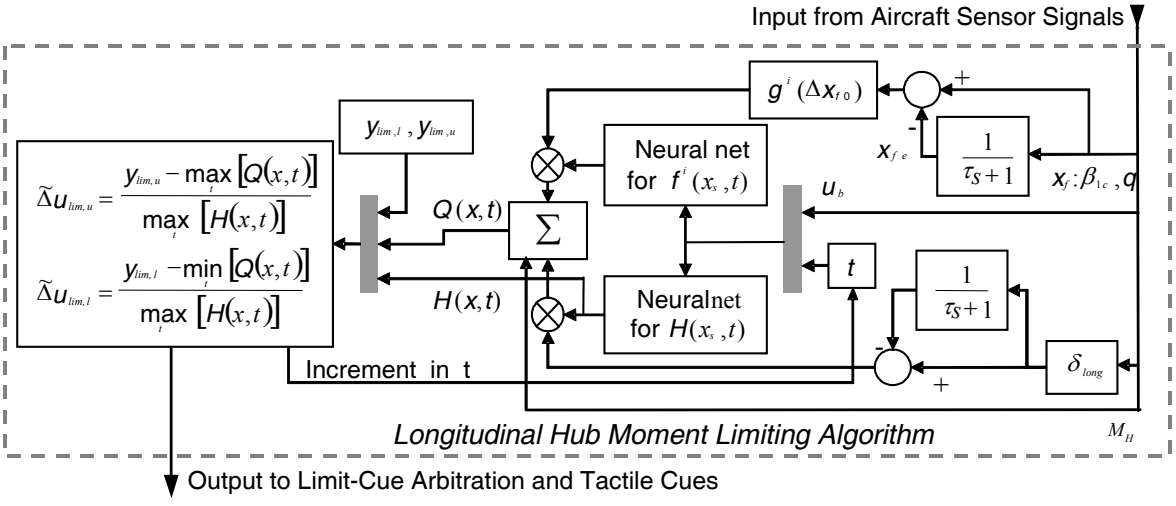

Figure 24. Schematic for Transient Peak Limit Cue

Limit Cue Output

This is limit number two. Like the ANN Blade Stall cue, this one sets the softstop position slightly before the critical control position and uses an abrupt constraint cue. The critical control position was used as the cue position. The softstop height was set at 0.75, which would create a softstop with three quarters the force required for maximum static deflection. The limit cue module provided two constraint vectors for the positive and negative hub moment constraints:

$$[N_{\lim} \quad u_{cue} \quad \Delta h_{cue} \quad \Delta \ell_{cue} \quad y \quad y_{\lim} \quad \lambda_{\Delta y}]$$
$$= [2 \quad u_{cue}^{+} \quad 1 \quad 0.04 \quad y \quad 20000 \quad \Delta y_{\lim}] \qquad (42)$$

$$[N_{\lim} \quad u_{cue} \quad \Delta h_{cue} \quad \Delta \ell_{cue} \quad y \quad y_{\lim} \quad \lambda_{\Delta y}]$$
$$= [2 \quad u_{cue}^{-} \quad -1 \quad 0.04 \quad y \quad -20000 \quad \Delta y_{\lim}] \qquad (43)$$

Limit Protection Performance

For purpose of the evaluation, the absolute hub moment limit was set to 20,000 ft-lb. This value does not represent the actual limit, but was selected in order to evaluate the performance under a restrictive flight envelope. Even so, the limit was not often approached accept for during extremely aggressive maneuvering. Thus, the evaluation maneuvers were defined to be so aggressive that the pilot would often move the cyclic control to the physical limits. Although such maneuvers might be considered unlikely, the idea was to evaluate the performance under "worst-case" scenarios, since those are the cases typically used for structural design.

The Attitude Capture and Swoop maneuvers were executed many times, but it's instructive to illustrate the performance of the cue by comparing nearly identical instances of the maneuvers with and without the tactile cue. Attitude variations for both the maneuvers are very closely spaced which allows good comparison to evaluate the effectiveness of the limit protection cues. Moreover, maneuver time for both the maneuvers are almost identical. It implies that the aircraft does not lose significant agility by restricting the hub moment to stay within the limits. Longitudinal stick position and longitudinal hub moment variation for these maneuvers are shown in Figure 25. Without cueing, the longitudinal hub moment shows peaks reaching up to 30,000 ft-lbs. But, with the limit protection system engaged, the hub moment stays within the limiting value of 20,000 ft-lbs. The points where the pilot encounters and follows the softstop constraints are circled in the figure. At these points, the hub moment reaches its limit almost exactly, without violating it. Note that there is a slight violation of hub moment just after 9 seconds in the maneuver. This is where the stick crosses the lower softstop. Here the pilot overrides the limit constraint softstop.

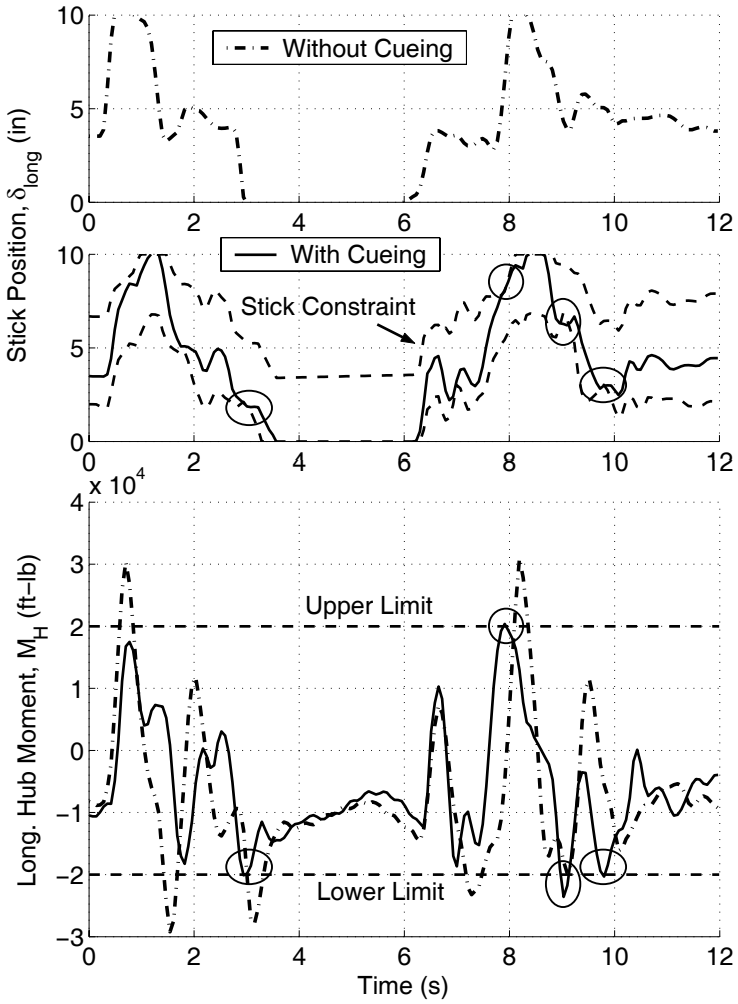

Figure 25. Attitude capture maneuver response with and without cueing.

Similar results for the swoop maneuver comparison are shown in Figure 26. Pitch attitude and total velocity variation with and without cueing are almost identical. Maneuver time is also the same for both the maneuvers. Stick position and hub moment variation are shown in Figure 26. Without cueing, the peak hub moment exceeds 30,000 ft-lb, but with cueing the peak hub moment stays very close to the limit of 20,000 ft-lbs. Again, the instances where the softstop guides the pilot are indicated by the circles in the figure. During the time interval of 6-8 seconds and 12-14 seconds, the stick input closely follows the upper and lower limit boundaries respectively. Without cueing, the stick input at these intervals shows sudden and large movements. But with cueing, the limit boundary appears to restrict the rate of the stick motion. It also indicates that the transient limits like hub moment are closely related to the rate of control stick input.

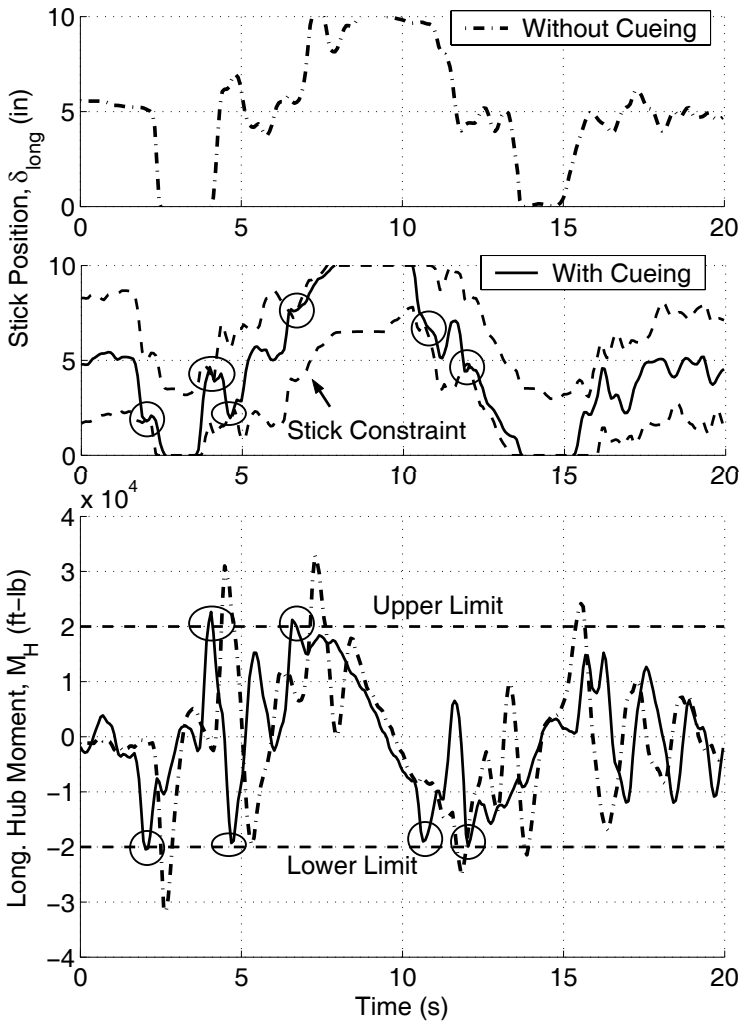

Figure 26. Swoop Maneuver response with and without cueing.

The pilots who flew the maneuver noticed the presence of the softstop cues. During the Attitude Capture maneuvers, the pilots felt that the cue "knocked" the sidestick back just before the pilot reached full aft stick displacement for the pitch up or full forward for the pitch down. The pilots did not consider the cue objectionable in such instances. It seemed to anticipate their control actions. It was the nature of the maneuver and the aircraft dynamics that the target attitude and the hub moment limit occurred at nearly the same time. The softstop was noticeably more intrusive (and least appreciated) when the pilot overshot the target attitude, especially in the Swoop maneuver. In these cases, both the forward and aft softstops sometimes came into play as the pilot tried to stabilize the aircraft at the target attitude. The pilots felt ricocheted back and forth between the softstops and considered the experience borderline objectionable, almost like interference.

This phenomenon can be seen at 4.0 and 4.5 seconds in Figure 26. This occurred in several of the maneuvers, during aggressive maneuvering in high speed forward flight. Typically, the forward and aft softstops were felt, at most, once each. After the half second or so that the forward and aft softstops "knocked" the pilot, the aircraft would reach the target attitude and the hub moment limit was no longer a factor.

A number of attitude capture and swoop maneuvers were performed in order to evaluate the possible performance and safety benefits of the hub moment limit protection system. The limit protection metric was a variation of the Integrated Limit Margin (ILM) which, in this case, was more descriptively named the Integrated Hub Moment Limit Exceedance Factor (IHMLEF). The factor combines violations of both maximum and minimum limits.

$$IHMLAF = \int_{t_0}^{t_f} \left| \min(0, \Delta y_{\lim}^{-}, \Delta y_{\lim}^{+}) \right| dt = \int_{t_0}^{t_f} \left| \min\left(0, \left(M - M_{\lim}^{-}\right), \left(M_{\lim}^{+} - M\right)\right) \right| dt \qquad (44)$$

Agility of the aircraft is measured in terms of maneuver time. The maneuver time was defined as the difference between the time when the pilot initiates the maneuver and the time when the response reaches and stays within the specifications signifying the end of the maneuver. Figure 27 and Figure 28 show the comparison of IHMLEF with and without cueing for attitude capture and swoop maneuver. Average maneuver time with and without cues for attitude capture maneuver is 12 seconds, implying the aircraft agility is not affected due to the cueing system. Average value for IHMLEF without cueing is 8100 ft-lb-s and with cueing is 1500 ft-lb-s, which amounts to 80% improvement. Average maneuver times with and without cueing for swoop maneuvers are 18 and 16 seconds respectively. Average values of IHMLEF without and with cues are 12100 ft-lb-s and 1800ft-lb-s, which amounts to about 85% improvement. Absolute values of peak hub moment for attitude capture and swoop maneuver are compared in Figure 29 and Figure 30. Average values of absolute peak hub moment for attitude and swoop maneuver without cueing are 32000 and 34500ft-lb respectively. For the same maneuvers, the values with cueing are 25300 and 25500 ft-lb respectively. It amounts to more than 20% reduction in absolute peak hub moment. Overall, the hub moment limit avoidance system should increase the safety and component life of the aircraft without adversely affecting the agility.

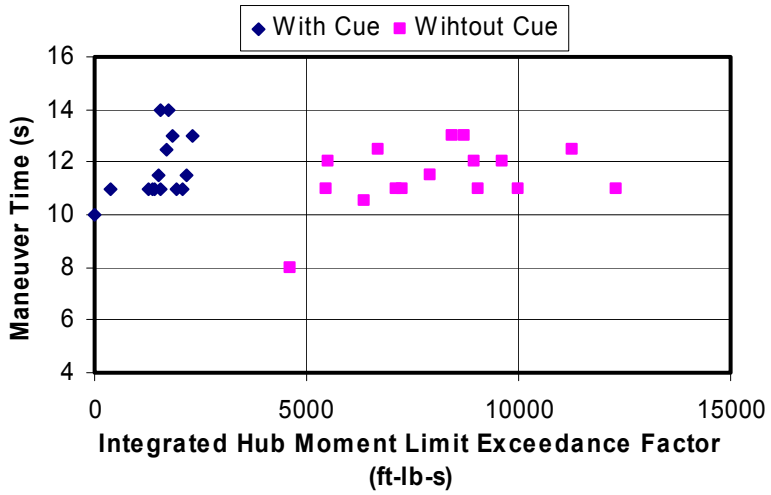

Figure 27. IHMLEF comparison for attitude capture maneuver

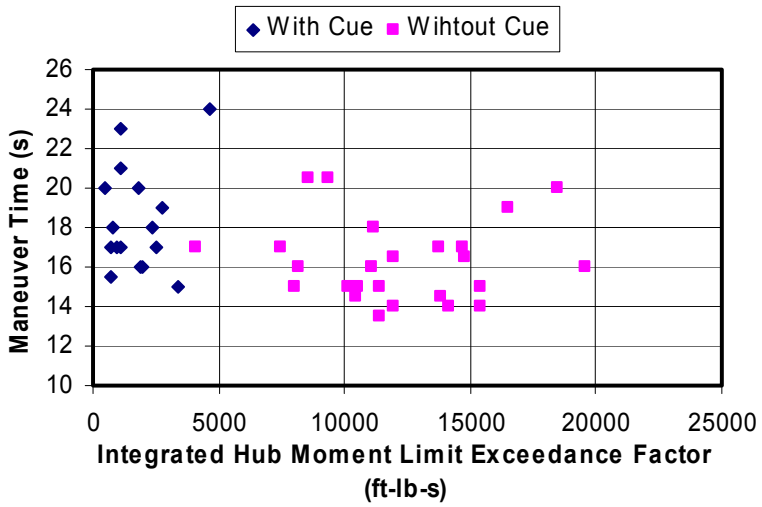

Figure 28. IHMLEF comparison for swoop maneuver

Conclusions

The maneuvers were flown aggressively, sometimes resulting in the controls moving to their physical hardstops or softstop constraint cues. The limit cue module was effective in predicting and providing an avoidance cue for the hub moment limit. The tactile cueing approach preserved the pilot's authority to over-ride the limit. The system did not inordinately restrict the agility of the aircraft. – the average maneuver time for the attitude capture maneuvers were nearly the same with or without the cue and the more dynamic Swoop was only slightly (12%) longer with the cue. In the maneuvers with limit protection,

the reduction in limit violations may indicate less fatigue wear to the structural components and may lead to in increased component life. Also, the reduced absolute peak hub moment may indicate reduced the risk of catastrophic structural failure.

Pilot comments indicated that the softstop cues were in some cases objectionable, particularly during very aggressive maneuvers when both the forward and aft limits were active together. Although the limit cue algorithm itself was effective, an improved method of limit protection (beyond a pure tactile cue) is desired. The remedy may be a better distribution between tactile cues and autonomous limit protection in the Arbitrator Module

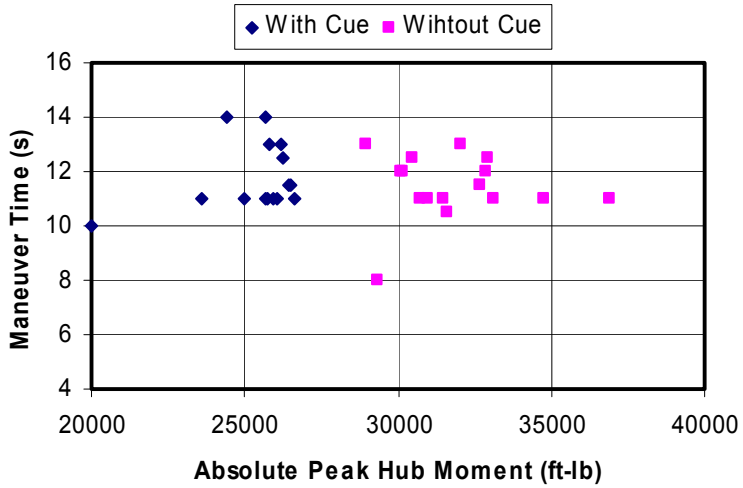

Figure 29. Absolute peak hub moment comparison for attitude capture maneuver

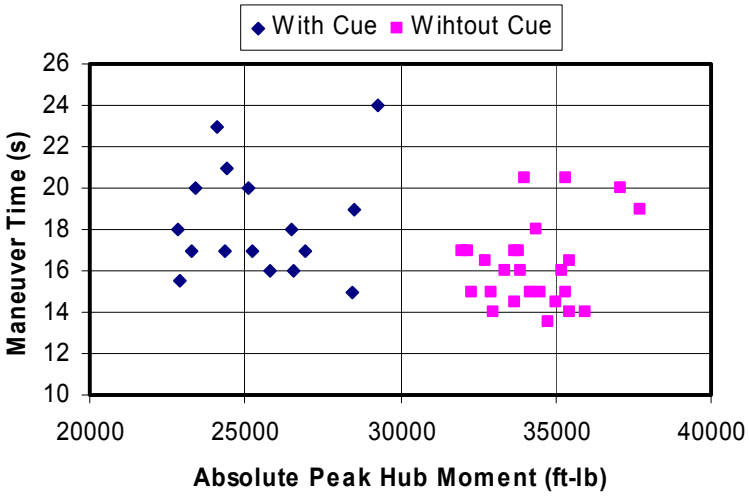

Figure 30. Absolute peak hub moment comparison for swoop maneuver

Arbitration Module

The Arbitration Module can be a complex element of an Open Platform for Limit Protection when the system has multiple, varied, and possibly conflicting limit cues – cues that must be arbitrated among and distributed to multiple points of the control system. But for the carefree maneuver system described here, the arbitration module has a fairly simple design that accommodates three sources of constraint cues, one alert cue, one transfer function cue, one friction cue, and control interfaces for tactile and visual displays.

Arbitrator Design and Output

Constraint Cue Selection

The constraint cue vector signals from the limit cue modules were divided into positive inequality control constraints, negative inequality control constraints, and equality constraints. The equality constraint algorithm, while not used by any of the limit cues would provide tactile detent cues, visual guidance pips, or control signals. The more conservative of the two types of inequality constraints is chosen (See Figure 31). That means that the positive constraint with the minimum cue position is chosen and the negative constraint.

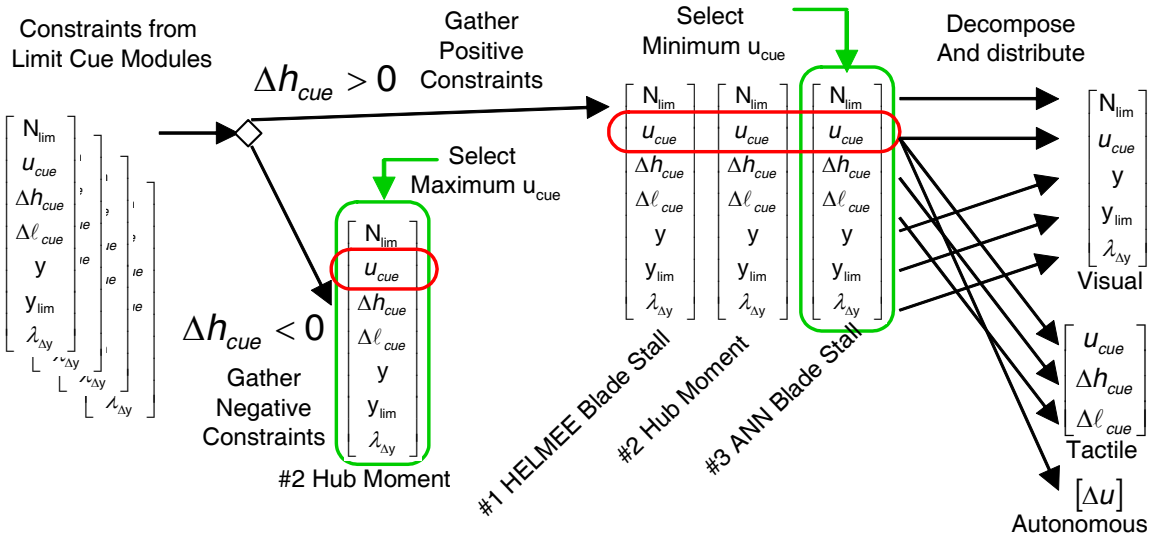

Figure 31. Conservative Constraint Selection

Alert Cue Selection

The alert cue is selected in a similar manner. The most conservative is chosen as that alert cue with the greatest amplitude among the alert cues

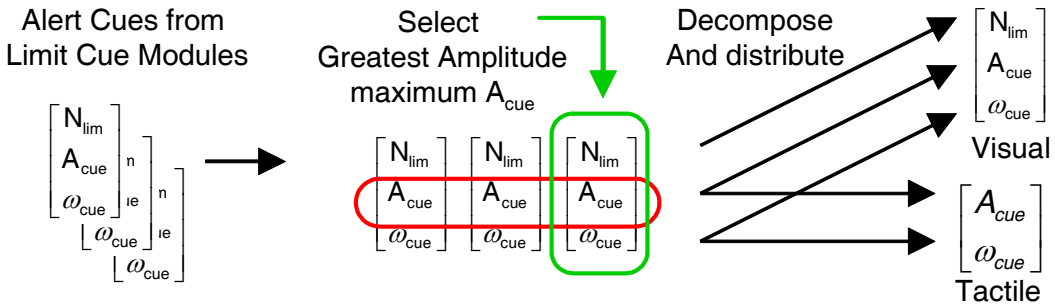

Figure 32. Conservative Alert Selection

Transfer Function and Friction Selection

The selection of the transfer function and friction cues is fixed and one-to-one. Only the PIO controllability limit provides these cues and they are fed through the arbitration module unchanged to the tactile interface.

Control Interface: Tactile Display

The control system interfaces for an OPLP based limit protection system are specific to the application. In this case the application is the RIPTIDE based flight simulation environment that uses a two-axis active sidestick (Figure 34) capable of all the force feedback cues described in chapter three: softstops, detents, bobweight dynamics, friction, and vibration.

Tactile Interface Design and Output

The tactile cue interface is a combination of C coded programs called as Simulink S-functions within the Simulink block diagram of the OPLP carefree maneuver system. These active sidestick S-functions send the parameters for the tactile cues to shared memory locations. A separate C code program reads that information and passes it though a point-to-point local area network to the active sidestick controller hardware.

The tactile cue parameters are computed from the limit protection cues from the Arbitration module as shown in Table 16. The transfer function cue defines the force-feel characteristics of the active sidestick as depicted in Figure 33. The pilot's communicates his control commands as his applied force. The active inceptor follows the dynamic response for displacement, in this case a second-order response with a natural frequency and a damping coefficient. Depending on the value chosen for the force/position command switch, μ, the inceptor subsystem provides a command signal based on the applied force, on the displacement response, or on a weighted combination.

Table 16. Limit Cue Conversions to Force Feedback

Limit Cue	Manifestation	Physical Qualities
Constraint	Softstop	Softstop force = $(RoM)k_f \Delta h_{cue}$
		Softstop length = $(RoM)\Delta \ell_{cue}$
		Softstop position = $(RoM)u_{cue}$
Alert	Vibration	Force Amplitude = $(RoM)k_f A_{cue}$
		Frequency = ω_{cue}
Transfer Function (See Figure 33)	Dynamics	Natural Frequency = ω_n
		Damping Coefficient = ζ
	Scaling	Force Scaling Factor, $K_{Fu} = \dfrac{K_0}{(RoM)k_f}$
		Displacement Scaling Factor, $K_{\delta u} = K_2(RoM)^{-1}$
Friction	Friction Force	Friction Force = $\mu(RoM)k_f$

The primary calculation here is the conversion of the nondimensional limit cues to the dimensional forces and displacements for the actual inceptor used. The designer chooses the radius of motion (RoM) and force gradient (k_f). The Radius of Motion was set at 25° for all the limit cues, but the different values for the force gradient were used. The PIO Limit Cue used k_f = 1.2 N/deg while the Hub Moment and Blade Stall cues used both that value and k_f = 1.6 N/deg. These gradient choices changed the amount of force required for maximum static deflection between 30 N and 40 N. These were the normalization values for forces.

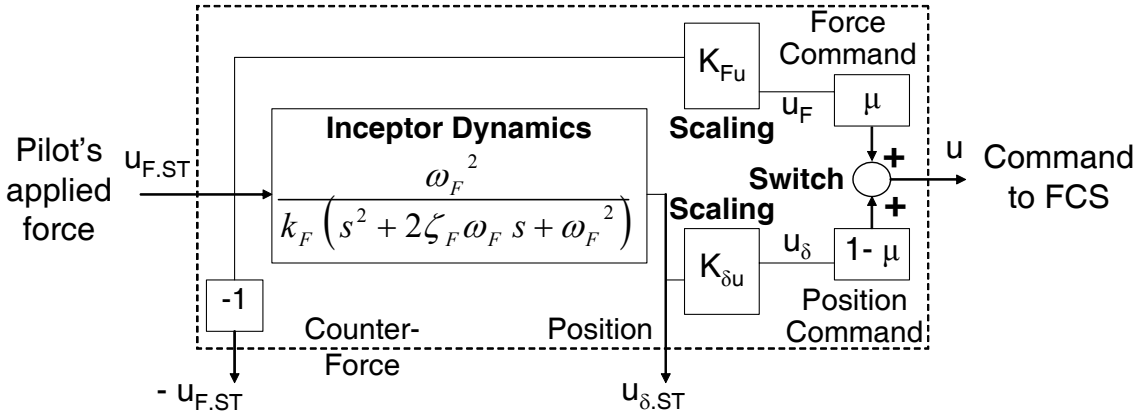

Figure 33: Force Feel Transfer Function

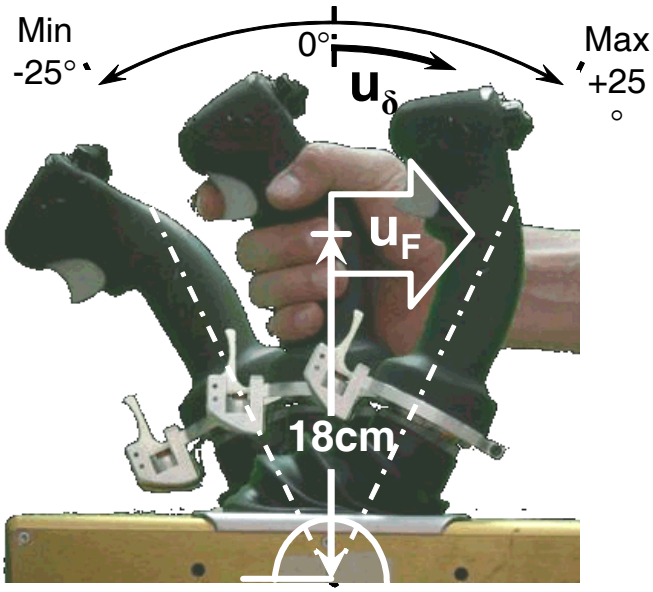

Figure 34: Active Sidestick Geometry

Control Interface: Visual Display

The visual interface design is specific to the RIPTIDE setup shown in Figure 16.

Visual Interface Design and Output

The visual cues appear as elements of the Heads Up Display (HUD) superimposed on the pilot's view. The limit cue information is passed to the HUD through an S-Function that saves constraint information to a shared memory location. A separate C code program creates the symbols, text, and colors using OpenGL commands for the Silicon Graphics Inc. OpenGL Performer rendering program.

The visual limit cues were simple, corroborating textual displays. When the constraint cue's Lagrange coefficient for limit margin ($\lambda_{\Delta y}$), becomes negative, the interface saves the limit identification integer (N_{lim}) and the value of the limit parameter (y) to the shared memory. The HUD component then changes the nominal display of simulation time to a textual display of the parameter value and the name of the limit as shown in Figure 35.

Another visual cue that may be driven by the constraint cue is a shape cue attached to the collective control position vertical scale. The style of visual cue is common and referred to as a vertical scale instrument. But unlike existing vertical scale instruments, which display limit parameters (like engine torque) and their maximum and minimum values, this visual indicator shows the control position (collective) and the location of the nearest limit constraint on that control axis.

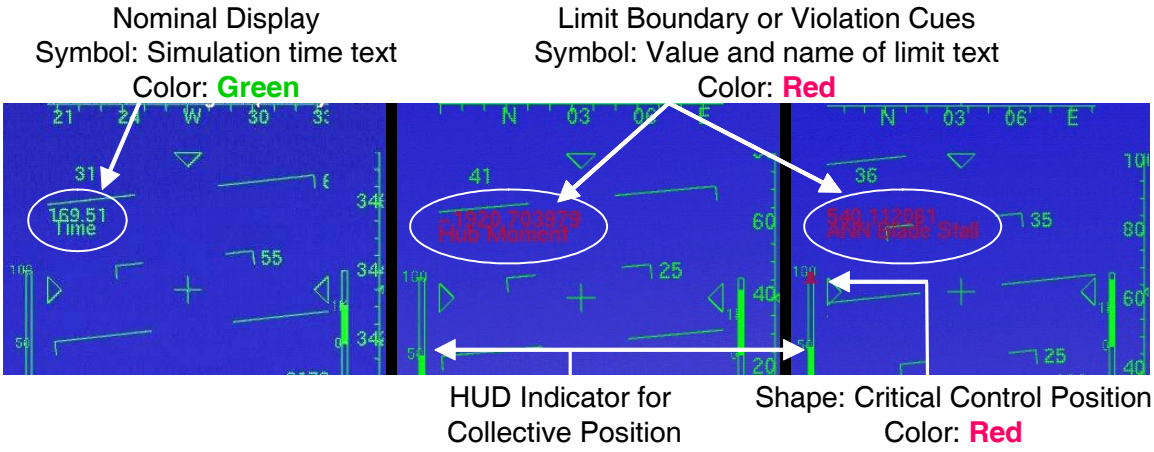

Figure 35. Heads Up Display Limit Cue

CHAPTER VI

CAREFREE MANEUVER DESIGN FOR A CONTROLLABILITY LIMIT

While pilot induced oscillation is a common term, it misleadingly implies that the pilot is the cause and that the event is oscillatory. Aircraft Pilot Coupling (APC) is a more accurate description of these closed loop events where neither the pilot nor the flight control system nor the aircraft are solely the source of the problem. Moreover, APC events range from minor bobbles to large-scale oscillations or to uncontrollable divergent flight. Severe APC events "are invariably new 'discoveries' that often occur in transient and unusual circumstances. To prevent their discovery by operational pilots under unfavorable circumstances, test pilots must be allowed some freedom to search for APC tendencies in simulations and flight tests."[93] But with limited time, money, and risk tolerance, an aircraft manufacturer can not completely explore and eliminate the possibility of PIO in some combination of uncontrolled variables and uncertainties that include changing pilots, modifications, environments, damages, malfunctions, and wear.

Pilot Induced Oscillation or, more accurately, Pilot Involved Oscillation (PIO) is a subset of Aircraft Pilot Coupling (see Figure 36) and has long been a flight control design consideration. The introduction of modern control system design specification and digital fly-by-wire flight control systems (FCS) has largely overcome the essentially linear category I PIO challenges to reveal subtler nonlinear category II and III PIO. Digital, fly-by-wire control systems can provide the pilot with familiar control response despite highly nonlinear flight dynamics, but they also sever the physical connection between the pilot and the aircraft and can mask the approach to controllability limits.

Emerging carefree maneuver technology is intended to protect vehicle limits and enable "carefree" flight for operational pilots. When the technology is incorporated into production aircraft, the intuitive tactile cues will allow ordinary pilots to safely and confidently maximize aircraft capabilities without undue in-cockpit attention to visual gauges and adherence to traditional handbook limits. Paradoxically, this performance multiplier may make operational pilots more likely than ever to encounter untested flight conditions prone to PIO. Consequently, limit protection systems should also include provisions to detect PIO controllability limits and provide avoidance cues.

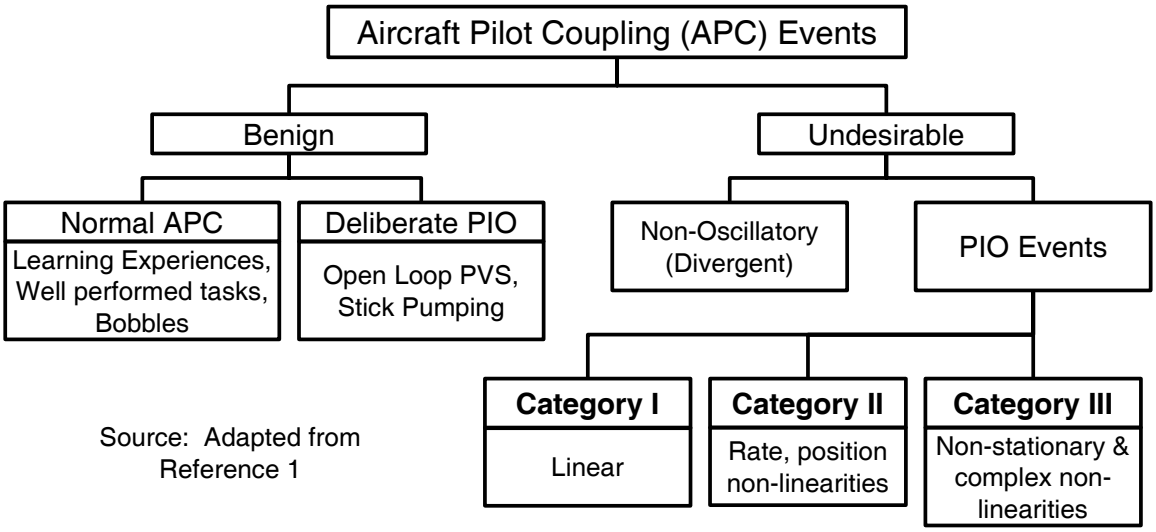

Figure 36: Taxonomy of APC Phenomenon

The Nature of the Limit

PIO is a controllability limit with many manifestations. Some of those manifestations (such as the category I events) have been studied and are understood to knowledge stage 7 (refer to Table 6) and design standards have been adopted to prevent them. However, the Category II and III events often have vehicle specific causes and knowledge of them may be an earlier stage of knowledge. However, the characteristics and qualities of a PIO event are known, and therefore can be detected, measured, and understood with the use of intelligent control methods (in this case fuzzy inference). The time scale of the limit varies, but PIO limit cycle times are typically 0.5 to 2.0 seconds. Divergent APC, while rare, can occur more quickly. This time scale, on the order of 1 second, means that cognitive cues are possible. Tactile cues and autonomous protections are also possible. The risk of PIO may be uncertain when new technologies are introduced that lead to unpredicted events and new forms of the phenomenon.

Limit Cue Design

This fuzzy logic PIO detector builds upon previous work into probabilistic neural detection of PIO[94] and real time parameter estimation[95]. It serves as a component of a PIO Limit Cue module with adjustable bobweight dynamics and friction cues.

Identifying Aircraft Pilot Coupling

Four primary indicators or distinguishing characteristics of a PIO event were designed into the fuzzy inference system and the fuzzy variable preprocessing. Every one was

drawn from the explicit conclusions, numerous cross-references, and case analyses presented in reference 1. These indicators are neither strictly necessary nor sufficient to define a PIO event, but "can provide useful warnings and design guidance." They are particularly applicable to category I and II PIO. Whenever possible, the specific qualities of an aircraft model's PIO propensity should be used to refine and quantify these indicators to improve the probability of correct detection and reduce false alarms. The general PIO indicators used for this fuzzy detector are as follows:

- The aircraft attitude lags the stick by nearly 180°. When systemic lags from any sources abruptly stretch the aircraft response to this degree, the pilot loses an accurate mental concept for aircraft control and may even suspect a control system malfunction.

- Pilot commands have very large amplitudes. When the pilot fails to recognize the changed nature of the aircraft response, he may interpret a delay as unresponsiveness and increase his command through the cockpit controls. This effective increase in the pilot gain exacerbates the delayed aircraft response and the pilot attempts to compensate with a larger reverse control movement. Such is the nature of diverging pilot induced oscillations.

- The main coupled frequency of the PIO falls within a range of approximately 0.3 to 1.5 Hz. This is a low frequency PIO range common for pilots operating in compensatory and synchronous modes. Higher frequency PIO events can exist, but they tend to be high-frequency limb-manipulator system coupling with high frequency aircraft modes. This higher frequency "ratchet" oscillation is too fast for cognitive pilot involvement. Oscillations slower than 0.3 hertz are rare. Any control system lags of this magnitude make the aircraft practically uncontrollable and lead to rapid divergence rather than oscillation.

- An element of the control system (such as a control surface actuator) is rate saturated. Rate saturation introduces a time delay into the overall control system only when the speed of control commands exceeds the capability of the actuator. Consequently, the aircraft reacts normally for a pilot flying typical flight maneuvers. But when the pilot maneuvers aggressively with high gain, for high precision tracking maneuvers, for example, the aircraft has a cliff-like control response.

The fuzzy logic inference system uses these same four indicators that a human "expert" would use to identify a PIO event. But before they can be applied, some signal

preprocessing is necessary to create fuzzy variables. Two signals, the inceptor control signal and the aircraft state signal, are pre-processed for frequency domain information. A third signal, the actuator position is processed for time domain information.

Although aircraft come in a wide range of sizes and configurations, and their cockpit inceptors take many forms, a general purpose fuzzy detector may still be effective. In a well designed aircraft, the control surface areas and their ranges of movement are sized to provide control authority between a minimum necessary for timely, confident maneuver and a maximum tolerable by a human pilot. The cockpit inceptor is likewise sized for human factors and mapped to aircraft responses bounded by the capabilities of the control surfaces. In an effort to generalize the fuzzy inference system, these design assumptions are adopted and the relevant inceptor, state, and actuator signals are non-dimensionalized during preprocessing.

The inceptor signal in this RIPTIDE environment is the physical displacement of the cockpit inceptor, a sidestick with a range of motion fore and aft 25°. It is normalized across its range of motion to [-1, 1]. The actuator position signal was likewise normalized across its range of movement to [-1, 1]. The aircraft state, aircraft pitch angle, was processed in degrees.

Real-Time Fourier Transform

Following the methodology presented in reference 95, the control and state signals are discretized at a 0.05 second sampling interval and scaled by the complex frequency factor. These sequences provide frequency content information that is accumulated in each respective finite Fourier transform. The recursive discrete transform has the form:

$$X_i(\omega_k) = X_{i-1}(\omega_k) + x_i\, e^{-j\omega_k(i\Delta t)} \tag{45}$$

The discrete Fourier transform is computed for a set of frequencies ranging from ω_k = 0.1 to 2.5 Hz (or 0.63 to 15.7 rad/sec). This encompasses the aircraft pilot coupling frequency range. The recursive relation is modified to consider only the frequency content of the recent past. A window of time (w) is defined and the frequency content of the signal before that window is removed from the transform:

$$X_i(\omega_k) = X_{i-1}(\omega_k) + x_i\, e^{-j\omega_k i\Delta t} + x_{(i-w)}\, e^{-j\omega_k(i-w)\Delta t} \tag{46}$$

This recursive finite Fourier transform, implemented across a vector of frequencies, and dimensionalized by window length was implemented in a Simulink® block diagram as shown in Figure 37. The FFT blocks provided a vector of discrete, finite Fourier transforms corresponding to the frequencies of interest.

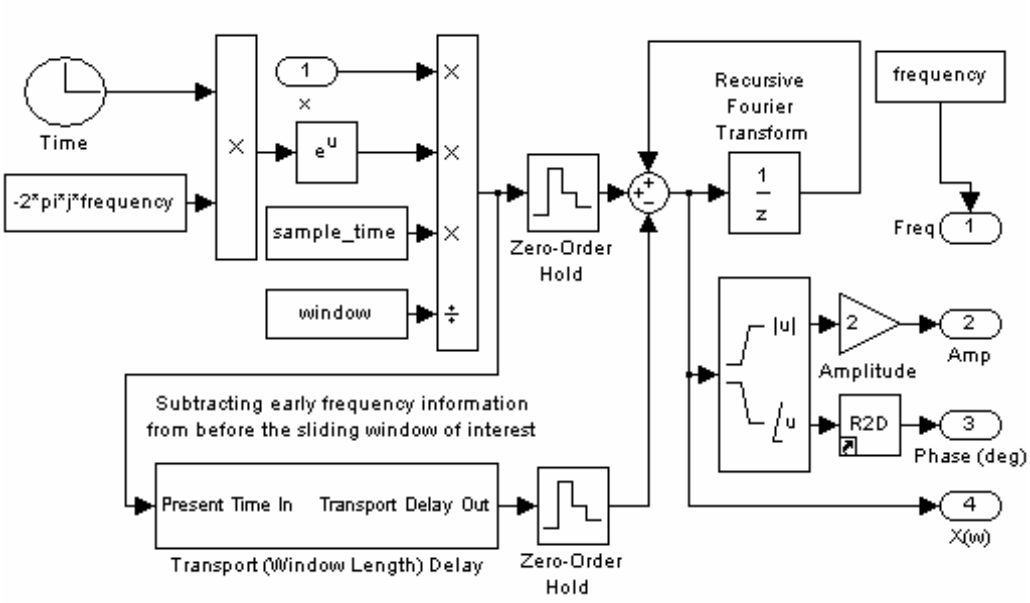

Figure 37: Recursive FFT Block Diagram

The remainder of the fuzzy variable preprocessing generally follows the methodology presented in reference 96 for a probabilistic neural detector for PIO. One difference is that the main frequency is selected as the component of the control signal with the largest amplitude rather than the frequency with the minimum phase lag. Also, the phase lag is not carried through as the degrees of lag but as the cosine of the phase lag. The cosine function served well to eliminate erroneous responses due to abrupt +/- 360° shifts in phase.

Once the main frequency is selected, the corresponding control and state amplitudes and the cosine of the phase lag become the fuzzy variable arguments of the fuzzy inference system as shown in Figure 38. The two time domain fuzzy variables are the magnitudes of the actuator speed and acceleration.

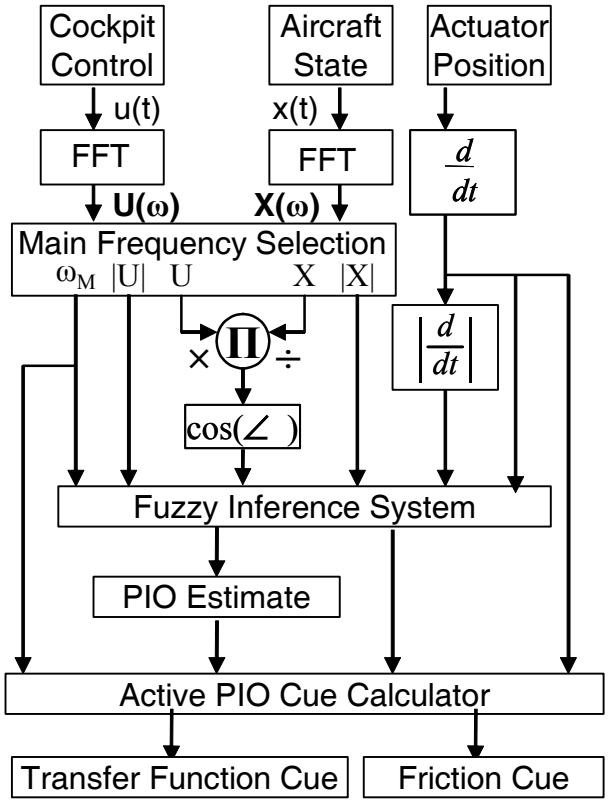

Figure 38: Preprocessing for PIO Limit Cue

Fuzzy Variables

For each of the fuzzy variables, a set of membership functions is defined to fuzzify them across their ranges of discourse. Some membership functions were ultimately deemed unnecessary and not included in any rule.

Main Control Frequency

The main control frequency fuzzy variable has three membership functions (Figure 39). The Nominal membership function uses a generalized bell curve centered at 0 Hz. This represents steady state trimmed flight or slow maneuvering. The APC Range function is a trapezoidal membership function that encompasses the 0.3 to 1.3 Hz range where coupled longitudinal oscillations occur in medium aircraft and helicopters. A notable example of this was the ADOCS helicopter PIO tendency (Ref. 1). The Over-controlling function represents high frequency movements beyond the bandwidth of the FCS-aircraft system.

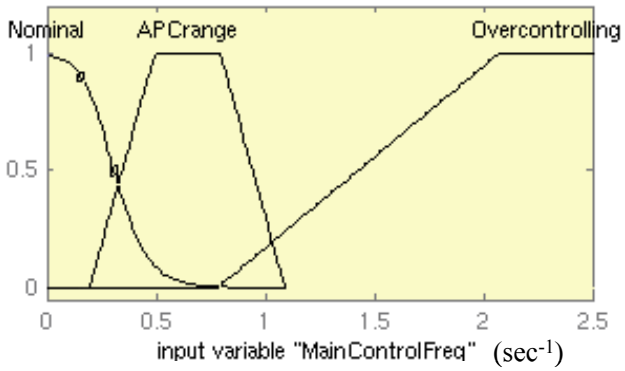

Figure 39: Main Control Frequency
Membership Functions

Main Stick Amplitude

The Main Stick Amplitude variable has only two bell curve membership functions (Figure 40). The Low function covers amplitudes less than about 30% of the inceptor radius of movement. The High function covers amplitudes over 60% of the radius of movement.

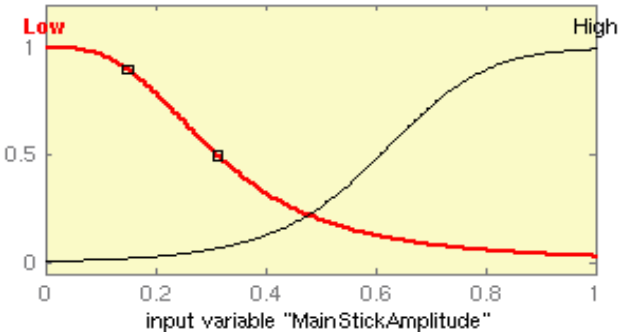

Figure 40: Main Stick Amplitude
Membership Functions

Cosine of Phase Lag (Main Frequency)

Three bell curved membership functions represent the -1 to +1 universe of discourse for the Cosine of Phase Lag variable (Figure 41). The Same Phase function covers values near +1 where the state nearly synchronizes with the inceptor. This is the normal flight mode for attitude command systems. The Lag 90 function covers values near zero where pitch leads or lags behind inceptor movements by 90º, as with normal rate

command systems. The Lag 180 function represents instances when the aircraft and the pilot are 180° out of phase.

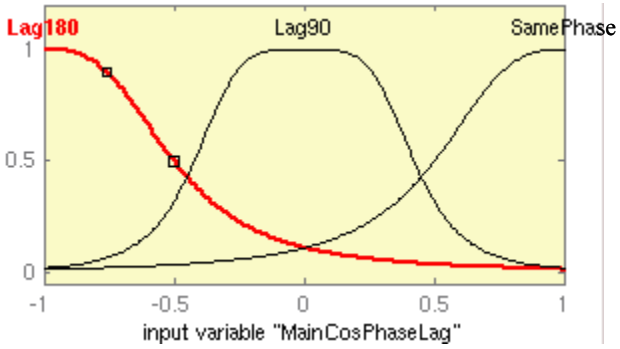

Figure 41: Cosine of Phase Lag for Main Control Frequency Membership Functions

Actuator Speed

No specific saturation rate is defined, but normalized actuator rates above 40% radius of movement per second are considered Speed Saturated. A trapezoidal membership function for Nominal rates is defined between 0.05 sec^{-1} and 0.40 sec^{-1}. The third function named Zero covers near zero actuator speeds (Figure 42).

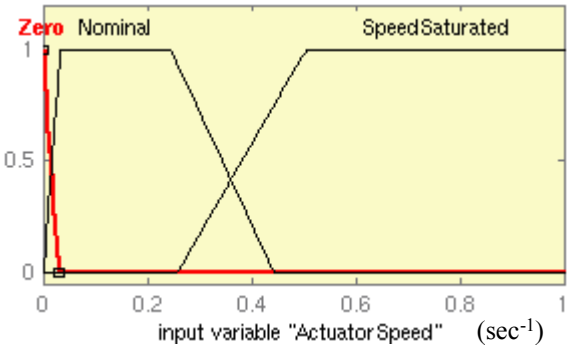

Figure 42: Actuator Speed Membership Functions

Actuator Acceleration

Actuator acceleration has two membership functions (Figure 43). The Zero function represents constant actuator speed while the Non-Zero function represents all other speeds.

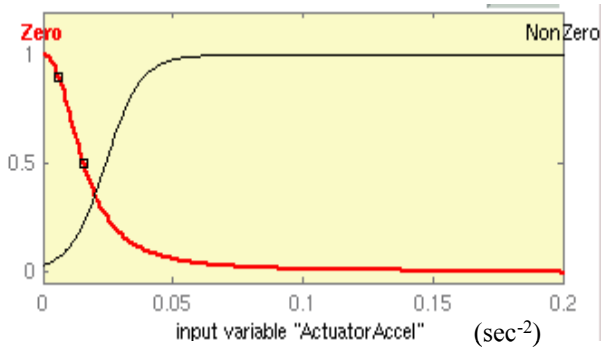

Figure 43: Actuator Acceleration Membership Functions

PIO Estimation

PIO Estimate is the fuzzy output variable and has two bell shaped membership functions (Figure 44): Low, meaning that this is not a PIO event; and High, meaning that it is. They are strongly weighted around 0 or 1 with low membership fulfillment in the mid-range. This accentuates the differences PIO and non-PIO events.

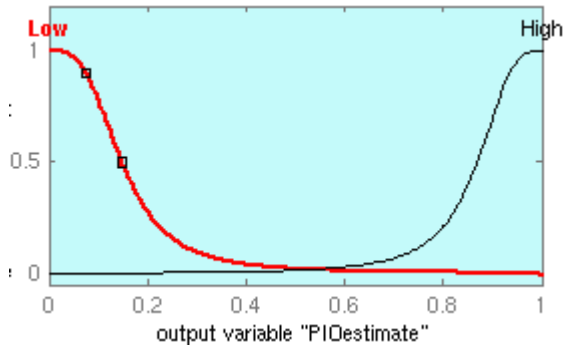

Figure 44: PIO Estimate Membership Functions

Fuzzy Rule Set

The pilot induced oscillation detector uses a Mamdani fuzzy inference system with minimum for implication and maximum for aggregation. The AND method is used for the minimum. Defuzzification is made from the centroid of the Max-min aggregate.

The single output is the PIO Estimate, which assesses whether the present flight condition is a PIO event. The output is not a binary decision of PIO or NOT PIO. It provides a continuous assessment of the PIO severity from 0 (meaning no PIO) to 1 (Severe PIO). The fuzzy rule set uses both positive rules that identify PIO characteristics

and negative rules that identify normal flight characteristics. The positive rules increase the PIO estimate while the negative rules discriminate normal but possibly oscillatory flight and decrease the PIO estimate. All the rules are equally weighted, except for the Phase Lag rule, which is doubly weighted.

Phase Lag Rule

	Fuzzy Variable		Membership Function
IF	MainControlFreq	is	APC_range
AND	MainStickAmp	is	High
AND	MainCosPhaseLag	is	Lag180
THEN	PIO Rating	is	High

The Phase Lag rule is a positive rule satisfied when the pilot and the aircraft are nearly 180° out of phase. It is given double the weight of the following rules because it is deemed the most reliable indicator of pilot induced oscillation.

Nominal Frequency Rule

IF	MainControlFreq	is	Nominal
THEN	PIO Estimate	is	Low

The Nominal Frequency Rule is a negative rule that identifies steady state, trimmed flight. In this flight condition, the recursive Fourier transforms lacks adequate high frequency content to provide a reliable the phase lag estimate for those frequencies, but the phase lag for the low frequencies may remain accurate.

Same Phase Rule

IF	MainCosPhaseLag	is	SamePhase
THEN	PIO Rating	is	Low

The Same Phase rule is a negative rule that identifies normal flight regardless of how extreme the maneuver may be. This rule counters the Phase Lag rule.

Actuator Saturation

IF	ActuatorSpeed	is	SpeedSaturated
AND	ActuatorAccel	is	Zero
THEN	PIO Rating	is	High

The positive Actuator Saturation rule applies to instances where the actuator speed is high while the acceleration is zero. This describes the qualitative nature of speed (rate) saturation without defining a particular saturation rate.

Nominal Actuator

IF	ActuatorSpeed	is	NOT SpeedSaturated
OR	ActuatorAccel	is	Non-Zero
THEN	PIO Rating	is	Low

The negative counter to the Actuator Saturation rule is this Nominal Actuator rule. This rule accounts for instances were the actuator has a constant speed as a normal result of intentional flight control.

Rule Surface

The rules operate together to form an assessment of pilot induced oscillation that can be depicted graphically for a set of input arguments (Figure 45 and Figure 46). The flat shelf at PIO Estimate = 0.37 is due to the partially satisfied positive Actuator Saturation rule. That PIO Estimate shelf slopes downward along the near left edges of the two figures due to the negative Same Phase rule and the negative Nominal Frequency rule respectively. The tall peak of PIO Estimate is due to the Phase Lag rule.

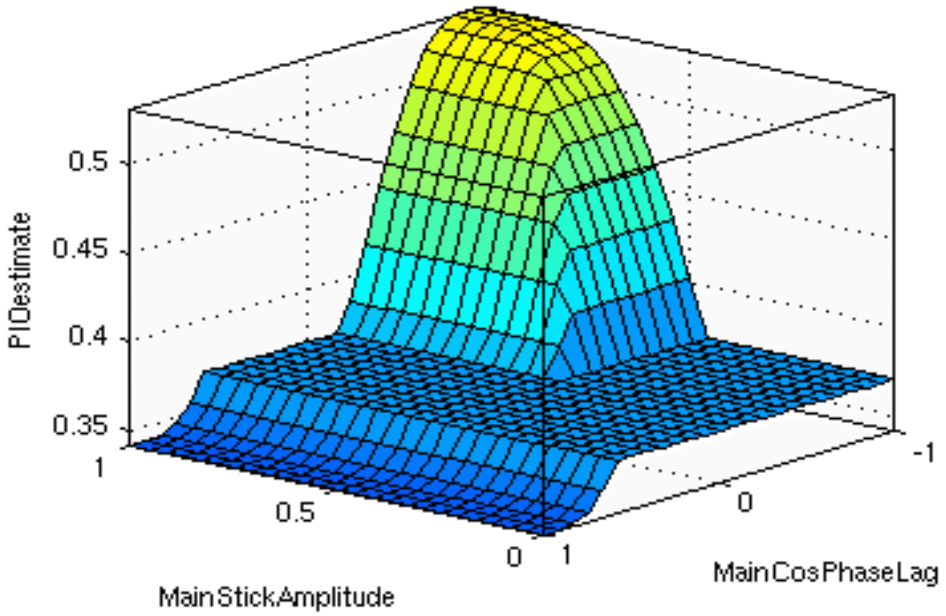

Figure 45: Rule Surface

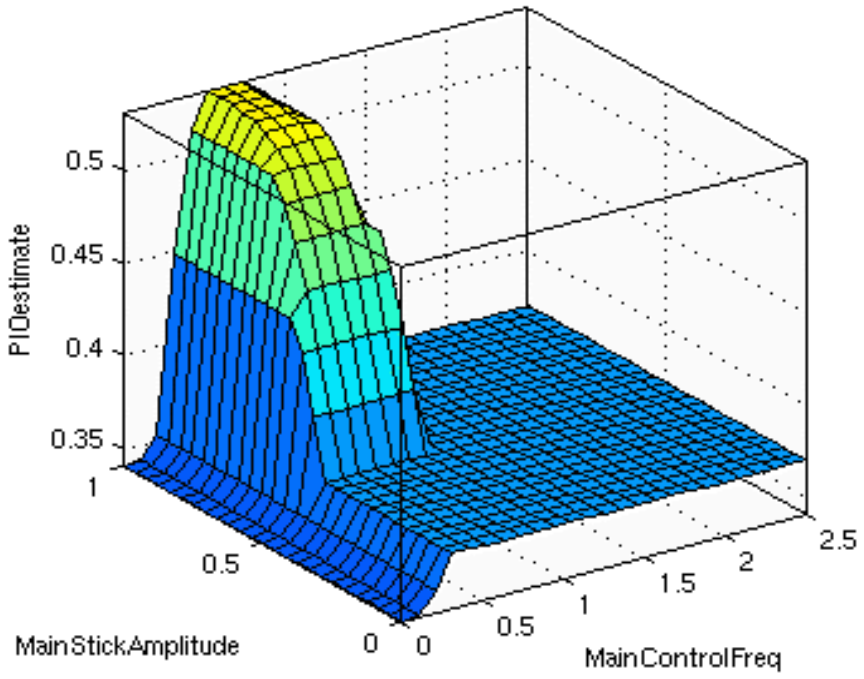

Figure 46: Rule Surface

Force Feel Dynamics in Closed Loop PIO

Considerable research into inceptor dynamics, handling qualities, and pilot induced oscillations provides the framework for understanding PIO and lessons for control systems design. Military Specifications quantified force feel requirements[97], introduced the use of an equivalent system for complex fly-by-wire flight control systems[98], but generally exclude the inceptor dynamics from the equivalent time delay calculation.

When the pilot and the airplane are modeled with describing functions, their open loop transfer function for a PIO limit cycle would be:

$$Y_P(s)Y_C(s) = -1 \tag{47}$$

If we extract the inceptor subsystem from the vehicle system the description becomes:

$$Y_P(s)Y_{FS}(s)Y_C(s) = -1 \tag{48}$$

But this implies an open loop analysis with neither intra-loop proprioceptive feedback from the inceptor to the pilot nor biodynamic feedback from the aircraft to the limb-manipulator system.

Closed loop assessment criteria, such as the Neal-Smith and Smith-Geddes[99] assume some form of pilot model, whether synchronous, compensatory, or more detailed switching models. Although debate persists regarding exactly how to account and design for inceptor dynamics, the desirable qualities of a cockpit inceptor are generally known. But to place those qualities in the context of an active inceptor cues for PIO, first consider a closed loop model to replace open loop models above.

For the purpose of examining the inceptor in various PIO events, the inceptor centered model (Figure 47) was adapted from several references [1,100,101,102.] It includes the stick force and displacement proprioceptive feedback and biodynamic reaction to aircraft accelerations but omits other noise introduced at the limb and stick.

The model shows three control signal feedback loops: the cognitive feedback to the pilot from the aircraft state (or perceived output), the biodynamic feedback from the aircraft to the limb-manipulator system, and the proprioceptive feedback from the inceptor to the pilot. The first two feedback loops distinguish two forms of PIO and the third offers a mechanism to address them.

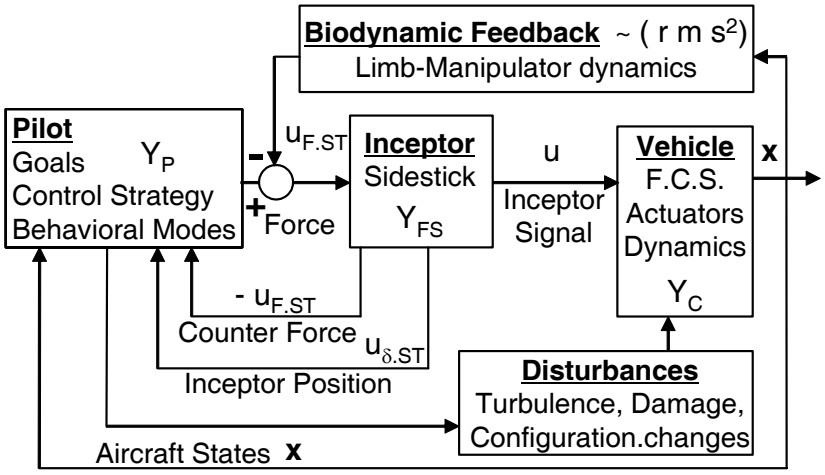

Figure 47: Inceptor-centric Pilot-Vehicle System

The outer loop accounts for the pilot's conscious efforts to control the aircraft. It includes the decisions he makes to accomplish mission goals. These decisions interact

with the vehicle over a few seconds and longer and lead to changes in environment and aircraft configuration which may also trigger changes in the effective dynamics of the total vehicle (including the flight control system, actuators, and aerodynamics). The pilot maintains a control strategy for his concept of the aircraft behavior and response. Within the context of that control strategy and the immediate mission goals, he adopts a behavioral mode. The assessment criteria approximate the pilot's control strategy and behavioral modes with the pilot models already mentioned.

Cognitive pilot involved oscillations, which manifest in frequencies less than about 1.5 Hz, are due to a sudden disconnect between the pilot's concept of the aircraft's response and its actual response. This disconnect is usually due to changes in the total effective vehicle dynamics, and results from combinations of actuator limits, control law changes, stick signal shaping, and so on.

The biodynamic feedback loop accounts for the effects of aircraft accelerations on the pilot's limb grasping the cockpit control. Roll ratchet, yaw chatter, and the less common pitch bobble are names for this form of PIO. The peaking frequency of these events is typically too fast for conscious involvement, above 1.5 Hz, and it is a non-cognitive PIO. It most commonly appears in aircraft with excess roll damping when the roll acceleration moves the pilot's forearm side to side on the center or sidestick. It is less common in pitch; where aircraft dynamics are slower and the larger mass of the forearm plus upper-arm reduce the peaking frequency to within the pilot's conscious ability to control it. Still, this type of feedback in pitch and roll has been destructive to helicopters making sliding landings that lead to forms of dynamic resonance.

The flight control system can address biodynamic feedback through inceptor signal prefiltering and appropriate rate damping. The inceptor dynamics can also counter excess control system roll damping with a greater damping. All of these solutions introduce an effective delay and reduce the bandwidth in an axis (roll) where rapid response is expected. This PIO tactile cue is a channel of information added to visual and aural cues, will not address non-cognitive forms of PIO.

Active Inceptor Dynamics

An active inceptor offers many forms of real-time alterable force (that is, counter-force) cues, including its nominal static force displacement relationship plus softstops, detents, shakers, force dynamics, and friction.

$$F_{ST} = F_{nom} + \sum_i F_{ss\,i} + \sum_j F_{\det j} + F_{\omega} + F_{\omega_F \zeta_F} + F_{fric} \tag{49}$$

The tactile cues for this PIO controllability limit use only force feel dynamics or friction. Other force cues (softstops, etc.) are not included $\left(F_{ST} = F_{\zeta_F \omega_F} + F_{fric}\right)$. The force feel dynamics of the SA-S-2D-1 active sidestick are second order, bobweight dynamics shown in Figure 33.

The pilot's force against the sidestick is the subsystem's input. It's output, u, is the input signal for the flight control system. In general, depending on the switch, an inceptor signal may be either a force command, $u = u_F$, a direct measurement of applied force; or a position command, $u = u_\delta$, where stick displacement resembles a second order system. An active inceptor can alter, in real time, each of the three parameters (force gradient, damping coefficient, and natural frequency) and it can serve as a force command stick or a position command stick and change modes during flight.

The scaling parameters, K_{Fu} and $K_{\delta u}$, of the inceptor model translate force or displacement into the normalized input signal for the flight control system. The control systems developed for RIPTIDE accept normalized signals between -1 and 1. The sidestick position is measured in degrees and its maximum 25° radius of motion implies that $K_{\delta u}$ has a minimum value of 0.04 deg^{-1}. The definition of K_{Fu} is not obvious because the pilot's maximum force is not artificially limited, as the radius of motion is. The nominal value will be set such that the static force required to displace the stick to its radius of motion equates to unity, $K_{Fu} = (k_F \, RoM)^{-1}$.

Findings by two studies suggest guidelines for the range of force-feel parameters. The first study[16] considered both force command and position command inceptors as center or side sticks. A force command stick (μ=1 in the switch in Figure 33), is commonly implemented as an isometric stick, and has the advantage of minimal forward loop dynamic lag and superior performance in tracking tasks. Its transfer function is simply:

$$Y_{FS} = \frac{u}{F_{ST}} = K_{Fu} \tag{50}$$

Its chief drawbacks are its denial of position as a tactile cue and its susceptibility to biodynamic feedback whose cure, command pre-filtering, adds a delay that offsets its low-lag advantage.

A position command stick (μ=0), transfer function is:

$$Y_{FS} = K_{\delta u} \frac{\omega_F^{\ 2}}{k_F \left(s^2 + 2\zeta_F \omega_F s + \omega_F^{\ 2} \right)} \qquad (51)$$

The study varied damping and natural frequency and found that handling qualities deteriorated with increasing effective dynamic delay, $\tau_e = 2\ \zeta_F / \omega_F$, but otherwise found pilot performance unchanged while natural frequency remained above about 2.2 Hz.. The second study[103] also considered inertia with regard to cyclic sticks in rotorcraft and found that stick frequencies even as low as 0.8 Hz were acceptable as long as the inertia of the stick was below an acceptable threshold.

PIO Tactile Cues

Three forms of tactile PIO avoidance cues were tested for a position command inceptor to address pilot over-controlling tendencies, actuator rate saturation, and altered aircraft dynamics during PIO. The active dynamics and friction cues were evaluated individually and in several variations, including both discrete on/off cues, where μ was binary; and gradual switching, with a continuous $\mu \in [0, 1]$. The latter variations were easily implemented with the Fuzzy PIO detector, which provided a continuous output between 0 and 1 that was linearly mapped to μ. The binary approach used a relay to turn on the cue at a threshold PIO Estimate level and leave it on until the PIO Estimate dropped below a lower value. The graphical results shown below are all versions with a binary μ because they better depict the performance of the cue in a shorter span of time.

Cueing Actuator Saturation with Friction

Actuator rate saturation and position saturation can cause or exacerbate a PIO event by abruptly increasing the phase lag. A friction force, triggered by the Actuator Saturation Rule in the Fuzzy PIO Detector, can inform the pilot of the onset of rate saturation.

Initially, the cue used a constant coulomb dynamic friction force triggered by a rate saturation detection rule-set within the Fuzzy PIO detector. With physical testing, the cue was found to be marginally useful while the friction remained low, below 5 N. Higher forces became objectionable and interfered with pilot control. While this variation of the cue did alert the pilot to the saturation, it did not provide a constructive intuitive correction because it also retarded even his corrective control reversals to counter saturation.

A more effective variation of this cue used uni-directional friction. The cue required the addition of a sixth rule to the Fuzzy PIO detector to distinguish between positive and negative rate saturations. Uni-directional friction cues pilot against exacerbating the rate saturation without hindering corrective movement. Because this form of friction does not hinder corrective action, a larger force (about 15 N) may be used to make the cue more noticeable and effective.

Cueing PIO with Active Dynamics

When examining the dynamical cues with respect to the pilot, it is helpful to partition the pilot's effective transfer function into control strategy and limb-manipulator behavior:

$$Y_P = \hat{Y}_P \left(\frac{U_\delta}{U_F} \right)^{-1} \tag{52}$$

The first term, $\hat{Y}_P$, represents the control intention that the pilot wants to communicate to the aircraft control system and the second term is the pilot's concept of the man-machine interface that is the position command inceptor. This "concept" is the actionable, internal element model mentioned on page 24.

The design of this active dynamics cue, presupposes a structural pilot model[104] where the human control strategy is based on the integration of proprioceptive and tactile sensory information rather than differentiation of visual cues. This model supports the demonstrated benefits of the "matched manipulator" concept[105] for control scenarios, which can include longitudinal PIO about a base attitude. This concept uses a force command sidestick (μ=1), and equation 4 holds with regard to the input to the flight control system. The human pilot senses the stick position, u_δ, and stick dynamics effectively appear in the numerator of the pilot's closed loop transfer function:

$$Y_P = \hat{Y}_P \frac{U_F}{U_\delta} = \hat{Y}_P \frac{k_F \left(s^2 + 2\zeta_F \omega_F s + \omega_F{}^2 \right)}{\omega_F{}^2} \tag{53}$$

If the stick dynamics match a second order vehicle system,

$$\frac{U_\delta}{U_F} \approx \frac{K_C \omega_C{}^2}{\left(s^2 + 2\zeta_C \omega_C s + \omega_C{}^2 \right)} = \frac{X(s)}{U(s)} = Y_C \tag{54}$$

the pilot realizes a direct gain control strategy :

$$Y_P Y_{FS} Y_C \approx \hat{Y}_P \left(k_F K_{Fu} K_C \right) \tag{55}$$

If the limit cycle of the aircraft in a PIO event can be dynamically approximated with second-order force feel dynamics, at least in a narrow frequency range around the PIO frequency, the pilot perceives the above transfer function of the aircraft system during a PIO event as:

$$Y_P Y_{FS} Y_C = \hat{Y}_P \frac{k_F K_{Fu} K_C \omega_C{}^2 \left(s^2 + 2\zeta_F \omega_F s + \omega_F{}^2 \right)}{\omega_F{}^2 \left(s^2 + 2\zeta_C \omega_C s + \omega_C{}^2 \right)} \tag{56}$$

Approximations for ω_C and ζ_C can be made with either of two methods. A simple method, used during manned evaluation of this cue, is to assume an appropriate value for an under-damped system such as $\zeta_C = 0.4$, and calculate the vehicle's effective natural frequency using ω_{PIO} as the effective damped frequency:

$$\overbrace{\zeta_C = \zeta_o}^{Assume} \rightarrow \omega_C = \frac{\omega_{PIO}}{\sqrt{1 - \zeta_o{}^2}} \tag{57}$$

For sustained or diverging coupled oscillations, the effective damping coefficient is small and any errors in the calculation of ω_C from ω_{PIO} would also be small.

An alternative method for approximating second order vehicle dynamics follows from the Fuzzy PIO detector preprocessing, which computes the finite Fourier transforms for the frequencies in the PIO range. Real time parameter estimation[106], though only truly accurate with linear systems, can still approximate ω_C and ζ using the FFTs for frequencies at and above the PIO peaking frequency, ω_{PIO}.

The inceptor system could introduce a second order lead or lag, but to minimize unpredictable interference with the flight control system, the sidestick natural frequency is set equal to the approximated natural frequency of the vehicle in a PIO event, ($\omega_F = \omega_C$). The stick damping coefficient, however, may be set lower than the approximated aircraft damping. The resulting transfer function, when the gains are properly set, provides a unity gain across the frequency spectrum except near the PIO frequency, where feedthrough is diminished as shown in Figure 48. At first glance, this result implies that the active dynamics cue is taking control authority away from the pilot, but the effect involves the pilot's conscious recognition of changing vehicle dynamics and his intentional adaptation to the PIO event.

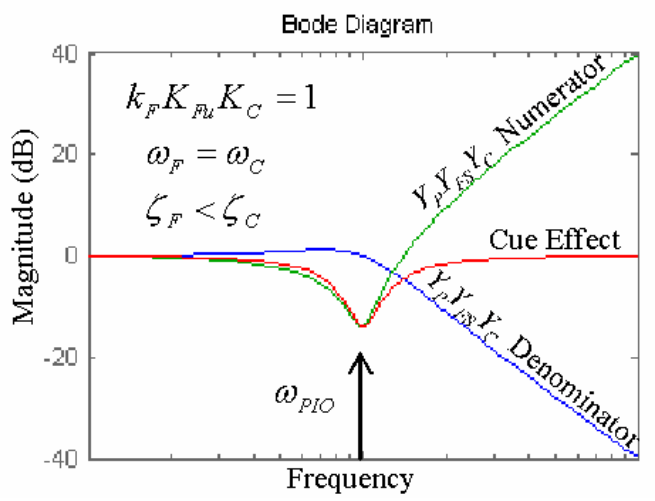

Figure 48: Bode Diagram of Active Dynamics Cue

Limit Cue Output

The inceptor nominally acts as a position command stick with a 25° radius of motion and baseline dynamics with an effective delay of $\tau_e = {}^{2\zeta}/_{\omega}$=0.074 sec:

ω_F = 3.0 Hz = 18.8 rad/sec ζ_F = 0.7 k_F = 1.2 N/° = 0.675 lb/°

Radius of Motion: 25° = 7.6 cm ← This is used to normalize position signals

Max Force required: 30 N = 16.9 lb ← This is used to normalized force signals

These settings were chosen to maximize stick bandwidth, minimize effective dynamic delay, and still provide a high resolution (large displacement) position cue. Also, the active inceptor used in the manned evaluation has mechanical stability limits that prevent high natural frequency and low damping combinations. The sidestick rotates around an 18 cm axis (Figure 34). Its displacement is measured in degrees; its response is measured as the force at the grip rather than a moment about its axis. Its radius of motion is 25°. The position gain was effectively $K_{\delta u} = {}^{1}/_{25°} = 0.04$ deg^{-1} but within the control system all positions are normalized and non-dimensionalized from [-25° +25°] to [-1 1] so the second order gain for the cue was simply K_2 = 1.0. The effective force gain $K_{Fu}={}^{1}/_{30N}$. The zero order gain was also K_0 =1.0.

Fully Off $$[N_{\lim} \quad \omega \quad \zeta \quad K_0 \quad K_2 \quad \mu]^T = [4 \quad 18.8 \quad 0.7 \quad 1.0 \quad 1.0 \quad 0.0]^T \quad (58)$$

The PIO Limit Cue Module provides a transfer function and a friction cue using the methods described above. This is limit number four. The nominal sidestick force-feel uses natural frequency ω_n=18.8 $^{rad}/_{sec}$ (= 3.Hz) and damping ζ = 0.7 in a position command mode, μ=0. As the fuzzy PIO detector switches the cue on, the transfer function changes to a very under-damped (ζ=0.1), force command stick (μ=1) with a natural frequency that matches the main PIO frequency calculated by the FFT preprocessing algorithm.

Fully On $$\begin{bmatrix} N_{\lim} & \omega & \zeta & K_0 & K_2 & \mu \end{bmatrix}^T = \begin{bmatrix} 4 & \omega_c & 0.1 & 1.0 & 1.0 & 1.0 \end{bmatrix}^T \quad (59)$$

The friction cue is nominally absent (μ_d= μ_s=0) but when rate limiting is detected and inceptor is moving in the same direction, the friction cue is turned on. The normalized cue of 0.5 will ultimately lead to a 15 N friction force cue.

$$\begin{bmatrix} N_{\lim} & \mu_f & \mu_s \end{bmatrix}^T = \begin{bmatrix} 4 & 0.5 & 0.5 \end{bmatrix}^T \quad (60)$$

Limit Protection Performance

Fuzzy PIO Predictor Evaluation

The fuzzy inference system is tested in piloted simulation within RIPTIDE with an artificial rate saturation inserted immediately after the inceptor signal. The pilot was already aware of the PIO propensity of the control system and simply performed climbs, descents, and pull-up push-over maneuvers of increasing rapidity and amplitude.

An excerpt of a flight (Figure 49) depicts a series of intentional longitudinal oscillations that segue into a coupled oscillation with rate saturation. Early in the 30-second sequence, main control frequency was 0.5 to 0.3 Hz, within the APC range, but the aircraft state remained in phase with the pilot's sidestick commands. Later, at approximately 108 seconds, the pilot increased the frequency (to 0.8 Hz) and amplitude (to 0.5) of his commands. The signal reached rate saturation, which abruptly caused the state to lag the control by 180°. The positive rules for PIO are fulfilled and the PIO Estimate increases from near 0.2 to over 0.5. The saw tooth pattern in the PIO Estimation is due to the Actuator Saturation rule acting on the abrupt changes in actuator speed and acceleration evident in the saw tooth power of the saturated control signal.

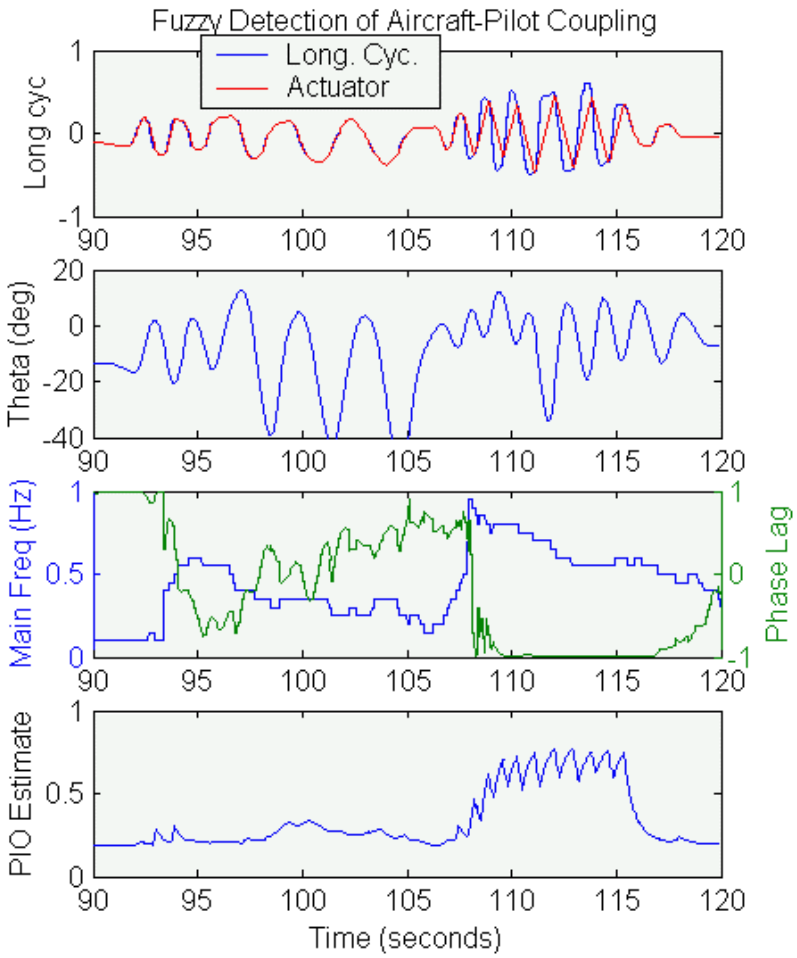

Figure 49: Intentional Oscillations into PIO

Because of its negative rules, the fuzzy detector can discriminate abnormal but non-coupled flight (Figure 50). Despite several seconds of large amplitude, high frequency sidestick movements, the PIO Estimate remains low. This is partly due to the Same Phase rule and partly due to Phase Lag rule with its APC Range membership function.

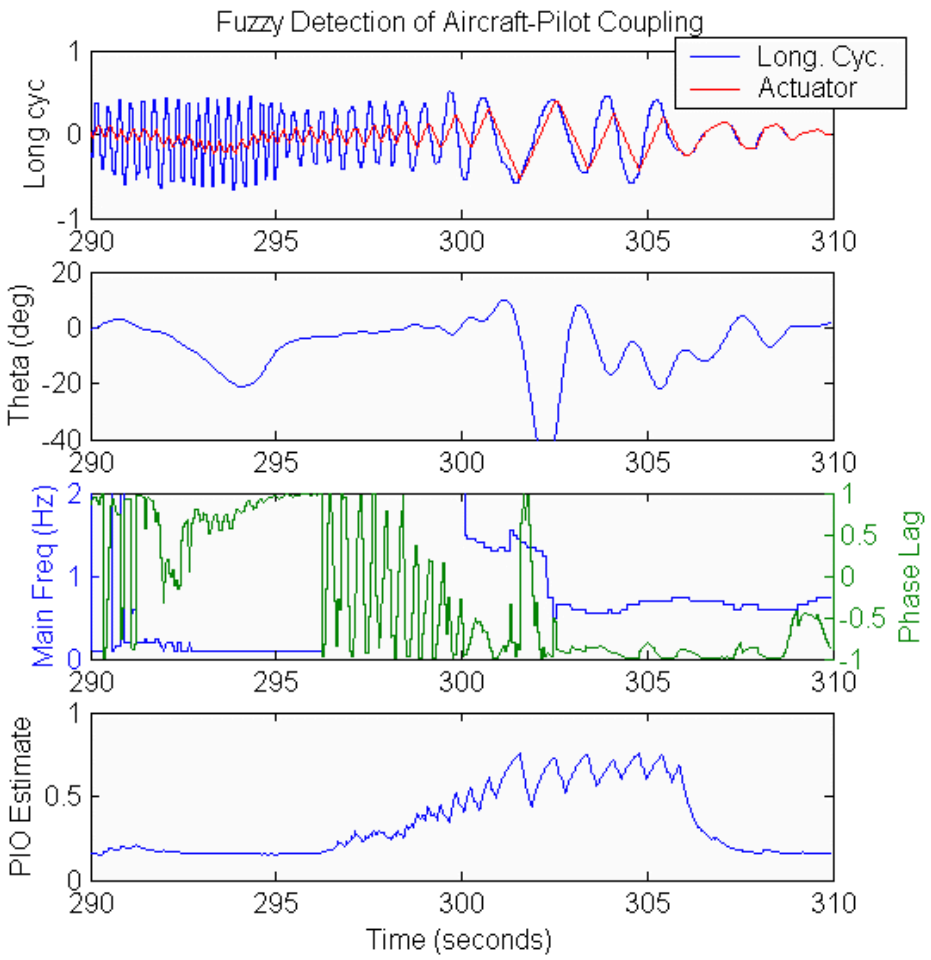

Figure 50: Over-controlling into PIO

Tactile Cue Evaluation

The cue was evaluated in manned simulation with an artificial rate limiting element applied to the inceptor output signal, u. The artificial rate saturation targeted an onset fully developed frequency of 1 Hz = 6.3 $^{RAD}/_{SEC}$ with a 100% radius of motion amplitude (A=1). Using the time domain relations for rate limiting properties (See Reference 1, Appendix C),

$$V_L = \omega_{ON-FD} A \sqrt{\frac{4}{\pi^2 + 4}} \qquad (61)$$

the rate limit, V_L, was set at 3.37 sec^{-1}. This implies onset of rate liming at 0.54 Hz for full amplitude inceptor output or, alternatively, onset in a 1 Hz signal at 54% amplitude.

When actuator rate saturation occurs, it typically occurs during the most rapid inceptor movement, near the center of the inceptor radius. Consequently, the friction force manifests during very rapid inceptor movement. The friction cue disappears as the pilot slows the inceptor to reverse movement and the actuator "catches up" to its commanded position. The tactile impression is that of a faint pulsing during movement not unlike minor hydraulic feedback. Because this is a motion cue, it is more noticeable with large displacement sticks. Figure 51 depicts a growing 1 Hz oscillation. In this figure, the force command gain remains constant, $K_{Fu}={}^{1}/_{30N}$, and the same gain is also applied to scale the 10 N friction force. The most noticeable cue effect is the flattened peak amplitudes.

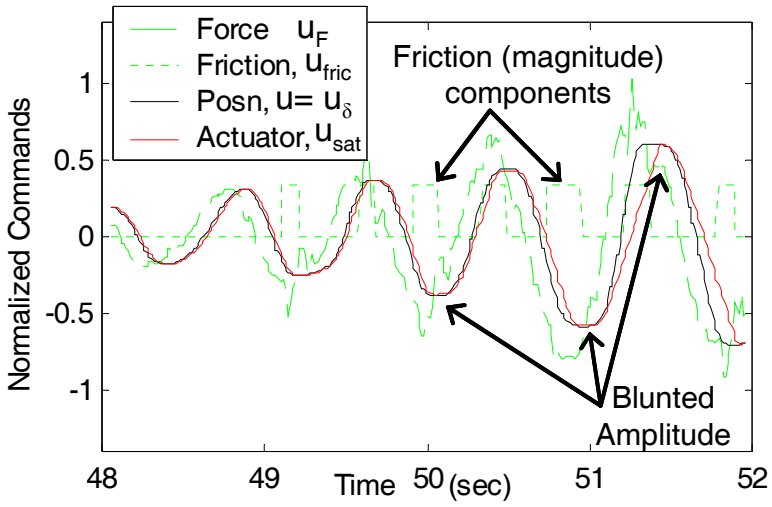

Figure 51: Cueing Saturation with Friction

In the evaluation of the active dynamics cue, the cue was turned on when the Fuzzy PIO Estimate reached 0.6 and remained on until it dropped to 0.3. The cue is effective in cases where the pilot understands that the change in stick dynamics reflects the change in the aircraft dynamics. Figure 52 depicts an oscillatory event with growing amplitude and onset of rate limiting. At 230.7 seconds, the PIO Estimate triggers the active dynamics cue where the command switches from position command to force command simultaneously with a change in bobweight characteristics. The stick frequency changes from the nominal 3 Hz to the 1 Hz PIO frequency calculated by the Fuzzy PIO Detector and damping drops from 0.7 to 0.1. In order to better explore the nature of this cue, these evaluations all took place with a constant 25° stick radius and position gain $K_{\delta u} = {}^{1}/_{25°}$. The gradient remained k_F = 1.2 N/° and the force gain remains $K_{Fu}={}^{1}/_{30N}$.

The immediate effect of the cue is a sudden drop in counter-force due to the lower damping on the fast moving stick. The lower force immediately reduces the force command, u_F. Meanwhile, the sidestick, with low damping and low frequency continues in a large amplitude oscillation. The pilot, still accustomed to a position command stick, adapts to the new stick dynamics to reduce the amplitude of the oscillation. The pilot senses the effective bandwidth of the stick, which resembles the instantaneous aircraft dynamics, and adapts his control strategy accordingly. The shift from position command to force command also eliminates the 0.74 second effective delay of the nominal stick dynamics to offset the delay caused by the rate limit.

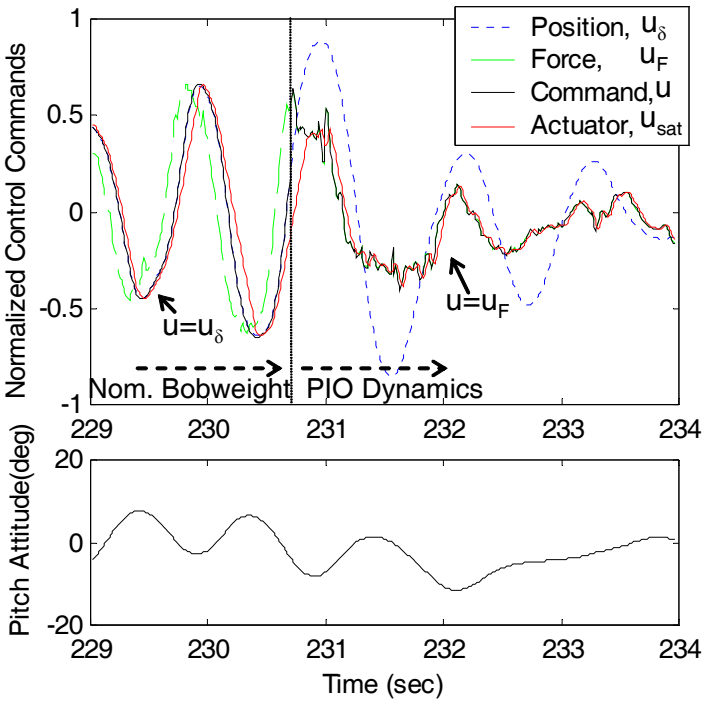

Figure 52: Effective PIO Active Dynamics Cue

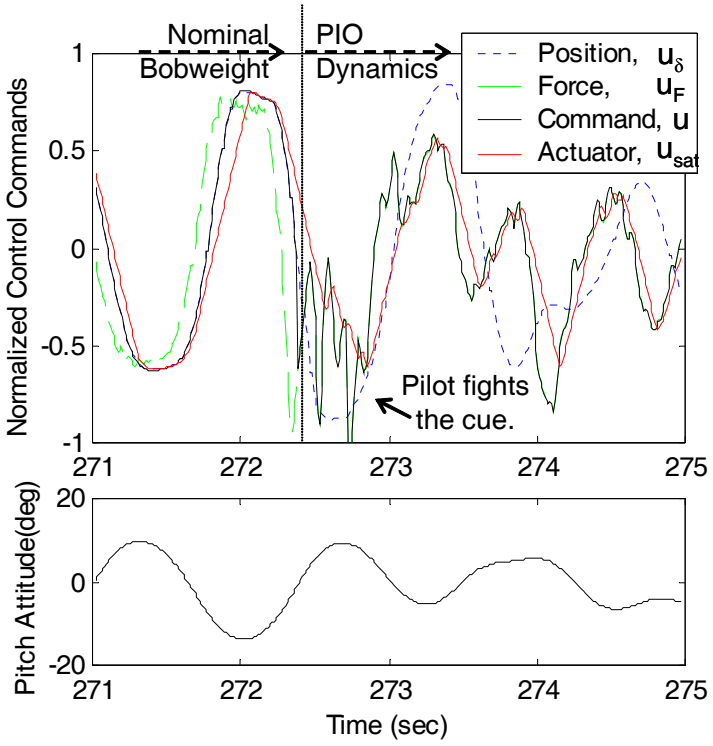

Figure 53: Mistrusted PIO Active Dynamics Cue

The cue is less effective when the pilot interprets the change in stick dynamics as a cockpit control malfunction. In another event (Figure 53), the pilot stiffens his grip to force the stick onto a desired path. The saturation washes out the resulting force command spikes and the recovery is less smooth that the previous example.

This fuzzy logic detector for aircraft pilot coupling and pilot induced oscillation provides a real time assessment that can trigger some form of compensation. It has strengths and weaknesses over similar mechanisms such as the probabilistic neural net. Both intelligent control methods require similar accurate signal preprocessing. But while a probabilistic neural net must be trained with flight event time histories which have been expertly classified as PIO or Non-PIO; a fuzzy predictor eliminates that middle step and directly assesses real time signals based on aircraft pilot coupling knowledge designed into its rule set. So this fuzzy detector can be applied more generally than a neural net trained for a specific aircraft type.

However, just as a neural net is only as effective as it's training, so too is a fuzzy inference system only as good as its rule set and membership functions. Only five non-redundant rules are used for the PIO Estimate. Their careful design is analogous to the

selection of orthogonal inputs for a neural net. The parsimonious rule set simplified analysis and tailoring of the membership functions for accurate coupling detection.

As new PIO knowledge is acquired, additional rules may be added. For example, the amplitude of the pitch attitude can be a valuable PIO indicator. It was included in developmental trials and did contribute marginally to the accuracy of the PIO Estimate. However, aircraft pitch amplitude may be judged severe or not depending on the pilot, the aircraft, and the mission. So for the sake of generality, simplicity, and robustness with respect to opinions of pitch severity, it was excluded from the final fuzzy inference system.

To improve the detector's accuracy, one may apply a neuro-fuzzy technique to train the PIO Estimate membership functions from time histories of expertly classified PIO and non-PIO time histories. This additional training can tune the fuzzy PIO identification with respect to an intended aircraft and a given human expert. Such a technique combines the structural simplicity of the fuzzy inference system with the trainable accuracy of a neural net.

The PIO tactile avoidance cues presented here explore three new elements for carefree maneuver systems: 1) They apply to a controllability limit rather than a structural limit, 2) They use a logic based detector rather than an arithmetic cue detector, and 3) The tactile interface uses friction and force-feel dynamics rather than displacement based force cues like soft stop constraints.

The tactile avoidance cues are found to be effective and suggest intuitive corrective responses that guide the pilot away from PIO events. A uni-directional friction force up to 40% of the maximum static deflection force can provide an effective, intuitive tactile cue that the pilot's stick movement exceeds some rate limitation within the total aircraft. This saturation cue is effective when there is a fundamental directional relationship between the rate limited element and the inceptor movement. It may not be appropriate for aircraft with unstable aerodynamics requiring multiple control surface actuator reversals during a maneuver.

An active dynamics cue alters the inceptor natural frequency and damping coefficient to approximate the aircraft effective dynamics with the bobweight quality of the sidestick. This "matched manipulator" concept can communicate the changed limited bandwidth of the aircraft during a PIO Event. As the pilot adapts to stick dynamics, he acknowledges and adapts to the dynamical limitations of the aircraft that cause the coupled oscillation.

CHAPTER VII

CONCLUSION

This Open Platform for Limit Protection provides an open design structure for Limit Protection Systems. The platform uses three stages of limit protection modules: limit Cue creation, limit cue arbitration, and control interface. A common set of limit cue modules provides four types of limit cue commands: constraints, alerts, transfer functions, and friction. An arbitration module selects the "best" or most appropriate from among these four limit protection cues and distributes it across the control system. This platform adopts a holistic approach to limit protection whereby it considers all potential interface points along the control path. Among the possible control interfaces are visual, aural, and tactile displays; and automatic command restraint shaping for autonomous limit protection.

For each of the platform functional modules, this thesis guides the control system designer through the design choices and explains the standardized information interfaces among the modules. The limit cue module design choices include the type of prediction, the prediction mechanism, the method of critical control calculation, and the type of limit cue. Special consideration is given to the nature of the limit, particularly the level of knowledge about it, and the ramifications for limit protection design, especially with respect to intelligent control methods such as fuzzy inference systems and neural networks.

Using the Open Platform for Limit Protection, a carefree maneuver system is designed that addresses the main rotor blade stall as a steady-state, structural limit, hub moment as a transient structural limit, and pilot induced oscillation as a controllability limit. The limit cue modules in this carefree maneuver system make use of static neural networks, adaptive neural networks, and fuzzy inference systems to detect or predict these limits. Visual (heads up display) and tactile (force-feedback) limit cues are employed. The carefree maneuver system is evaluated with manned simulation using a General Helicopter (GENHEL) math model of the UH-60 Black Hawk, a projected, 53° field of view for the pilot, and a two-axis, active sidestick for cyclic control.

The Open Platform for Limit Protection reduces the effort required for initial limit protection design by defining a practical structure that still allows considerable design freedom. The platform reduces lifecycle effort through its open engineering systems approach of decoupled, modular design and standardized information interfaces.

Findings

Open platform advantages

The Open Platform for Limit Protection adopts an open engineering systems approach to guide the design of limit protection systems. A carefree maneuver system that adopts the OPLP structure uses well defined functional modules and standardized information interfaces. Information flows in one direction through the OPLP modules, allowing them to remain decoupled. This facilitates the addition and replacement of new limit modules and extensibility to new control interfaces. The OPLP approach simplified the creation and combination of the carefree maneuver applications described herein. The standardized information interface facilitated the parallel development and integration of limit protection cues.

The hub moment SNN limit cue and the Blade Stall ANN limit cue modules were designed, prototyped, and examined independently but simultaneously. The limit cue designers were geographical separated, an increasingly common collaboration challenge today. They faced communication challenges and coordination problems. The standard information interface for the limit cue output (i.e. the constraint vector) greatly simplified the problem of integrating the two limit cues in the same carefree maneuver system. Because of this, and because the entire system is software based, the designers were able to exchange SIMULINK models by electronic mail; copy and paste the improving iterations of the modules into the greater carefree maneuver system; connect the signals; and test fly the new product.

Limit protection taxonomy

In the process of developing the modular structure of this platform, the design of modern limit protection system was analyzed and the taxonomy of functions, means, methods, and mechanisms was cataloged. The lists and descriptions of design choices within this document are not exhaustive, but define the scope of options and suggest a systematic approach for limit protection control systems design to replace closed, ad hoc, or generic control systems design methods.

Riptide prototyping environment

The RIPTIDE / Simulink based design, prototype, and testing environment proved to be a valuable tool that streamlined the development of new control systems. The collection of relatively inexpensive hardware and software tools is well suited for continued use, collaborative control systems design, and growth.

Dynamics and friction can be useful tactile cues

The use of active force-feel dynamics and friction had not been tried as limit protection cues, but they can be useful means of communicating the dynamical nature of a controlled system such as an aerospace vehicle. Unidirectional friction, when not excessive, communicates a nonlinear quality or discontinuity, such as a rate limited element, in the aircraft flight control system. Active dynamics, using the "matched manipulator" concept can communicate the effective frequency response on an aerospace vehicle, whether in PIO or not.

Benefits of adaptive neural networks

Adaptive limit protection algorithms, such as the adaptive dynamic trim method, are well suited for open engineering applications because they are robust to changes in the vehicle and other uncertainties. Adaptive mechanisms can enable "all-purpose" limit protection modules to model, predict, and protect limits as the environment or aircraft changes. The adaptive dynamic trim blade stall cue tested applied to the UH-60 provided good limit predictions despite intentional changes in aircraft configuration (gross weight and center of gravity location). The static neural network based predictors (such as the blade stall or hub moment) are accurate only for their trained flight conditions.

Improved safety with negligible loss of agility

Results from the experiments involving the blade stall and hub moment cues confirm findings of earlier tactile limit avoidance studies: Overall limit protection, and therefore general safety, improved considerably with the use of a capable limit protection (cueing) system with tactile limit avoidance cues. These safety gains do not significantly reduce the agility or effectiveness of the vehicle and its control system.

Active biodynamic Pilot Involved Oscillation

Tactile constraint cues (softstops) can be made abrupt with short lengths, or more gradual with longer lengths. In the former case, the cue is precise and resembles a step-force jump. But when the softstop location is dynamic and commanded by an active limit protection system, a force cue can affect the limb-manipulator orientation. This is a biodynamic feedback loop. Because of this, a pilot involved oscillation similar to roll ratchet can develop. Minor examples of this are visible in Figure 19 at 79.5 seconds and in Figure 23 at 170 seconds. During the development of these limit cues, more severe active biodynamic PIO events occurred that were objectionable and harmed overall controllability of the vehicle. They were aggravated by abrupt softstops, limit prediction

algorithms highly sensitive to the inceptor position on an active axis, and limit cue algorithms that had intrinsic oscillatory tendencies (such as the adaptive dynamic trim blade stall limit cue). This is another PIO manifestation. Depending on the design of the limit prediction algorithms and the nature of the force feedback cues, these may be category I, II, or III PIO events. The events discovered in the carefree maneuver applications tested here are the nonlinear category III events due to the highly nonlinear nature of the limit prediction algorithms and the complex dynamics of the pilot's limb and inceptor along the longitudinal axis.

Recommendations

Determine the true vehicle limits

Knowledge about the dynamical nature of the limited parameter is one thing, but knowing its true maximum or minimum limit is another question with an inadequate answer. The question becomes: Why is a parameter like hub moment, vertical load, is or engine torque limited at all? Every system is composed of sub-systems and in the same way, each limit is composed of simultaneous and chained subordinate limits. The answer to these questions may be found partly in an aircraft's original design specifications for the original aircraft. Decomposing the major limits would require the cooperation of the manufacturers and their suppliers and access to relevant proprietary design criteria.

The gross limits provided in an aircraft operating manual are conservative simplifications and concatenations of many subordinate limits set during detailed design. The progressive decomposition every major limit to the subordinate limits will increase the complexity of the limit envelope by replacing a gross constraint with multiple fine constraints. The process would enlarge the flight envelope. An extensible limit protection system with adaptive limit cue modules would be able to manage the increased complexity and enable the safe envelope expansion.

Study the trade-off between limit protection and fatigue limits.

The Integrated Limit Margin and similar metrics are assumed to be proportional to the fatigue wear on the vehicle caused by sustained limit violations. But the connection between the metric and actual fatigue wear or maintenance demands has not been definitively made. A comprehensive evaluation of fatigue wear may lead to a better appreciation of the safety vs. performance compromise and more useful metrics with which to evaluate voluntary limit protection systems.

Study the design benefits of an organic limit protection system.

A detailed study of the aircraft design process in light of the potential of capable limit protection systems may discover that aircraft designers may relax overly conservative safety factors to allow the design of lighter, higher performing aircraft that rely on active limit protection systems instead of brute structural strength.

Extend to other tactile cues.

Temperature, surface texture, and electric shock should be examined as potentially useful and intuitive limit protection cues, but investigating their potential would require some hardware additions to an active sidestick. A heat exchange element in the stick grip could be used to generate temperatures related limits, such as engine turbine temperature. Surface texture may be a useful tactile indicator of boundary layer conditions along a key control surface. Mild shock could be driven as an alert to draw attention to key events.

Continue to develop the Arbitration module.

As the carefree maneuver system grows, the arbitration module must grow with it. Increased use of intelligent control methods is called for. The arbitration module will become the embodiment of limit knowledge and how limits can be protected. This is the most under-researched and underdeveloped element of the limit protection systems.

Implement within the Open Control Platform (OCP).

This OPLP is well suited for software enabled control platforms such and as the Open Control Platform. The carefree maneuver system using the OPLP offers some of the same qualities as the OCP: Adaptability, Plug-and-play extensibility, Interoperability, and openness. The OCP is an avenue for continued research of carefree maneuver systems, whether manned or unmanned.

Develop a common limit avoidance and obstacle platform.

Depending upon how obstacles, hazards, and limits are defined, they may be addressed with the same mechanisms. A study of obstacles defined as physical limits may lead to a demonstration of an OPLP based obstacle avoidance algorithm.

Develop tactile cues for regulatory limits.

Tactile cues have not yet been developed for regulatory limits. These may take the form of tactile guidance cues along the boundaries of flyable airspace and air routes.

Develop design standards to address active biodynamic PIO .

The active biodynamic PIO will remain a problem until aeronautical design standards are created to progressively eliminate the linear and nonlinear causes of the phenomenon. Coincidentally, the PIO Limit Cue presented here may be an appropriate solution. It could be adapted to address this problem by monitoring the softstop position versus the inceptor position instead of monitoring inceptor position versus aircraft pitch attitude. The “APC Range” membership function would shift to capture the more rapid set of frequencies of the excitable modes of the limb-manipulator system.

Continue development of adaptive limit protection mechanisms.

In the form it was tested here, the adaptive dynamic trim limit cue is effective, but not without shortcomings, particularly the oscillatory prediction and its sometimes jittery tactile softstop. Such adaptive methods have great potential and enhance the advantages of open systems. Research and testing of such limit cue modules should continue.

REFERENCES

1 National Research Council, “Aviation Safety and Pilot Control: Understanding and Preventing Unfavorable Pilot-Vehicle Interactions,” National Academy Press, Washington, D.C., 1997.

2 Defence Systems Daily, “Eurofighter completes carefree handling trials,” http://defence-data.com/eft/eftpage06.htm. (Dated 23 July 2002).

3 Air Force Flight Test Center, Public Affairs, “F-22 Raptor ‘Carefree abandon’,” http://www.edwards.af.mil/articles98/docs_html/splash/apr98/cover/carefree.htm. . (Cover story of April 1998, Accessed June 2004)

4 United States Army Safety Center. “Army Safety Statistics,” http://safety.army.mil/home.html. (Accessed March 2004.)

5 Shappell, Scott A., Wiegmann, Douglas A., “Human Error and General Aviation Accidents: A Comprehensive, Fine-Grained Analysis Using HFACS”, Office of Aerospace Medicine: Washington, DC.

6 Wiegmann, Douglas A., Shappell, Scott A., “A Human Error Analysis of Commercial Aviation Accidents Using the Human Factors Analysis and Classification System (HFACS)”, Aerospace Medicine Technical Report No. DOT/FAA/AM-01/3. Office of Aerospace Medicine: Washington, DC. February 2001.

7 Bell Augusta Aerospace Company., “The BA609 Aircraft”, http://www.bellagusta.com/html/theAircraft/ba_609/index.html. (Accessed April 2004.)

8 The Boeing Corporation, “V-22 Osprey,” http://www.boeing.com/rotorcraft/military/v22/flash.html. (Accessed August 2004.)

9 BAE Systems, , “BAE Systems to Develop Active Inceptors for Joint Strike Fighter,” Press Release, http://www.baesystems.com/newsroom/2002/apr/120402news2.htm, (Dated 12 April 2002, Accessed June 2004.)

10 Howitt, Jeremy, “Carefree Maneuvering In Helicopter Flight Control”, American Helicopter Society 51st Annual Forum, Fort Worth, TX, USA, May 9-11, 1995.

11 Whalley, M. S., “A Piloted Simulation Investigation of Helicopter Limit Cueing”, USAATCOM TR 94-A-020, NASA TM-108851, October 1994.

12 Einthoven, P. E., Miller, D. G., and Thiers, G., “Tactile Cueing Experiments with a 3-Axis Active Sidestick Controller”, American Helicopter Society 57th Annual Forum, Washington, D.C., USA, May 8-11, 2001.

13 Dones F., Dryfoos J.B., McCorvey D.L., Hindson W.S., “An Advanced Fly-by-Wire Flight Control System Designed for Airborne Research – Concept to Reality”,

Proceedings of the 56th Annual Forum of the American Helicopter Society, Virginia Beach, Virginia, May 2-4, 2000.

14 Mistree, F., Allen, J., Karandikar, H., Shupe, J., and Bascaran E., "Learning How to Design: A Minds-On, Hands-On, Decision-Based Approach" Course Notes for a course "Designing Open Engineering Systems," Georgia Institute of Technology, Spring 2002.

15 Miller, D., Einthoven, P., Morse, C., Wood, J., "HACT Flight Control System (HFCS) Control Law Overview", Proceedings of the American Helicopter Society 58th Annual Forum Proceedings, Montreal, Canada, June 11-13, 2002.

16 Suh, N., "The Principles of Design," Oxford University Press, 1990.

17 Ulrich, K., "The role of product architecture in the manufacturing firm," Research Policy, Massachusetts Institute of Technology, Sloan School of Management, Cambridget, Massachusettes, 1995.

18 Erens, V., Verhulst, K., "Architectures for Product Families," Computers in Industry, Vol. 33, p. 165-178, Elsevier Publishers, 1997.

19 Booch, Grady. "Object-Oriented Analysis and Design with Applications," The Benjamin/Cummings Publishing Company, Inc., Redwood City, California, 1994.

20 Bertrand Meyer, "Object-Oriented Software Construction", Prentice Hall, 2nd Edition, March 21, 2000.

21 Leslie, R.A., Geyer, D.W., Cunningham, K., Glaab, P.C., Kenney, P. S., and Madden, M.M., "LaRS++ An Object-Oriented Framework for Real-Time Simulation of Aircraft," AIAA Modeling and Simulation Technologies Conference and Exhibit, Boston Massachusetts, August 10-12, 1998.

22 Hawley, P., Urban, T., "Object Oriented Simulation Architecture," AIAA Modeling and Simulation Technologies Conference and Exhibit, Providence, Rhode Island, Aug. 16-19, 2004.

23 Tchon, K., "Object-oriented programming for a temporal adaptive Navier-Stokes solver," Aerospace Sciences Meeting and Exhibit, 33rd, Reno, NV, Jan. 9-12, 1995.

24 Katsurayama, H., Komurasaki, K., Arakawa, Y., "Application of Object-Oriented Design Patterns to CFD Code with AMR Technique," University of Tokyo, Tokyo, Japan, 42nd AIAA Aerospace Sciences Meeting and Exhibit, Reno, Nevada, Jan. 5-8, 2004.

25 Cambier, L., Gazaix, M., "elsA - An efficient object-oriented solution to CFD complexity," AIAA Aerospace Sciences Meeting and Exhibit, 40th, Reno, Nevada, Jan. 14-17, 2002.

26 T. Fritz and L. Long, "A Parallel, Object-Oriented Unsteady Vortex Lattice Method for Flapping Flight," 42nd AIAA Aerospace Sciences Meeting and Exhibit, Reno, Nevada, Jan. 5-8, 2004.

27 Malone, B., Woyak, S., “An object-oriented analysis and optimization control environment for the conceptual design of aircraft,” Aircraft Engineering, Technology, and Operations Congress, Los Angeles, California, Sept. 19-21, 1995.

28 Pfaender, H., DeLaurentis, D., Mavris, D., “An Object Oriented Approach for Conceptual Design Exploration of UAV-Based System-of-Systems,“ 2nd AIAA "Unmanned Unlimited" Conference, Workshop and Exhibit, San Diego, California, September 15-18, 2003.

29 Ahlqvist, A., Jamal F. Nayfeh J., Kodiyalam, S., Zarda, P.R., “Object oriented multidisciplinary design optimization,” AIAA/USAF/NASA/ISSMO Symposium on Multidisciplinary Analysis and Optimization, Long Beach, California, September 6-8, 2000.

30 Glaab, P.C., Madden, M.M., “A generic object-oriented implementation for flight control systems,“ AIAA Modeling and Simulation Technologies Conference and Exhibit, Portland, Oregon, Aug. 9-11, 1999.

31 Wills, L., Kannan, S., Sander, S., Guler, M., Heck, B., Prasad, J.V.R., Schrage, D., Vachtsevanos, G., “An Open Platform for Reconfigurable Control,” IEEE Control Systems Magazine, June 2001.

32 Whalley, M., Achache, M., “Joint U.S./France Investigation of Helicopter Flight Envelope Limit Cueing”, American Helicopter Society 52nd Annual Forum, Washington D.C. 4-6 June, 1996.

33 Wolfdietrich, H., “Flying by Wire – Eurofighter Flight Control System,” Aerospace, AIAA, No. 1, April 2000.

34 Corps, S.G., “Airbus A320 Side Stick and Fly By Wire – An Update,” Proceedings of the SAE 5th Aerospace Behavioral Engineering Technology Conference, Long Beach, California, 1987.

35 anon., “777 Flight Reference Manual,” United Airlines, 16 October 1998.

36 RAH-66 Comanche Development Program, System Specification, 2000-315-512-1, April 1993.

37 King, D.W., Dabundo, C., Kisor, R.L., Agnihotri, A., “V-22 Load Limiting Control Law Development.” American Helicopter Society 49th Annual Forum, St. Louis Missouri, May 19-21, 1993.

38 Iloputaife, O., “Design of Deep Stall Protection for the C-17A,” Proceedings of the AIAA Guidance, Navigation and Control Conference, San Diego, California, July 1996.

39 Horn, J.F., Calise, A.J., Prasad, J.V.R., “Flight Envelope Limiting Systems Using Neural Networks,” Proceedings of the AIAA Atmospheric Flight Mechanics Conference, Boston, Massachusetts, August 1998.

40 Horn, J.F., Calise, A.C., Prasad, J.V.R, “Flight Envelope Limit Detection and Avoidance for Rotorcraft”, Journal of the American Helicopter Society, Vol. 47, (4), October 2002.

41 Yavrucuk, I., Prasad, J.V.R., “Automatic Limit Detection and Avoidance for Unmanned Helicopters,” Proceedings of the American Helicopter Society 57th Annual Forum, Washington D.C., May 2001,

42 Prasad, J.V.R., Yavrucuk, I., Unnikrishnan, S., “Adaptive Limit Prediction and Avoidance for Rotorcraft,” Proceedings of the European Helicopter Forum, Bristol, U.K., September 2002.

43 Yavrucuk, I., Prasad, J.V.R., Calise, A.J., “Adaptive Limit Detection and Avoidance for Carefree Maneuvering,” Proceedings of the AIAA Atmospheric Flight Mechanics Conference, Montreal, Canada, August 2001,

44 Schage, D., Vachtsevanos, G., “Software Enabled Control for Intelligent UAV’s,” August 2000, Proceedings of the AIAA Atmospheric Flight Mechanics Conference, Denver, Colorado.

45 Johnson, E.N. and Schrage, D.P., "The Georgia Tech Unmanned Aerial Research Vehicle: GTMax," Proceedings of the AIAA Guidance, Navigation, and Control Conference, 2003.

46 Anon., “Minimum Performance Specifications for TCAS Airborne Equipment,” Radio Technical Committee on Aeronautics (RTCA), Washington, D.C., Doc. RTCA/DO-185, 1983.

47 Yang, L.C., Kuchar, J.K., “Performance Metric Alerting: A New Design Approach for Complex Alerting Problems,” IEEE Transactions on Systems, Man and Cybernetics-Part A: Systems and Humans. Vol. 32, No.1, January 2002.

48 Song, L., Kuchar, J.K., “Dissonance Between Multiple Alerting Systems Part 1: Modeling and Analysis,” IEEE Transactions on Systems, Man, and Cybernetics—Part A: Systems and Humans, Vol.33, No.3, May 2003.

49 Song, L., Kuchar, J.K., “Dissonance Between Multiple Alerting Systems Part 2: Avoidance and Mitigation,” IEEE Transactions on Systems, Man, and Cybernetics—Part A: Systems and Humans, Vol.33, No.3, May 2003.

50 A. R. Prichett, “Simultaneous design of cockpit display of traffic information and air traffic management procedures,“ AIAA and SAE 1998 World Aviation Conference, Anaheim, California, Sept. 28-30, 1998

51 Amy R. Pritchett, Richard Barhydt, R. J. Hansman (MIT, Cambridge, MA), and Eric N. Johnson, “Flight simulator testing of cockpit traffic displays using robust situation generation ” AIAA Flight Simulation Technologies Conference, San Diego, CA, July 29-31, 1996, Technical Papers.

52 Whalley, M.S., Keller, J.F., Roos, J., and Buckanin, R., “Helicopter Active Control Technology Demonstrator Program,” Proceedings of the American Helicopter Society 57th Annual Forum, Washington D.C., May 2001.

53 Einthoven, P., Miller, D., Nicholas, J., and Margetich, S., “Tactile Cueing Experiments with a Three Axis Sidestick,“ Proceedings of the American Helicopter Society 57th Annual Forum, Washington D.C., May 2001.

54 Einthoven, P., Morse, C., “Energy Management,” Proceedings of the American Helicopter Society Crew Systems Design Specialists Meeting, Philadelphia, PA, October 9-11, 2002.

55 Einthoven, P., Miller, D., “The HACT Vertical Controller,” Proceedings of the American Helicopter Society 58th Annual Forum Proceedings, Montreal, Canada, June 11-13, 2002.

56 Cooper, G.E., “A Survey of the Status of and Philosophies Relating to Cockpit Warning Systems,” NASA CR-152071, NASA Contract No. NAS2-9117, December 1977.

57 Randle, R.J., Larsen, W.E., Williams, D.H., “Some Human Factors Issues in the Development and Evaluation of Cockpit Alerting and Warning Systems.” NASA RP-1055, January 1980.

58 Berson, B.L., Po-Chedley, D.A., Boucek, G.P., Hanson, D.C., Leffler, M.F., Wasson, R. L., “Aircraft Alerting Systems Standardization Study – Vol. II – Aircraft Alerting System Design Guidelines,” DOT/FAA/RD-81/38II, Boeing Rep. No. D6-49976TN, Contract No. DOT-FA79WA-4268, January 1981.

59 Proctor, P., “Integrated Cockpit Safety System Certified,” Aviation Week and Space Technology, April 6, 1998.

60 Massey, C.P., Wells, P., “Helicopter Carefree Handling Systems.” Royal Aeronautical Society Conference on Helicopter Handling Qualities and Control, London, UK, November 1988.

61 Howitt, J., “Carefree Manoeuvring in Helicopter Flight Control,” Proceedings of the 51st Annual Forum of the American Helicopter Society, Ft. Worth, TX, May 1995.

62 Rollet, P., and Mezan, S., “Active Control Technology to Improve Mission Effectiveness,” Proceedings of the American Helicopter Society 55th Annual Forum, Montreal, Quebec, Canada, May 1999,

63 Handcock, A., Lanes, R., Johns, S.L., and Charlton, J.H.M, “Benefits of Advanced Control Technology,” Proceedings of the American Helicopter Society 56th Annual Forum, Virginia Beach, VA, May 2000.

64 Wright, G.P., Lappos, N.D., “Helicopter Maneuver Envelope Enhancement (HelMEE) Study,” USAAVSCOM TR-89-A-001, NASA CR 177542, September 1989.

65 The MathWorks. http://www.mathworks.com/products, (Accessed May 2004.)

66 Advanced Realtime Control Systems, Inc., http://www.arcsinc.com. (Accessed June 2004)

67 Jex, H.R., “Problems in Modeling Man-Machine Control Behavior in Biodynamic Environments,” Proceedings of the Seventh Annual Conference on Manual Control, Washington, D.C., 1972.

68 Hess, R.A., “Model for Human Use of Motion Cues in Vehicular Control,” AIAA Journal of Guidance, Vol. 13, No. 3, May-June 1990.

69 Jeram, G., “Open Design for Helicopter Active Control Systems,” Proceedings of the American Helicopter Society 58th Annual Forum Proceedings, Montreal, Canada, June 11-13, 2002.

70 Bohn, R., “Measuring and Managing Technological Knowledge,” Sloan Management review, Fall 1994.

71 anon., “Handling Qualities Requirements for Military Rotorcraft,” U.S. Army AMCOM Aeronautical Design Standard, ADS-33D-PRF, May 1996.

72 Hess, R.A., “A Qualitative Model of Human Interaction with Complex Dynamical System,” IEEE Transactions on Systems, Man, and Cybernetics,” Vol. SMC-17, No. 1, January / February 1987.

73 Horn, J.F. and Sahani, N., “Detection and Avoidance of Main Rotor Hub Moment Limits on Rotorcraft,” AIAA Journal of Aircraft, Vol. 41,(2), March-April 2004, pp.372-379.

74 Sahani, N., Jeram, G., Horn, J., Prasad, J.V.R., “Hub Moment Limit Protection Using Static Neural Networks,” Proceedings of the American Helicopter Society 60th Annual Forum, Baltimore, Maryland, June7-10, 2004.

75 Unnikrishnan, S., Jeram, G., Prasad, J.V.R., “Tactile Limit Avoidance Cueing Using Adaptive Dynamic Trim,” Proceedings of the American Helicopter Society 60th Annual Forum, Baltimore, Maryland, June7-10, 2004.

76 Jeram, G., Prasad, J.V.R., “Tactile Avoidance Cueing for Pilot Induced Oscillation,” American Institute of Aeronautics and Astronautics Atmospheric Flight Mechanics Meeting, Austin, Texas, 11-14 August 2003.

77 Whalley, M., “A Piloted Simulation Investigation of a Helicopter Limit Avoidance System Using a Polynomial Neural Network”, USAATCOM TR 97-A-004, NASA TM-1998-112220, January 1998.

78 Horn, J.F., Calise, A.C., Prasad, J.V.R, “Flight Envelope Cueing on a Tilt-Rotor Aircraft Using Neural Network Limit Prediction”, Journal of the American Helicopter Society, Vol. 46, (1), January 2001.

79 Sahasrabudhe, V., Spaulding, R., Faynberg, A., Horn, J., Sahani, N., “Simulation Investigation of a Comprehensive Collective-Axis Tactile Cueing System,” Proceedings of the American Helicopter Society 58th Annual Forum Proceedings, Montreal, Canada, June 11-13, 2002.

80 Yavrucuk, I., Prasad, J.V.R., Calise, A., “Adaptive Limit Detection and Avoidance for Carefree Maneuvering”, American Institute of Aeronautics and Astronautics, Guidance and Navigation Conference, Montreal, Canada, August 6-9, 2001.

81 Prandini, M., Hu, J., Lygeros, J., Sastry, S., “A Probabilistic Approach to Aircraft Conflict Detection,” IEEE Transactions on Intelligent Transportation Systems, Vol. 1, Issue 4, December 2000.

82 Yang, L., “Aircraft Conflict Analysis and Real-Time Conflict Probing Using Probabilistic Trajectory Modeling,” Ph.D. Dissertation, Department of Aeronautics and Astronautics, Massachusetts Institute of Technology, Cambridge, Massachusetts 2000.

83 Army Field Manual FM 1-203, Fundamentals Of Flight, 9 September 1983.

84 Gilson, R.D., Fenton, R.F., “Kinesthetic-Tactual Information Presentations – Inflight Studies,” IEEE Transactions on Systems, Man, and Cybernetics, Vol. SMC-4, No. 9, pp.531-535.

85 Leuthardt, E., Gerwin, S., Wolpaw, J., Ojemann, J., Moran, D., “A brain–computer interface using electrocorticographic signals in humans”, Journal of Neural Engineering (Volume 1, No 2, pages 63-71).

86 Kennedy, P., Andreasen, D., Ehirim, P., King, B., Kirby, T., Mao, H., Moore, M., “Using human extra-cortical local field potentials to control a switch,” Journal of Neural Engineering (Volume 1, No 2, pages 72-77).

87 Jeram, G Prasad, J.V.R., "Fuzzy Logic Detector for Aircraft Pilot Coupling and Pilot Induced Oscillation," Proceedings of the 59th American Helicopter Society Annual Forum, Phoenix, Arizona, May 2003.

88 Mansur, M.H., Frye M., Mettler B., Montegut M., “Rapid Prototyping and Evaluation of Control Systems Designs for Manned and Unmanned Applications”, Proceedings of the American Helicopter Society 56th Annual Forum, Virginia Beach, Virginia, May 2-4, 2000.

89 Howlett, J., “UH-60A Black Hawk Engineering Simulation Program: Volume I – Mathematical Model,” NASA CR 166309, December 1981.

90 Yavrucuk, I., Prasad, J. V. R., and Calise, A. J., “Adaptive limit detection and avoidance for carefree maneuvering," Proceedings of the AIAA Atmospheric Flight Mechanics Conference, Montreal, Canada, August 2001.

91 Yavrucuk, I., Prasad, J. V. R., and Calise, A. J., “Carefree maneuvering using adaptive neural networks," Proceedings of the AIAA Atmospheric Flight Mechanics Conference, Monterey, California. August 2002.

92 Lewis, F. L., Yesildirek, A., and Liu, K., “Multilayer neural-net robot controller with guaranteed tracking performance," Proceedings of the IEEE Transactions on Neural Networks, March 1996.

93 National Research Council, “Aviation Safety and Pilot Control: Understanding and Preventing Unfavorable Pilot-Vehicle Interactions,” National Academy Press, Washington, D.C., 1997.

94 Raimbault, N., Fabre, P., “Probabilistic Neural Detector of Pilot Induced Oscillations (PIO),” AIAA Guidance, Navigation, and Control Conference and Exhibit, 6-9 August, 2001.

95 Morelli, E.A., “Real-Time Parameter Estimation in the Frequency Domain,” Journal of Guidance, Control, and Dynamics, Vol. 23, No. 5, Sep-Oct 2000.

96 Raimbault, N., Fabre, P., “Probabilistic Neural Detector of Pilot Induced Oscillations(PIO),” AIAA Guidance, Navigation, and Control Conference and Exhibit, 6-9 August, 2001.

97 Department of Defense Interface Standard, – Flying Qualities of Piloted Airplanes, MIL-F-8785B, 1968.

98 Department of Defense Interface Standard, – Flying Qualities of Piloted Airplanes, MIL-F-8785C, 1980.

99 Smith, R.H., and Geddes, N.D., “Handling Quality Requirements for Advanced Aircraft Design: Longitudinal Mode,” AFFDL-TR-78-154, August 1997.

100 Hess, R.A., “Analyzing Manipulator and Feel System Effects in Aircraft Flight Control,” IEEE Transactions on Systems, Man, and Cybernetics, Vol. 20, No. 4, 1990.

101 van Passen, M. M., “Biophysics in Aircraft Control – A Model of the Neuromuscular System of the Pilot’s Arm,” Faculty of Aerospace Engineering, Delft University of Technology, Delft, Netherlands, 1994.

102 Johnston, D.E., Aponso, “Design Considerations of Manipulator and Feel System Characteristics in Roll Tracking,” NASA CR-4111, 1988.

103 Watson, D.C., Schroeder, J. A., “Effects of Stick Dynamics on Helicopter Flying Qualities,” AIAA Paper No. 90-3477, 1990.

104 Hess, R. A., “A Model-Based Theory for Analyzing Human Control Behavior,” Advances in Man-Machine Systems Research, Vol. 2, 1985.

105 Herzog, J.H., “Manual Control Using the Matched Manipulator Control Technique,” IEEE Transactions on Man-Machine Systems, Vol. MMS-9, No.3, 1968.

106 Morelli, E.A., “Real-Time Parameter Estimation in the Frequency Domain,” Journal of Guidance, Control, and Dynamics, Vol. 23, No. 5, September-October 2000.

VITA

Born through the familial convergence of pensive Fins, pragmatic Slovenians, and passionate Italians, Geoffrey James Jeram enjoyed a happy and carefree childhood amid extended family on the lakefront estates of Ashtabula, Ohio. In late childhood, among homes, forests, lakes, and state institutions, including The Ohio State University, he raised and schooled himself in science, philosophy, history, and simplicity.

As he came of age, with the Doomsday Clock only six minutes to midnight, he leapt to the service of God and Country. Despite family objections, he set aside his primogeniture to accept an appointment to the United States Military Academy. One of the Brave and the Few, Geoffrey graduated with Bachelors of Science degrees in Electrical Engineering and in Mechanical Engineering and with a regular army commission to the Aviation Branch. After an abbreviated Grand Tour, he reported for active duty at a remote post in Alabama and was given the Kiowa Warrior helicopter as his steed. He earned his spurs as an air cavalryman with the Second Dragoons at Fort Bragg and rapid promotion followed. Later, as a Captain with the 2nd Infantry Division and 101st Airborne Division (Air Assault), he developed into a respected and capable leader, logistician, and soldier of the Republic; securing peace for America and fostering liberty abroad.

Ignoring desperate veiled evil, the leaders of Earth enjoyed relative quietude in the final autumn of the second millennium. Unheeded, Geoffrey turned to academia at the Georgia Institute of Technology. He entered the School of Aerospace Engineering, pursuing the discipline of flight mechanics and intelligent control systems in research for the Army and NASA. His early work, the precursor of his doctoral thesis, was quickly recognized by the American Helicopter Society with the 2002 Robert L. Lichten Award. Other awards and recognition followed. Four years of cloistered intellectual rigor passed and he completed his Masters of Science in Aerospace Engineering, Masters of Business Administration, and Doctorate of Philosophy. Then he turned his face to the nation, a people resolved, and he set his eyes upon the sky. And he stood at a focus, as a cynosure, where he had been and always hoped to be: at the very Nick of Time.

Geoffrey's hobbies and pastimes include the study of classical literature, aviation, world military history, American history, cosmology, botany & zoology, oil painting & sketching, cinema, bagpiping, wilderness sports, travel, and adventure.